ISBN 0-315-57146-2

BACTERIAL LEACHING STUDY
OF A COMPLEX Cu-Zn SULFIDE ORE

By

HECTOR M. LIZAMA

A Thesis

Submitted to

the Faculty of Graduate Studies and Research

The University of Manitoba

In Partial Fulfillment

of the Requirements for the Degree

Doctor of Philosophy

1989

BACTERIAL LEACHING STUDY OF A COMPLEX Cu - Zn SULFIDE ORE

BY

HECTOR M. LIZAMA

A thesis submitted to the Faculty of Graduate Studies of the University of Manitoba in partial fulfillment of the requirements of the degree of

DOCTOR OF PHILOSOPHY

ABSTRACT

Strains of *Thiobacillus ferrooxidans* and *Thiobacillus thiooxidans* isolated from the Flin Flon mine of Hudson Bay Mining and Smelting Co., Ltd. were able to leach complex sulfide ore samples containing Cu, Zn, and Fe while the laboratory ATCC cultures could not. In both shake-flask and small-scale column leaching experiments Zn was leached preferentially over Cu although this effect was less with the columns. *T. ferrooxidans* and *T. thiooxidans* appeared to leach sulfide ores by different mechanisms and it was possible to preferentially leach Cu or Zn by choice of organisms and leaching conditions. Column experiments with different ore particle sizes showed bacterial leaching activity to be proportional to the available surface area of ore and inversely proportional to the ore particle size. On the basis of these experiments, a large-scale column leaching experiment with 1.8 tons of ore was carried out with successful results. The mine isolates were also tested in detailed kinetic studies of Fe^{2+} and FeS_2 oxidation. In the course of these experiments, some anomalous properties were seen with the *T. ferrooxidans* isolates where their Fe^{2+} oxidizing activities were competitively inhibited by increasing concentrations of cells. This was not seen with the ATCC cultures.

ACKNOWLEDGEMENTS

I would like to thank Dr. I. Suzuki for his guidance, generosity, and patience during the course of this work, as well as for giving me the best PhD project one could ask for.

I would also like to thank Dr. R.G.L McCready for his help and his input into the project. Many thanks to Patrick D. Tackaberry, Travis L. Takeuchi, and J.K. Oh for their companionship and technical assistance. The author also acknowledges the National Science and Engineering Research Council of Canada for a Postgraduate Scholarship, The University of Manitoba for a Graduate Fellowship, and Manitoba Energy and Mines, Hudson Bay Mining and Smelting Co., Ltd., and CANMET for making a contract possible under the Canada-Manitoba Mineral Development Agreement.

I am forever grateful to my wife, Arlene, and to my parents for their continuous moral support and encouragement.

And last, I would like to thank "Tobi" for providing me with a continuous supply of clean glassware.

TABLE OF CONTENTS

PART II: APPLIED STUDIES (continued)

LIST OF FIGURES

PART I: BASIC STUDIES

PART I: BASIC STUDIES (continued)

PART I: BASIC STUDIES (Continued)

PART II: APPLIED STUDIES

PART II: APPLIED STUDIES (continued)

LIST OF TABLES

PART I: BASIC STUDIES

PART II: APPLIED STUDIES

PART II: APPLIED STUDIES (continued)

ABBREVIATIONS

Eh	- redox potential
EP	- electrode potential
GSH	- reduced glutathione
HP	- high phosphate
LP	- low phosphate
PD	- pulp density
SFORase	- sulfur-ferric iron oxidoreductase
SM	- south main

INTRODUCTION

The two principal organisms involved in the bacterial leaching of sulfide ores are the chemolithotrophic bacteria *Thiobacillus ferrooxidans* and *Thiobacillus thiooxidans*, both being acidophiles with an optimum pH for growth around 2 to 3. Both organisms are gram negative, rod-shaped bacteria found naturally in acidic soil environments (12, 35, 38) such as acid mine drainage or tailings piles. Both are strict aerobes, their requirements for carbon being met solely by assimilating carbon dioxide.

T. ferrooxidans obtains its metabolic energy from the oxidation of ferrous iron to ferric and sulfur or sulfide to sulfate, with molecular oxygen being the electron acceptor (30, 47, 68). The ferric iron produced by bacterial oxidation eventually precipitates as ferric hydroxide or jarosite in the presence of sulfate even under acidic conditions. *T. thiooxidans* also obtains its metabolic energy from the oxidation of sulfur or sulfide to sulfate but is not capable of oxidizing iron. The various metabolic reactions carried out by these two bacteria have been reviewed (28, 30, 35, 54, 68). Although their metabolism requires an acidic external environment for growth, the intracellular pH of *T. ferrooxidans* and *T. thiooxidans* is close to neutrality (15, 29, 32).

Because of their unique metabolism, various sulfide minerals can be oxidized by *T. ferrooxidans* and *T. thiooxidans*, resulting in the production of acid and the solubilization of metals. The applications of this biological process for the profitable recovery of metals from refractory ores is becoming increasingly important in the mining industry. The present study deals with both fundamental and applied work with *T.*

ferrooxidans and *T. thiooxidans* strains isolated from mine water samples.

PART I

BASIC STUDIES

Part of this work is available elsewhere:

Isamu Suzuki, Hector M. Lizama, and Patrick D. Tackaberry. Competitive Inhibition of Ferrous Iron Oxidation by *Thiobacillus ferrooxidans* by Increasing Concentrations of Cells. Applied and Environmental Microbiology. 1989, Vol. 5, pp. 1117-1121.

Hector M. Lizama and Isamu Suzuki. Synergistic Competitive Inhibition of Ferrous Iron Oxidation by *Thiobacillus ferrooxidans* by Increasing Concentrations of Ferric Iron and Cells. Submitted to: Applied and Environmental Microbiology.

Hector M. Lizama and Isamu Suzuki. Rate Equations and Kinetic Parameters of the Reactions Involved in the Pyrite Oxidation by *Thiobacillus ferrooxidans*. Submitted to: Applied and Environmental Microbiology.

INTRODUCTION

Little is known about the kinetics of Fe^{2+} and pyrite oxidation by thiobacilli. In the first part of this study, an attempt was made to study these in detail. An interesting cell concentration effect was observed in Fe^{2+} oxidation by a *T. ferrooxidans* strain isolated from a mine site. The effect was in the form of an increase in the apparent Michaelis constant (K_m value) caused by increasing concentrations of cells. This could be explained by the assumption of a bacterial cell functioning as an Fe^{2+} oxidizing enzyme system also interacting with another cell in such a way that it competes with Fe^{2+} for the latter's Fe^{2+} binding site. The effect was not observed with the laboratory ATCC strain used.

Competitive inhibition of Fe^{2+} oxidation by increasing concentrations of Fe^{3+} was also studied in detail and in conjunction with the cell-cell competitive inhibition effect on the *T. ferrooxidans* mine isolate. The kinetics observed suggested a cooperative or synergistic type of inhibition by cells and Fe^{3+}. The binding of cells to one another seemed to hinder Fe^{3+} binding to cells and vice versa.

The oxidation kinetics of pyrite (FeS_2) by resting cells of *T. ferrooxidans* and *T. thiooxidans* was also studied. In order to give perspective to the bacterial activities observed, the kinetics of chemical oxidation of pyrite by oxygen and Fe^{3+} were first established. The mine isolates of *T. ferrooxidans* and *T. thiooxidans* tested both displayed cell-cell competitive inhibition kinetics when oxidizing unwashed pyrite which liberated Fe^{2+} and possibly sulfur and sulfide upon contact with the reaction mixture. Washed pyrite, which did not undergo this type of

instant solubilization upon wetting, did not elicit cell-cell competitive inhibition kinetics with the *T. ferrooxidans* mine isolate. These results provided insights as to the mode of pyrite oxidation by *T. ferrooxidans*.

In the second part of this study, the interactions of chalcopyrite ($CuFeS_2$) and sphalerite (ZnS) with pyrite were studied in shake-flask leaching experiments with and without inoculation with mine isolates of *T. ferrooxidans*, *T. thiooxidans*, or both cultures. In addition, short-term steady-state oxidation experiments were carried out in Warburg experiments with resting cells of these cultures. The experiments showed that pyrite helped the leaching of chalcopyrite and sphalerite. The *T. ferrooxidans* mine isolate was capable of leaching pyrite, chalcopyrite, and sphalerite although it required a period of adaptation for sphalerite leaching. The *T. thiooxidans* mine isolate stimulated Zn extraction from sphalerite and Fe from pyrite but did not stimulate Cu extraction from chalcopyrite. These experiments helped to give an insight as to the mineral-mineral interactions involved in the leaching of sulfide minerals by bacteria.

HISTORICAL

Iron oxidation

The mechanism for Fe^{2+} oxidation in *T. ferrooxidans* remained elusive for many years until the discovery of a novel blue copper protein, rusticyanin, which was found to undergo reduction during the oxidation of Fe^{2+} with O_2 (16). Rusticyanin was found to oxidize Fe^{2+} and transfer the electrons to cytochrome-*c*. Even though it was a small protein (molecular weight = 16300), containing only one Cu atom, it was present in high concentrations (up to 5% of the cell protein) and was located in the periplasmic space (17). From this information a model for the oxidation of Fe^{2+} by *T. ferrooxidans* was proposed in which Fe^{2+} was oxidized to Fe^{3+} outside the cell membrane by rusticyanin (33). Only the electrons would be transferred to the inside of the cell by cytochrome-*c* to cytochrome oxidase where water would be formed from O_2 and H^+:

OUTSIDE: $Fe^{2+} \rightarrow Fe^{3+} + e-$

INSIDE: $2e- + \frac{1}{2}O_2 + 2H^+ \rightarrow H_2O$

The model was very attractive because it stipulated that the extracellular oxidation of Fe^{2+} was coupled to the generation of a transmembrane proton electrochemical potential, $\Delta\mu_{H^+}$ (31). This potential could be explained by the separation of the primary (Fe^{2+}/Fe^{3+}) and terminal (O_2/H_2O) reactions by the coupling membrane. At the same time, the internal consumption of H^+ would explain how the cell maintains an internal pH that is close to neutrality.

The only problem with the model was that the kinetics of the Fe^{2+}-rusticyanin reaction were orders of magnitude slower than those required

in bacterial iron oxidation (10, 67). This was explained by the stipulation that the true substrate of rusticyanin was not aqueous Fe^{2+} but Fe^{2+} complexed to a polynuclear Fe^{3+} complex. *T. ferrooxidans* contains a ferric iron complex coat on its cell surface that behaves as a system of Fe^{3+} ions strongly interacting with each other through dipole interactions and exchange coupling (31, 32). Thus it was proposed that Fe^{2+} could be oxidized at the outer cell wall by a bound Fe^{3+} ion, the resulting equivalent rapidly moving through the polynuclear Fe^{3+} coat to rusticyanin at the periplasmic surface (31).

Another explanation may be that rusticyanin is not the primary Fe^{2+} oxidant at all; recently, an enzyme has been purified which directly oxidizes Fe^{2+} and reduces cytochrome *c*-552. This enzyme, Fe^{2+}-cytochrome *c*-oxidoreductase, is a periplasmic enzyme with a molecular weight of 63000 and reduces rusticyanin only in the presence of cytochrome-*c* (25). Kinetic studies have not yet been carried out on this new enzyme so it is not clear whether it, or rusticyanin is the true Fe^{2+} oxidant in iron oxidation.

Sulfur oxidation

Sulfur oxidation in *T. ferrooxidans* was thought to occur by a similar mechanism as in other thiobacilli until it was discovered that *T. ferrooxidans* cells could oxidize sulfur using Fe^{3+} as the electron acceptor, instead of O_2 (66). Under anaerobic conditions, *T. ferrooxidans* reduced Fe^{3+} stoichiometrically with elemental sulfur, producing 6 moles of Fe^{2+} and 1 mole of SO_4^{2-} from 6 moles Fe^{3+} and 1 mole of elemental sulfur. When O_2 was supplied, the Fe^{2+} produced was immediately reoxidized by iron oxidase with a stoichiometric consumption of 1.5 moles O_2 per 6

moles Fe^{2+} oxidized (66).

The enzyme responsible was found to be a 46000 molecular weight dimer composed of two identical subunits of 23000 daltons each and was denoted as sulfur-ferric iron oxidoreductase (65). The enzyme reduced 4 moles of Fe^{3+} with 1 mole of elemental sulfur under anaerobic conditions to give 4 moles of Fe^{2+} and 1 mole of SO_3^{2-}. Glutathione was required for the reaction, probably to open up the sulfur ring and provide a GSH-sulfur open-ended molecule for the enzyme to attack (69). A new sulfite oxidase enzyme was also discovered which oxidized sulfite to sulfate, utilizing Fe^{3+} as the electron acceptor in anaerobic conditions (63). The sulfur-ferric iron oxidoreductase enzyme was localized in the periplasm while the new sulfite oxidase was localized in the plasma membrane (63, 65).

The model for ferric iron-mediated sulfur oxidation was established as a cyclical process:

$S^o + 3H_2O + 4Fe^{3+} \rightarrow SO_3^{2-} + 6H^+ + 4Fe^{2+}$	SFORase
$SO_3^{2-} + H_2O + 2Fe^{3+} \rightarrow SO_4^{2-} + 2H^+ + 2Fe^{2+}$	chemical/sulfite oxidase
$6Fe^{2+} + 1\frac{1}{2}O_2 + 6H^+ \rightarrow 6Fe^{3+} + 3H_2O$	iron oxidase
$S^o + 1\frac{1}{2}O_2 + H_2O \rightarrow SO_4^{2-} + 2H^+$	overall

The periplasmic sulfur-ferric iron oxidoreductase (SFORase) reduces Fe^{3+} with elemental sulfur to give Fe^{2+} and sulfite. The sulfite can be chemically or enzymatically oxidized by Fe^{3+} to give Fe^{2+} and sulfate. The resulting Fe^{2+} produced can then be oxidized by the iron oxidase system to provide energy for the cell. The overall reaction is indistinguishable from the classical oxygen-mediated sulfur oxidation by other thiobacilli (54). *T. ferrooxidans* growing on sulfur retained the activities of both the ferric iron reducing system and the iron oxidase system, suggesting

that even when growing on sulfur the bacterium is actually relying upon iron oxidation for its energy requirements (64).

Sulfur oxidation in *T. thiooxidans* has not been defined and several methods of oxidation have been postulated (29, 54). An extracellular mechanism has been proposed in which the electrons derived from sulfur oxidation enter the cell through the inner membrane, leaving H^+ and HSO_3^- outside (15). A similar reaction would also take place in the oxidation of sulfite:

OUTSIDE: $S^o + 3H_2O \rightarrow HSO_3^- + 5H^+ + 4e-$

$HSO_3^- + H_2O \rightarrow HSO_4^- + 2H^+ + 2e-$

INSIDE: $1\frac{1}{2}O_2 + 6H^+ + 6e- \rightarrow H_2O$

OVERALL: $S^o + 1\frac{1}{2}O_2 + H_2O \rightarrow HSO_4^- + H^+$

If this were true, then the protons produced by sulfur oxidation could be released outside the cell while cytochrome oxidase would use the electrons to consume H^+ within the cell to maintain neutral cytoplasmic pH when protons enter the cell through the ATP synthetase (15). The proposed mechanism has received widespread support by many researchers (11, 27, 29).

A more classical mechanism for the oxidation of sulfur by *T. thiooxidans* involves a sulfur oxygenase whose role is to oxidize sulfur to sulfite, the key intermediate in the oxidation of sulfur to sulfate (70). This sulfur oxidizing enzyme has not yet been purified but has been found and partially characterized in other thiobacilli as well as *T. thiooxidans* (55). The role of elemental sulfur oxidation in *T. thiooxidans* can be perceived simply as a way for the cell to obtain sulfite for its energy requirements. This is because sulfite can be oxidized through the sulfite oxidase pathway which involves oxidative phosphorylation (54).

This pathway basically consists of channeling electrons through cytochrome-*c* to cytochrome oxidase:

$$SO_3^{2-} + 2\text{cyt-}c(ox) + H_2O \rightarrow SO_4^{2-} + 2\text{cyt-}c(red) + 2H^+$$

$$2\text{cyt-}c(red) + \tfrac{1}{2}O_2 + 2H^+ \rightarrow 2\text{cyt-}c(ox) + H_2O$$

Both sulfite oxidase and cytochrome oxidase have been found in *T. thiooxidans* (45). Sulfite oxidation has been localized in membrane fractions where sulfite can be oxidized with either O_2 or cytochrome-*c* (40). The mechanism of sulfite oxidation in *T. thiooxidans*, however, is still not clear since not as much research has been done as with other thiobacilli.

Pyrite oxidation

The oxidation of pyrite by *T. ferrooxidans* is thought to involve both a direct and an indirect process (9, 46). The direct process involves a bacterial attack on the pyrite surface while the indirect process is a chemical one, involving the attack of ferric iron upon pyrite. Neither of these processes is completely understood. The complete oxidation of pyrite by *T. ferrooxidans* can be described by the reaction (35):

$$2FeS_2 + 7\tfrac{1}{2}O_2 + H_2O \rightarrow Fe_2(SO_4)_3 + H_2SO_4$$

Time-dependent binding of *T. ferrooxidans* cells to pyrite has been reported (23), although the bulk of bacterial Fe^{2+} oxidizing activity has remained in suspension rather than attached. Indeed, it has been suggested that pyrite-bound *T. ferrooxidans* cells may be oxidizing sulfur primarily over iron, the cells preferentially binding at pyrite crystal dislocation sites where sulfur availability is several orders of magnitude higher than at other sites in the crystal (3). There is evidence to support this, as *T. ferrooxidans* has been observed to grow preferentially at sites of

crystal dislocation in both pyrite (7, 61) and sulfur prills (22).

Recent studies with attached *T. ferrooxidans* growing on sulfur prills show that not only is Fe^{2+} oxidizing activity not lost, but is also similar in both free and attached cells (21). These experiments have also shown that sulfur oxidation is not affected by Fe^{2+} and iron oxidation is not completely inhibited by sulfur, suggesting that the Fe^{2+} oxidizing activity of *T. ferrooxidans* in ore is equivalent to its total Fe^{2+} oxidizing activity. The newly proposed sulfur ferric iron oxidoreductase system (64, 66) could account for *T. ferrooxidans* being able to simultaneously oxidize the iron and sulfur moieties of pyrite. However, this alone does not clarify the role of free and attached cells with respect to sulfur and iron oxidizing activities.

The oxidation of pyrite by ferric iron, also known as "indirect leaching mechanism" (46) has been more extensively studied (44, 53). The proposed overall reaction is:

$$FeS_2 + 14Fe^{3+} + 8H_2O \rightarrow 15Fe^{2+} + 2SO_4^{2-} + 16H^+$$

The chemical attack of Fe^{3+} upon pyrite is thought to be an electrochemical one: the presence of Fe^{3+} during *T. ferrooxidans* oxidation maintains a high redox potential (Eh) of the liquid medium compared to the electrode potential (EP) of the pyrite. This potential difference has been denoted as the "driving force" of pyrite oxidation by *T. ferrooxidans* (35). A surface reaction has also been proposed in which a sequential attack by hydrated Fe^{3+} weakens the Fe-S bonds in the pyrite crystal, forming thiosulfate ($S_2O_3^{2-}$) which is further oxidized to sulfate (53).

There have been no significant studies of pyrite oxidation by *T. thiooxidans*. Because this bacterium is only able to oxidize the sulfide

moiety of pyrite, its mode of oxidation probably involves a direct bacterial attack (30), analogous to the oxidation of elemental sulfur. *T. thiooxidans* must come into contact with sulfur in order for the oxidation to occur (29); *T. thiooxidans* cells have been observed "attacking" sulfur particles (28). This attachment of cells to sulfur has also been shown to be energy-dependent (72). Studies have shown that sulfur oxidation by *T. thiooxidans* is facilitated by wetting agents or surfactants (1) which probably increase the force of adhesion between water and sulfur, facilitating contact. A possible wetting agent may be the lipid phosphatidylinositol which is produced by growing cultures of *T. thiooxidans* (58).

MATERIALS AND METHODS

Materials

All chemicals and reagents used were of reagent grade and obtained commercially. Elemental sulfur and ferric sulfate were obtained from British Drug Houses Ltd., Toronto. All soluble salts, including ferrous sulfate, were obtained from Fisher Scientific Co., Fairlawn, N.J., U.S.A. Sulfuric acid (concentrated, 96% by weight, 36 N) was also obtained from Fisher Scientific Co. The reagent *o*-phenanthroline was obtained from Sigma Chemical Co., St. Louis, Mo., U.S.A. All reagents and media were prepared using glass-distilled water.

Mineral samples

The mineral samples used in these experiments had been ground to -140 mesh (100 μm particle diameter by microscopic observation). Sphalerite and pyrite sample No. 1 had been kindly supplied to us by Dr. M. J. Osbourne from the Department of Geological Sciences. The No. 1 pyrite sample contained 45.0% Fe, 42.3% S, and 12.7% impurities. The sphalerite sample contained 63.5% Zn, 27.2% S, and 9.3% impurities. Chalcopyrite was obtained from Carolina Biological Supply Co., Burlington, N.C., U.S.A. and contained 22.1% Cu, 19.4% Fe, 27.6% S, and 30.9% impurities. Pyrite sample No. 2 had been supplied to us by the Mines Branch of Manitoba Energy and Mines. This pyrite sample contained 45.9% Fe, 45.1 S, and 9% impurities.

Organisms and growth conditions

Two *T. ferrooxidans* and one *T. thiooxidans* strains were used in this study. *T. ferrooxidans* strain SM-4 and *T. thiooxidans* strain SM-6 were

isolated from the Flin Flon mine as discussed in Part II. The *T. ferrooxidans* laboratory strain used was ATCC 19859.

The growth medium for *T. ferrooxidans* contained 0.1 g K_2HPO_4, 0.4 g $(NH_4)_2SO_4$, 0.4 g $MgSO_4 \cdot 7H_2O$ and 33.3 g $FeSO_4 \cdot 7H_2O$ per liter (49) and was adjusted to pH 2.3 with H_2SO_4. The ferrous sulfate solution was filter-sterilized separately and mixed with the autoclaved remaining components. Each culture batch of *T. ferrooxidans* was grown in six 1 L Erlenmeyer flasks containing 400 mL medium (10% inoculum) each at 25°C on a rotary shaker at 130 rpm. Cells were harvested at the late-log phase by centrifugation at 13000 x g for 10 minutes, after removal of insoluble ferric iron by filtration through Whatman No. 1 filter paper followed by low speed centrifugation (100 x g for 10 minutes). Cells were washed twice in medium without ferrous sulfate. Finally, a cell suspension was made to a concentration of 50 mg wet cells per mL in medium without ferrous sulfate.

T. thiooxidans SM-6 was grown in 2.7 L Fernbach flasks containing 1 L of the *T. ferrooxidans* medium without ferrous sulfate, hereafter refered to as HP medium (as discussed in Part II), plus 50 g powdered elemental sulfur sprinkled over the liquid surface. A 2.5% inoculum was used to grow the cells stationary for five days at 28°C. At this time, the cells were filtered through Whatman No. 1 filter paper to remove the sulfur. The cell suspension was washed in HP medium and resuspended in the same to a concentration of 50 mg wet cells per mL.

Methods

Preparation of heat-killed cells

For the preparation of cells with no Fe^{2+} oxidizing activity, 0.5 mL

of *T. ferrooxidans* SM-4 cell suspension was heated for 10 minutes at 80°C, the inactive dead cells washed with 10 mL of HP medium before resuspension in the original volume. For the preparation of cells with no sulfur oxidizing activity, 0.5 mL of *T. thiooxidans* SM-6 cell suspension was heated for 5 minutes at 100°C and used without washing.

Ferrous iron oxidizing activity

The rate of Fe^{2+} oxidation was determined by measuring the rate of O_2 consumption in a Gilson oxygraph with a Clarke electrode at 25°C. The reaction mixture was 1.2 mL, containing HP medium and microliter volumes of cell suspension (50 mg wet cells per mL) and 0.1 M $FeSO_4 \cdot 7H_2O$ at pH 2.3. In the inhibitor studies, Fe^{3+} was added in the form of 50 mM $Fe_2(SO_4)_3 \cdot 6H_2O$ in microliter volumes. The reaction was started with the addition of Fe^{2+} as substrate and the initial rate of O_2 consumption (nmol O_2 per minute) was taken as the reaction rate (v). The reaction rate was plotted against the concentration of Fe^{2+} in double reciprocal plots of Lineweaver and Burk (43).

Pyrite oxidizing activity

The rate of pyrite oxidation was determined by measuring the rate of O_2 consumption using standard manometric technique (79) in a Warburg manometer with 16 mL double-sidearm flasks (Brownhill Scientific Co.) at 30°C. The reaction mixture was 3.2 mL, containing HP medium and specified volumes of cell suspension (50 mg wet cells per mL of *T. ferrooxidans* or *T. thiooxidans*) and mg ammounts of No. 2 pyrite. The reaction mixtures were allowed to equilibrate for 20 minutes prior to the start of the reaction which was initiated by tipping the cells.

Sometimes the No. 2 pyrite was washed with HP medium prior to use.

This was done by stirring 10 g in 100 mL of medium for several hours at room temperature, followed by filtration (to remove liquid) and drying in a dessicator for several days. In this study, pyrite concentrations were expressed as % pulp density (PD), which is defined as:

$$PD = \frac{\text{weight of solid (g)}}{\text{total liquid volume (mL)}} \times 100$$

The linear rate of O_2 consumption (μM O_2 per minute) was taken as the reaction rate (v). The reaction rate was plotted against the PD in double reciprocal plots of Lineweaver and Burk (43).

Spontaneous pyrite dissolution assay

The spontaneous dissolution of washed No. 2 pyrite was monitored using a modification of the *o*-phenanthroline method (4). Pyrite was shaken in HP medium for several hours. The liquid was removed by decantation after centrifugation of the pyrite slurry at 13000 x g for 10 minutes. The washed pyrite was then resuspended in fresh HP medium for the start of the experiment. The pyrite slurries were shaken in a 30°C water bath in a manner analogous to the conditions in a Warburg apparatus (reciprocal shaking). Various time samples of liquid (50 μL) were taken, diluted in HP medium, and centrifuged to remove pyrite particles. One mL aliquots of supernatant were mixed with one mL of 0.1% *o*-phenanthroline solution and assayed for soluble Fe^{2+} at 500 nm in a Hewlett-Packard Diode Array Spectrophotometer 8452A. The reaction was carried out for one hour.

Assay of indirect leaching by ferric iron

Ferric iron-mediated Fe^{2+} solubilization from No. 2 pyrite was also monitored using the modified *o*-phenanthroline method (4). Pyrite was washed as with the spontaneous dissolution experiments and resuspended in HP medium containing specified ammounts of Fe^{3+} in the form of $Fe_2(SO_4)_3$•

$6H_2O$. The pyrite-Fe^{3+} slurries were shaken reciprocally in a 30°C water bath as with the spontaneous dissolution experiments. Time samples of liquid (50 µL) were taken, diluted in HP medium, and centrifuged. One mL aliquots of supernatant were mixed with one mL of 0.1% *o*-phenanthroline and assayed for soluble Fe^{2+} at 500 nm. The reaction was carried out for one hour.

Shake-flask leaching experiments

The experiments were carried out in 250 mL Erlenmeyer flasks containing 90 mL of HP medium plus 10 mL inoculum of *T. ferrooxidans* or *T. thiooxidans* or both and 5 g of sulfide mineral sample. The flasks were incubated at 25°C on a rotary shaker at 150 rpm for several days. When the sulfide mineral was leached in the presence of pyrite, 5 g of mineral sample plus 5 g of No. 1 or No. 2 pyrite were used. Periodically, 4 mL samples of slurry were collected aseptically and frozen in order to halt bacterial activity. The samples were thawed, filtered through Whatman No. 1 filter paper, and centrifuged at 13000 x g for 10 minutes. The clear samples were then analyzed for Cu, Zn, and Fe by atomic absorption spectrophotometry at the Manitoba Provincial Soil Testing Laboratory.

Washing of pyrite with HCl

The No. 1 and No. 2 pyrites were washed with 3 N HCl. Washing consisted of stirring 50 mL of a 10% slurry (5 g in 50 mL) in 3 N HCl with a magnetically-driven stirring bar overnight at room temperature. After washing the samples were again washed with distilled water under suction filtration through a Whatman No. 1 filter paper three times. The samples were then dried for 48 hours in a dessicator with $CaCl_2$ under vacuum.

Oxidation of mineral samples

Oxidation of mineral samples by resting cells was monitored by measuring the steady-state rate of O_2 consumption in a Warburg manometer (79). The reaction mixture was 3.2 mL, containing HP medium and 0.2 mL of cell suspension (50 mg wet cells per mL of *T. ferrooxidans* or *T. thiooxidans*) and 100 mg of sulfide mineral. The reaction was allowed to equilibrate for 20 minutes prior to the start of the reaction which was initiated by tipping the cells and sulfide mineral. When the sulfide mineral was oxidized in the presence of pyrite, the pyrite (No. 1 or No. 2) was always present as part of the reaction mixture while the other mineral sample was tipped from the sidearm. The reaction was allowed to proceed for several hours before the steady-state rate was monitored for 2 hours. At the end of the experiment, The reaction mixture was collected and processed for atomic absorption analysis (see shake-flask sampling).

RESULTS

Iron oxidation kinetics

Cell-cell competitive inhibition

At fixed concentrations of cells, the rates of Fe^{2+} oxidation (nmol O_2 per minute) of both *T. ferrooxidans* strains increased with increasing $[Fe^{2+}]$ following typical saturation kinetics and giving linear double reciprocal plots. When the Fe^{2+} oxidation rate was determined at varying concentrations of cells, however, the results with the mine isolate SM-4 were anomalous and different from the laboratory strain ATCC 19859.

The double reciprocal plots at varying SM-4 cell concentrations (Fig. 1) showed a family of lines which intersected at different points on the X-axis, the K_m value appearing to increase with increasing cell concentration. When the reaction rate was converted to the specific activity of Fe^{2+} oxidation (nmol O_2 per minute per mg wet cells, or v_{sp}) and plotted again in a double reciprocal manner against $[Fe^{2+}]$ (Fig. 2), a family of lines now intersected the Y-axis at the same point, characteristic of a typical competitive inhibition. Thus, the Fe^{2+} oxidizing activity of a unit cell (or enzyme system) was competitively inhibited by other cells with respect to $[Fe^{2+}]$.

The laboratory strain ATCC 19859, on the other hand, showed no anomalous results in its double reciprocal plots at varying cell concentrations (Fig. 3). A family of lines converged on the same point on the X-axis, the K_m value not changing with cell concentration.

A more direct demonstration of a competitive inhibition by cells was accomplished by carrying out the experiments in the presence of heat-

Figure 1. Effect of Fe^{2+} concentration on the Fe^{2+} oxidizing activity of various concentrations of SM-4. The O_2 consumption rate (v) was determined as nmol O_2 per minute at 25°C at various Fe^{2+} concentrations.

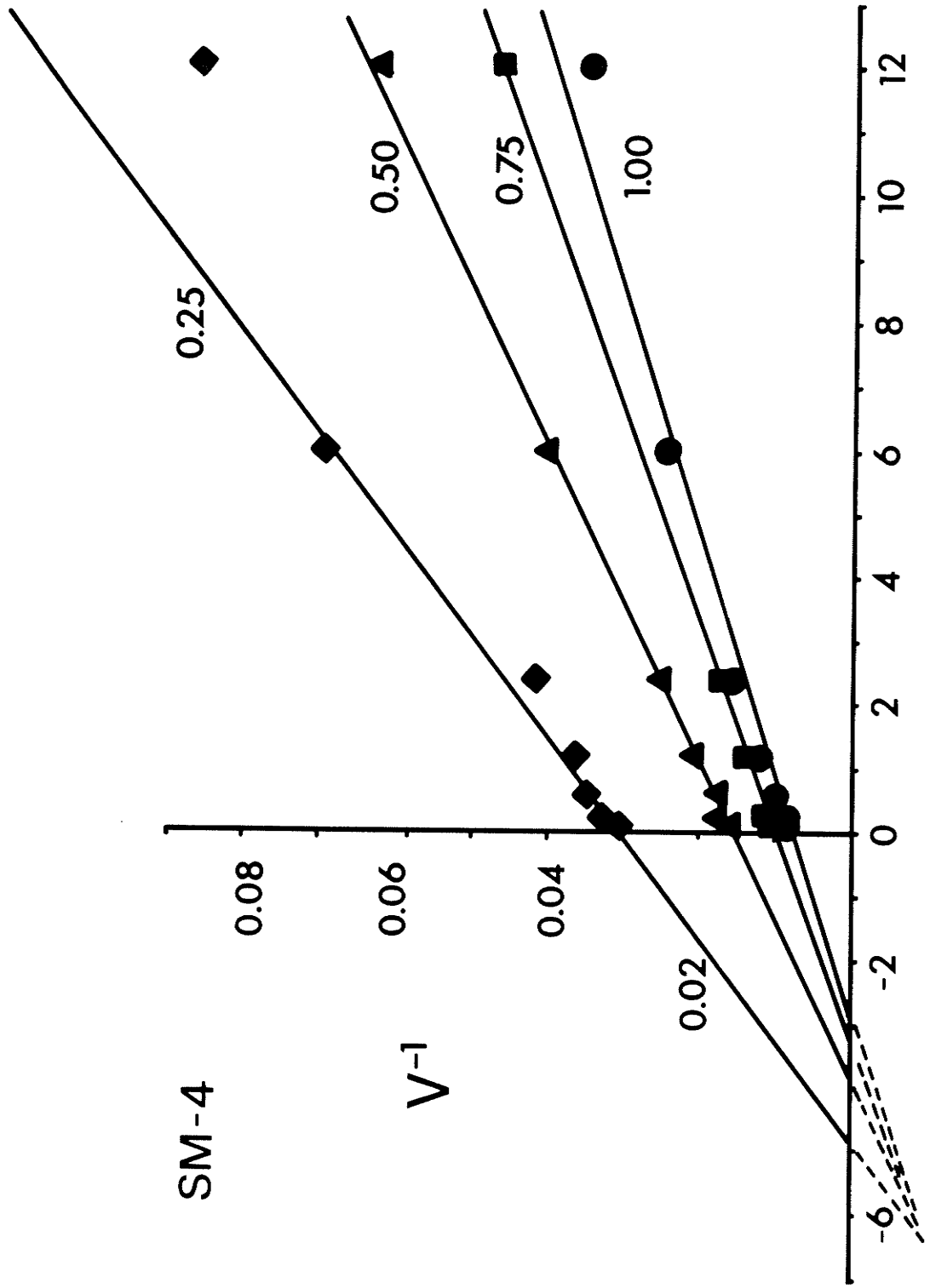
SM-4
V^{-1}
0.08
0.06
0.04
0.02
0.25
0.50
0.75
1.00
-6
-2
0
2
4
6
8
10
12
$[Fe^{2+}]^{-1}$ mM^{-1}

Figure 2. Competitive inhibition of Fe^{2+} oxidizing activity of SM-4 cells by increasing concentrations of cells. The specific activity (v_{sp}) was calculated from the data in Fig. 1 as nmol O_2 per minute per mg wet cells. The insert is a replot of the slopes to obtain the K_i' value in mg wet cells per mL.

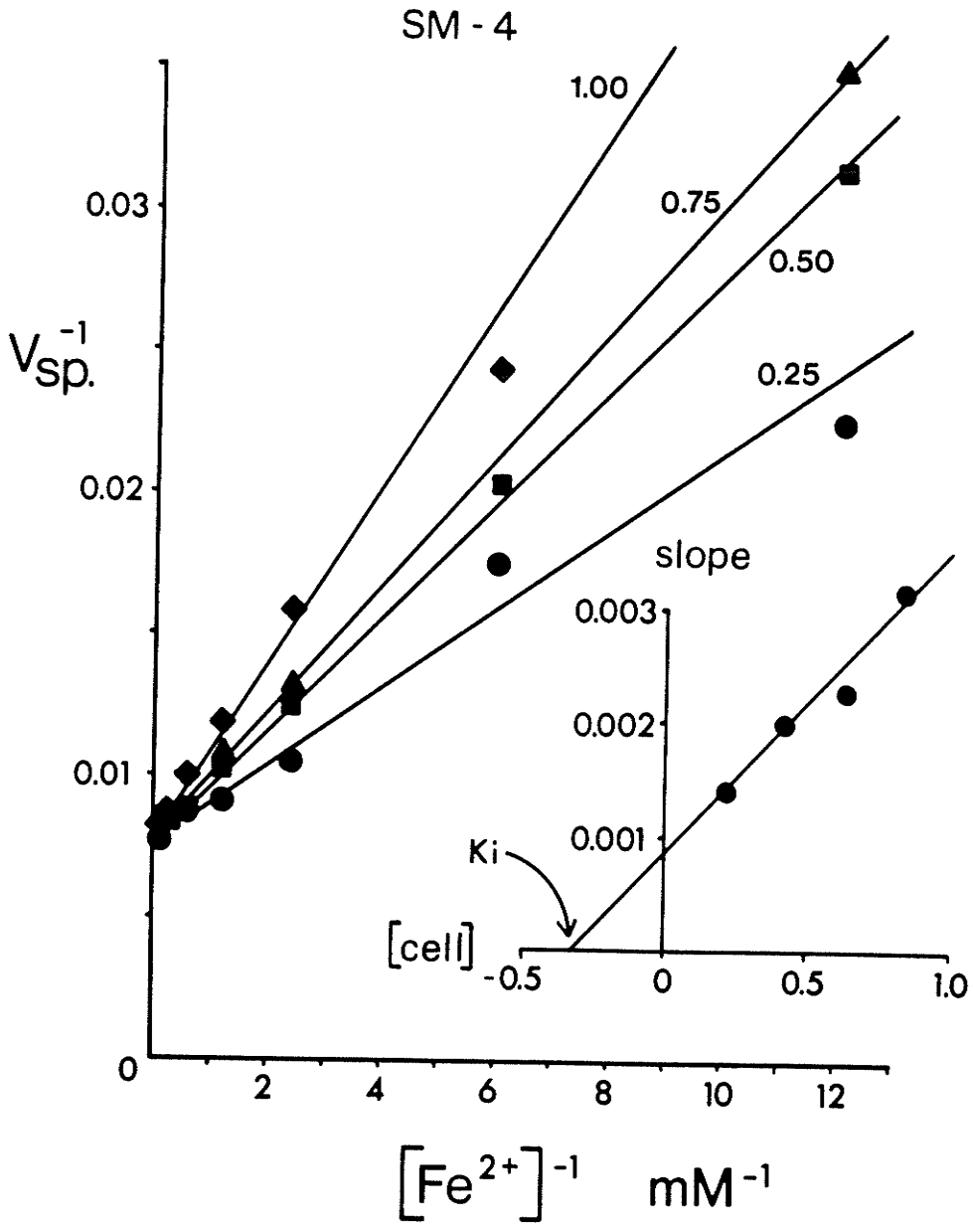
SM - 4
1.00
0.75
0.50
0.25
0.03
0.02
0.01
0
$V_{sp.}^{-1}$
slope
0.003
0.002
0.001
Ki
[cell]
-0.5
0
0.5
1.0
2
4
6
8
10
12
$[Fe^{2+}]^{-1}$ mM^{-1}

Figure 3. Effect of Fe^{2+} concentration on the Fe^{2+} oxidizing activity of various concentrations of ATCC 19859. Experimental conditions were the same as those described in the legend to Fig. 1.

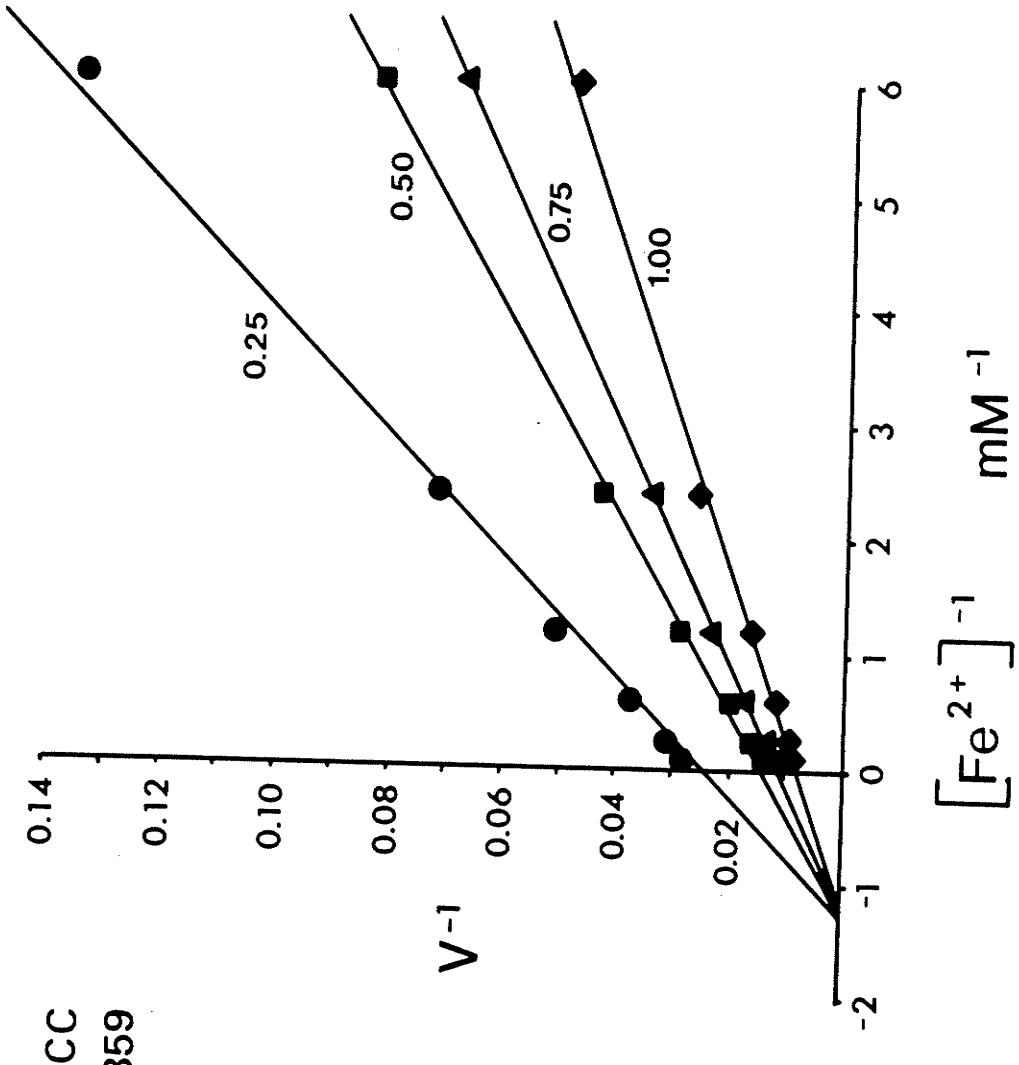
ATCC
19859
0.25
0.50
0.75
1.00
0.14
0.12
0.10
0.08
0.06
0.04
0.02
V^{-1}
-2
-1
0
1
2
3
4
5
6
$[Fe^{2+}]^{-1}$ mM $^{-1}$

inactivated SM-4 cells. As shown in Figure 4, these inactivated dead cells inhibited the Fe^{2+} oxidation by active SM-4 cells competitively with respect to $[Fe^{2+}]$. The extent of inhibition was lower than with live cells, probably due to the effect of heat treatment.

The experimental results can be explained as follows.

If each *T. ferrooxidans* cell (C) has *m* number of an enzyme system (E) capable of oxidizing Fe^{2+} (S) to Fe^{3+} (P) with oxygen, the rate of O_2 consumption (v) is expressed:

$$E + S \underset{k_2}{\overset{k_1}{\rightleftarrows}} ES \xrightarrow{k_3} E + P + O_2 \text{ consumption}$$

$$\text{and } v = \frac{k_3[E][S]}{[S] + K_m} = \frac{mk_3[C][S]}{[S] + K_m} \qquad \text{where } K_m = \frac{k_2 + k_3}{k_1}$$

If each cell also acts as a competitive inhibitor of another cell with respect to Fe^{2+}:

$$E + I \underset{k_5}{\overset{k_4}{\rightleftarrows}} EI \qquad \text{and } [I] = n[C]$$

$$\text{then } v = \frac{k_3[E][S]}{[S] + K_m(1 + I/K_i)} = \frac{mk_3[C][S]}{[S] + K_m(1 + n[C]/K_i)}$$

where K_i is the inhibitor constant k_5/k_4.

If we make $mk_3 = k_3'$ and $K_i/n = K_i'$, then the rate equation becomes

$$v = \frac{k_3[C][S]}{[S] + K_m(1 + [C]/K_i')}$$

and in the double reciprocal form:

$$\frac{1}{v} = \frac{1}{k_3'[C]} + \frac{K_m}{k_3'[C]}\left(1 + \frac{[C]}{K_i'}\right)\left(\frac{1}{[S]}\right)$$

The plots of 1/v versus 1/[S] will show a family of lines at

Figure 4. Competitive inhibition of Fe^{2+} oxidizing activity of SM-4 cells by heat-inactivated cells. Experimental conditions were the same as those described in the legend to Fig. 1, except that the amount of active SM-4 cells used was 0.25 mg. Where indicated, heat-inactivated dead cells were present at 1 or 2.5 mg in the reaction mixture.

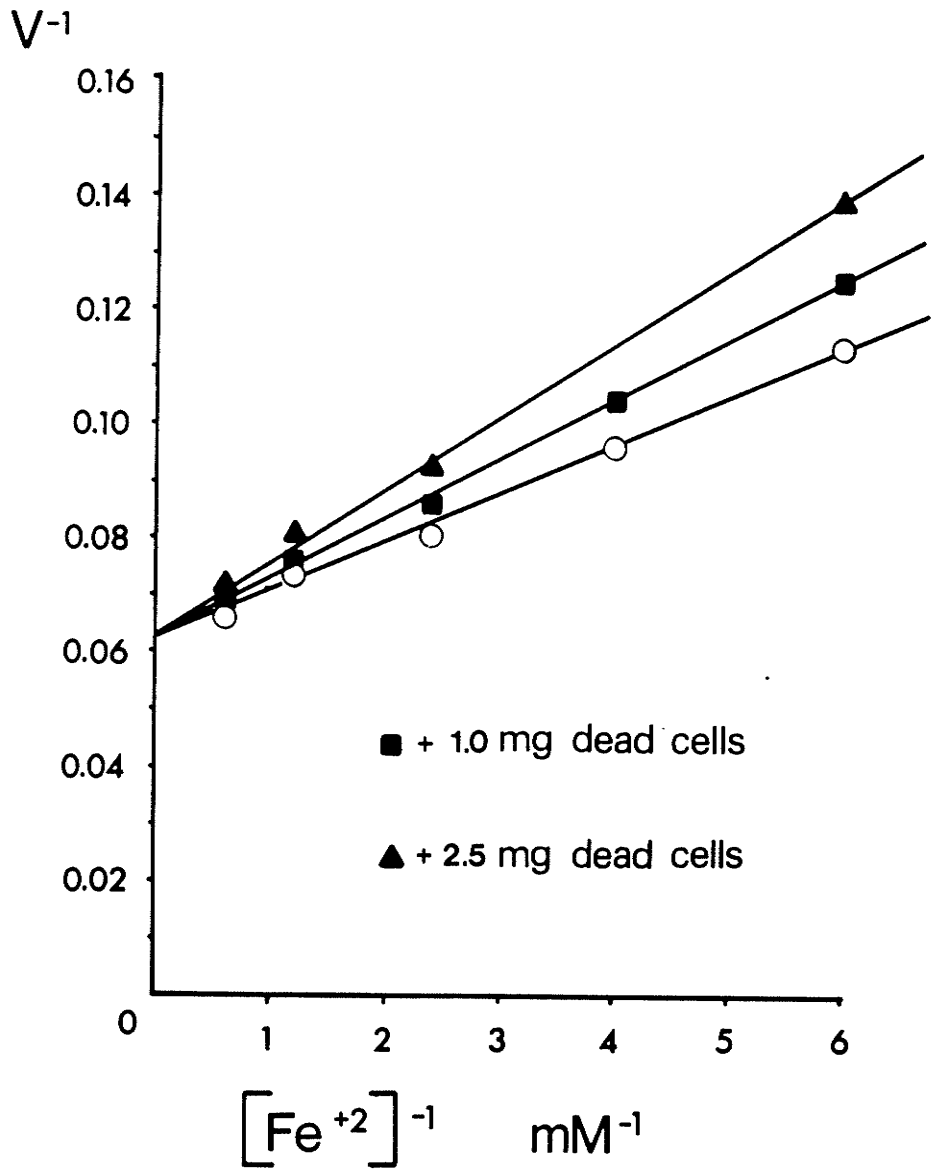
V-1
0.16
0.14
0.12
0.10
0.08
0.06
0.04
0.02
0
1
2
3
4
5
6
■ + 1.0 mg dead cells
▲ + 2.5 mg dead cells
[Fe+2]-1 mM-1

different cell concentrations with Y-intercepts at $1/k_3[C]0$ and X-intercepts at $-1/\{K_m(1 + [C]/K_i')\}$ (see Fig. 1). The maximal reaction rate (V_{max}) would be equivalent to $k_3'[C]$.

If the observed reaction rate, v, is converted to the specific activity, v_{sp}, by dividing v by the cell concentration, [C], the equation obtained is

$$v_{sp} = \frac{k_3'[S]}{[S] + K_m(1 + [C]/K_i')}$$

and in the reciprocal form

$$\frac{1}{v_{sp}} = \frac{1}{k_3'} + \frac{K_m}{k_3'}(1 + \frac{[C]}{K_i'})(\frac{1}{[S]})$$

Now the plots of $1/v_{sp}$ versus $1/[S]$ at different cell concentrations will show a family of lines converging on the Y-axis at $1/k_3'$ with changing slopes corresponding to $(K_m/k_3')(1 + [C]/K_i')$ (Fig. 2). The slope replots against [C] will give a straight line intersecting the Y-axis at (K_m/k_3') and the X-axis at $(-K_i')$ (inset, Figure 2).

The rate and kinetic constants obtained for the two *T. ferrooxidans* strains are listed in Table 1. The rate constant k_3 is similar for both strains. The Fe^{2+} K_m value for ATCC 19859 is not affected by the cell concentration, while the K_m value for SM-4 is a minimum value which increases with increasing cell concentration. The K_i' value is the cell concentration which doubles the experimental K_m value.

Synergistic inhibition by cells and ferric iron

The oxidation of Fe^{2+} by *T. ferrooxidans* SM-4 cells was competitively inhibited by Fe^{3+} at three fixed concentrations of cells (0.25, 0.50, and 1.00 mg wet cells per 1.2 mL) as shown in the double reciprocal plots in Figure 5. The replot of slopes against the Fe^{3+} concentrations (Fig. 6)

TABLE 1. Rate and kinetic constants for Fe^{2+} oxidation (I)

Strains	k_3' nmol O_2 per minute per mg wet cells per mL	K_m mM Fe^{2+}	K_i' mg wet cells per mL
ATCC 19859	143	0.08	-
SM-4	125	0.11	0.33

Figure 5. Competitive inhibition of Fe^{2+} oxidizing activity of *T. ferrooxidans* SM-4 cells by Fe^{3+} at three fixed concentrations of cells: 0.25 (A); 0.50 (B); and 1.00 (C) mg wet cells in 1.2 mL reaction volume. The concentrations of inhibiting Fe^{3+} were 0, 2, 8, and 16 mM as indicated. Experimental conditions were the same as those described in Figure 1.

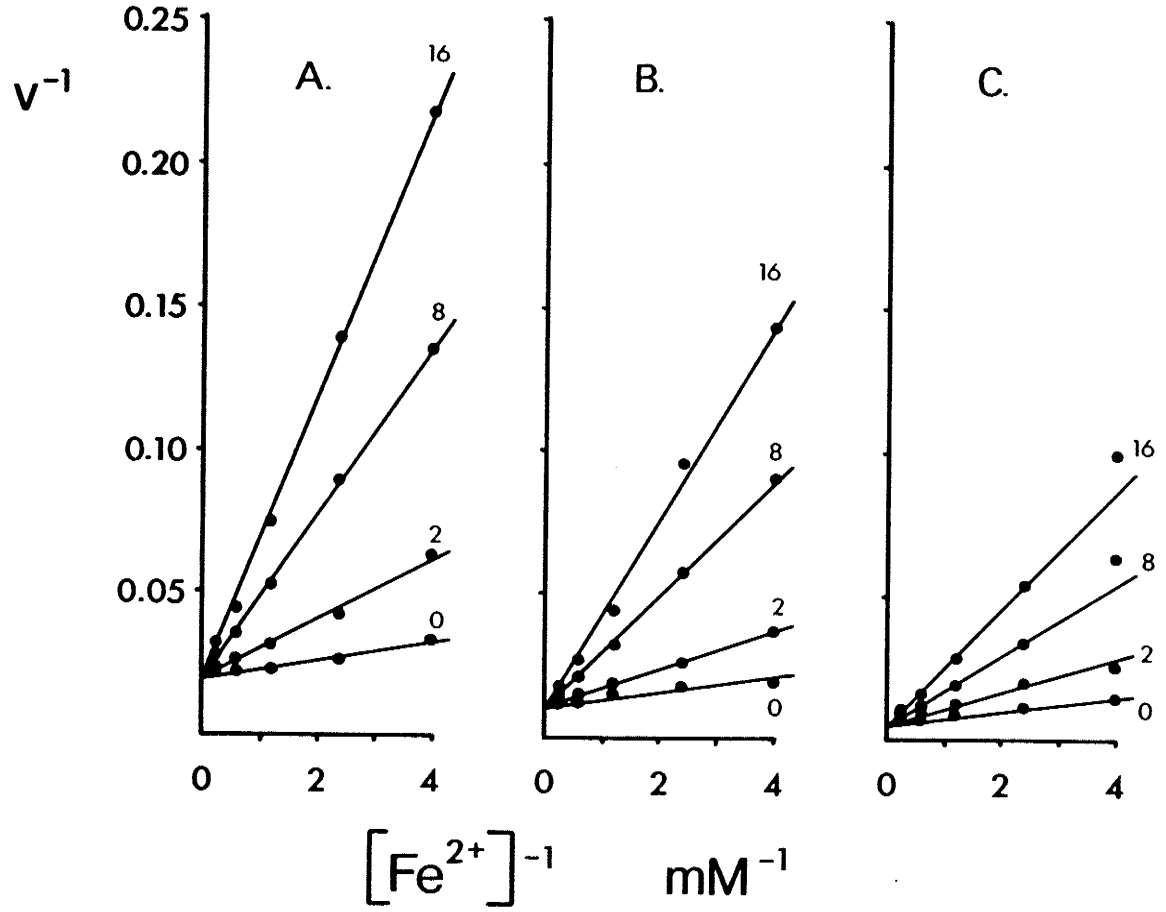
V^{-1}
0.25
0.20
0.15
0.10
0.05
A.
B.
C.
16
8
2
0
0
2
4
$[Fe^{2+}]^{-1}$ mM^{-1}

Figure 6. Replots of slopes from Figure 5 against Fe^{3+} concentration. The three lines correspond to the three fixed cell concentrations used, indicated here in mg amounts. The inset is a secondary replot of the slope versus the increase of cell concentration in (mg wet cell per mL)$^{-1}$. The line has a slope equivalent to $K_m/(k_3' K_{if})$ and a Y-intercept equivalent to $K_m/(k_3' K_i' K_{if})$.

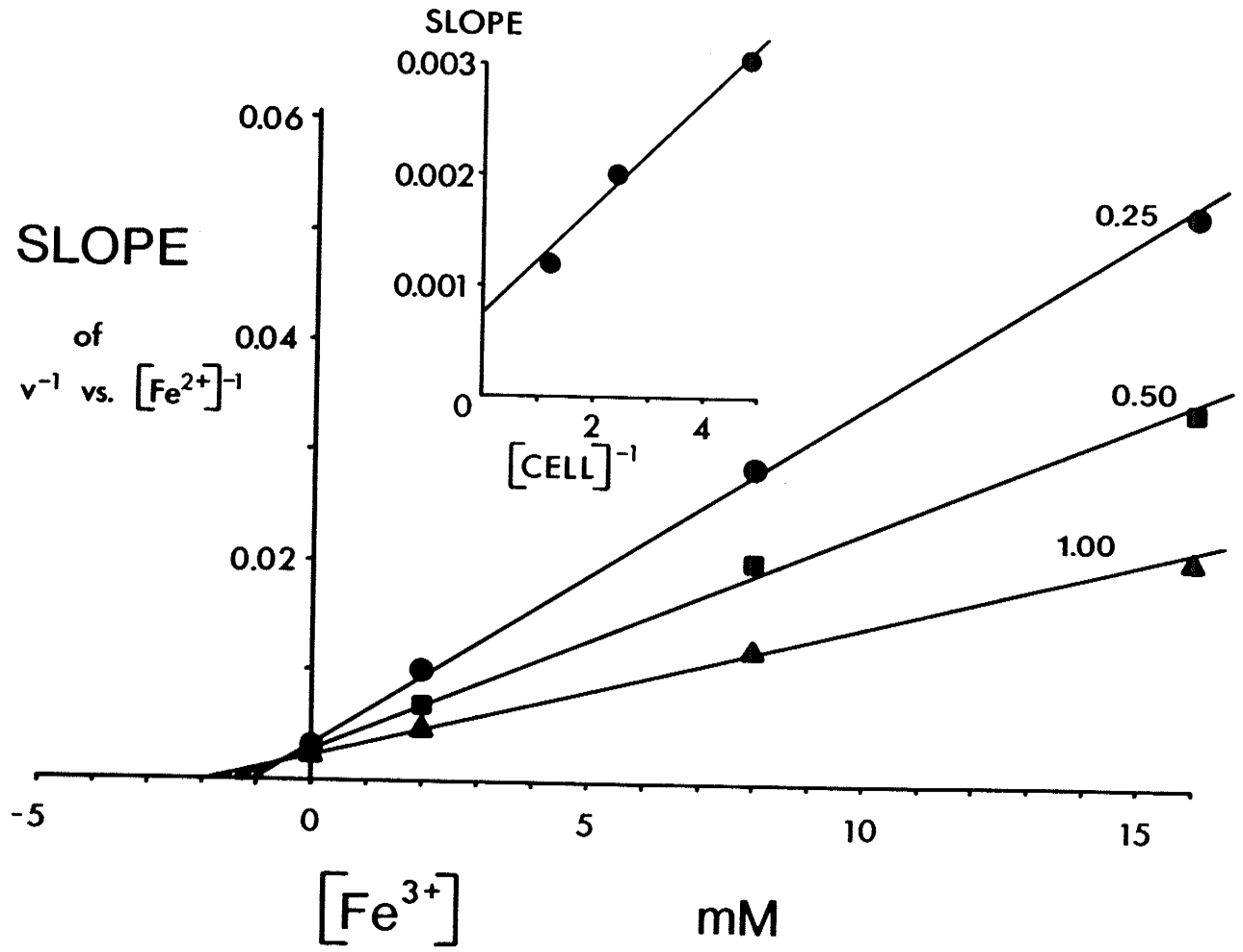
SLOPE
0.003
0.002
0.001
0
2
4
[CELL]$^{-1}$
SLOPE
of
v^{-1} vs. $[Fe^{2+}]^{-1}$
0.06
0.04
0.02
0.25
0.50
1.00
-5
0
5
10
15
$[Fe^{3+}]$
mM

indicated that increasing cell concentrations lowered both the slopes and Y-intercepts, but increased the values of the apparent inhibition constants for Fe^{3+} (the positive values of X-intercepts). The secondary replot of slope change from Figure 6 showed that the slope increased with the reciprocal of cell concentration (Figure 6 inset).

When the data were plotted at fixed Fe^{3+} concentrations (0, 2, 8, and 16 mM Fe^{3+}), the patterns in Figure 7 were obtained where increasing cell concentrations lowered both the Y-intercepts and slopes, and characteristically increased the apparent K_m values, similar to the previous results. If the reaction rate, v, was converted to the specific activity, v_{sp}, and plotted in a double reciprocal manner against the Fe^{2+} concentration, the resulting plots (Fig. 8) showed the competitive inhibition by increasing concentrations of cells at the four fixed Fe^{3+} concentrations of 0 - 16 mM. The replot of slope against cell concentration (Fig. 9) indicated a stronger inhibition by cells at higher Fe^{3+} concentrations.

These results can be explained if Fe^{3+} and cells both compete with Fe^{2+} for the Fe^{2+} oxidation sites of cells and the binding of one inhibitor (Fe^{3+} or cell) does not exclude the binding of the other (cell or Fe^{3+}) but only inhibits it.

The inhibition of an enzyme (E) by two competitive inhibitors (I and X) with respect to the substrate (S) in the formation of product (P) has been discussed by Segel (59) and can be expressed by the reactions:

$$E + S \underset{k_2}{\overset{k_1}{\rightleftarrows}} ES \xrightarrow{k_3} E + P, \qquad \text{where } K_m = \frac{k_2 + k_3}{k_1}$$

$$E + I \underset{k_5}{\overset{k_4}{\rightleftarrows}} EI, \qquad \text{where } K_i = \frac{k_5}{k_4}$$

$$E + X \underset{k_7}{\overset{k_6}{\rightleftarrows}} EX, \qquad \text{where } K_x = \frac{k_7}{k_6}$$

and in additon, $EI + X \underset{k_9}{\overset{k_8}{\rightleftarrows}} EIX$ and $EX + I \underset{k_{11}}{\overset{k_{10}}{\rightleftarrows}} EIX$

The formation of EIX distinguishes the synergistic system from the inhibition by mutually exclusive inhibitors. The rate equation derived for this system (59) can be expressed as:

$$v = \frac{k_3[E][S]}{[S] + K_s(1 + [I]/K_i + [X]/K_x + [I][X]/\alpha K_i K_x)}$$

where v is the reaction rate; [E], [S], [I], and [X] are concentrations of E, S, I, and X; K_i and K_x are inhibitor constants for I and X; K_s is the dissociation constant for ES (k_2/k_1) and is the same as K_m, the Michaelis constant, when $k_2 >> k_3$. When binding of one inhibitor does not affect the binding of the other, $\alpha = 1$, $K_i = k_5/k_4 = k_{11}/k_{10}$, and $K_x = k_4/k_6 = k_9/k_8$.

Remembering the previously derived rate equation for the competitive inhibition of *T. ferrooxidans* Fe^{2+} oxidation by increasing concentrations of cells:

$$v = \frac{k_3'[C][Fe^{2+}]}{[Fe^{2+}] + K_m(1 + [C]/K_i')}$$

where [C] is the concentration of cells, k_3' is k_3 times the number of enzymes per cell, $[Fe^{2+}]$ is the concentration of Fe^{2+}, and K_i' is K_i divided by the number of inhibitors per cell.

Figure 7. Effect of Fe^{2+} concentration on the Fe^{2+} oxidizing activity of various concentrations of cells at four fixed concentrations of Fe^{3+}: A, 0; B, 2; C, 8; D, 16 mM. The concentrations of cells used were (as indicated) 0.25, 0.50, and 1.00 mg wet cells in 1.2 mL reaction volume. The data shown are the same as in Figure 5.

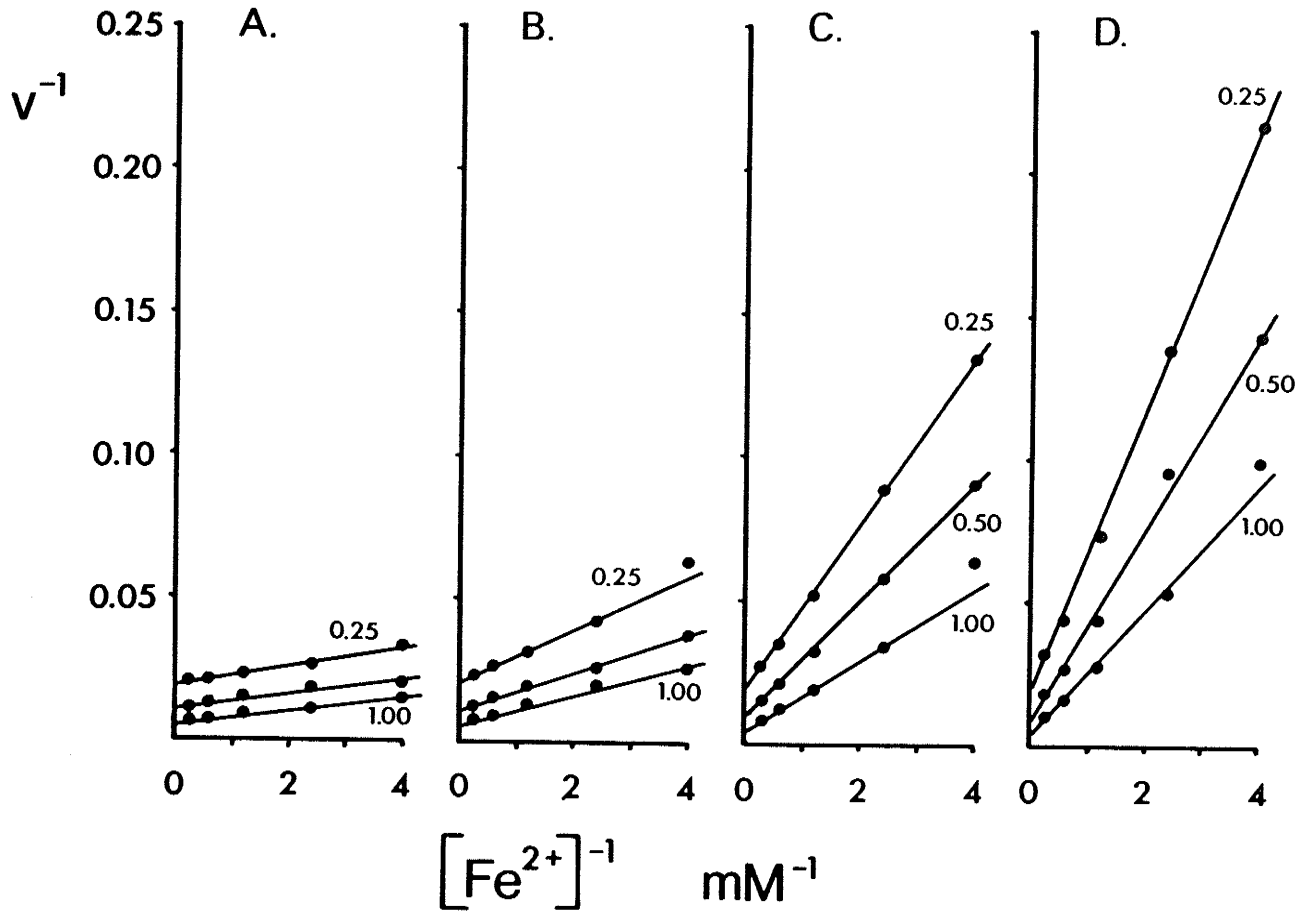
A.
B.
C.
D.
v^{-1}
0.25
0.20
0.15
0.10
0.05
0.25
1.00
0.25
1.00
0.25
0.50
1.00
0.25
0.50
1.00
0
2
4
$[Fe^{2+}]^{-1}$ mM^{-1}

Figure 8. Competitive inhibition of Fe^{2+} oxidizing activity of SM-4 cells by increasing concentrations of cells at four fixed Fe^{3+} concentrations: A, 0; B, 2; C, 8;, D, 16 mM. The specific activity (v_{sp}) was calculated from the data in Figure 7 as nmol O_2 per minute per mg wet cells. The concentrations of cells used were (as indicated) 0.25, 0.50, and 1.00 mg wet cells in 1.2 mL reaction volume.

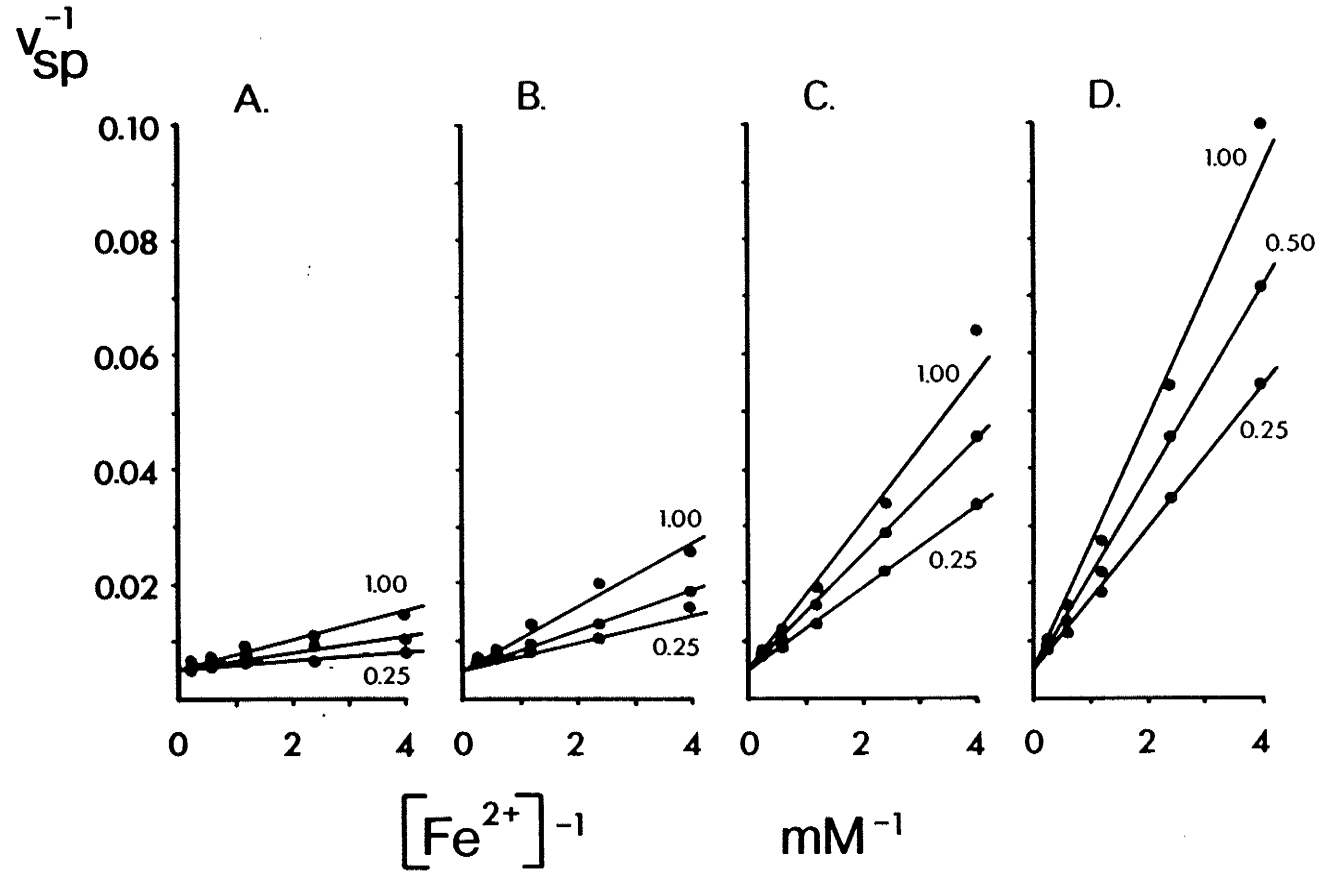
v_{sp}^{-1}
A.
B.
C.
D.
0.10
0.08
0.06
0.04
0.02
1.00
0.25
0.50
0
2
4
$[Fe^{2+}]^{-1}$
mM^{-1}

Figure 9. Replot of slopes from Figure 8 against cell concentration. The four lines correspond to the four Fe^{3+} concentrations used, indicated in mM. The top inset is a secondary replot of the slope versus the Fe^{3+} concentration in mM. The line has a slope equivalent to $K_m/(k_3' K_i' K_{if})$ and a Y-intercept equivalent to $K_m/(k_3' K_i')$. The bottom inset is a replot of the Y-intercept versus the Fe^{3+} concentration in mM. The line has a slope equivalent to $K_m/(k_3' K_{if})$ and a Y-intercept equivalent to K_m/k_3'.

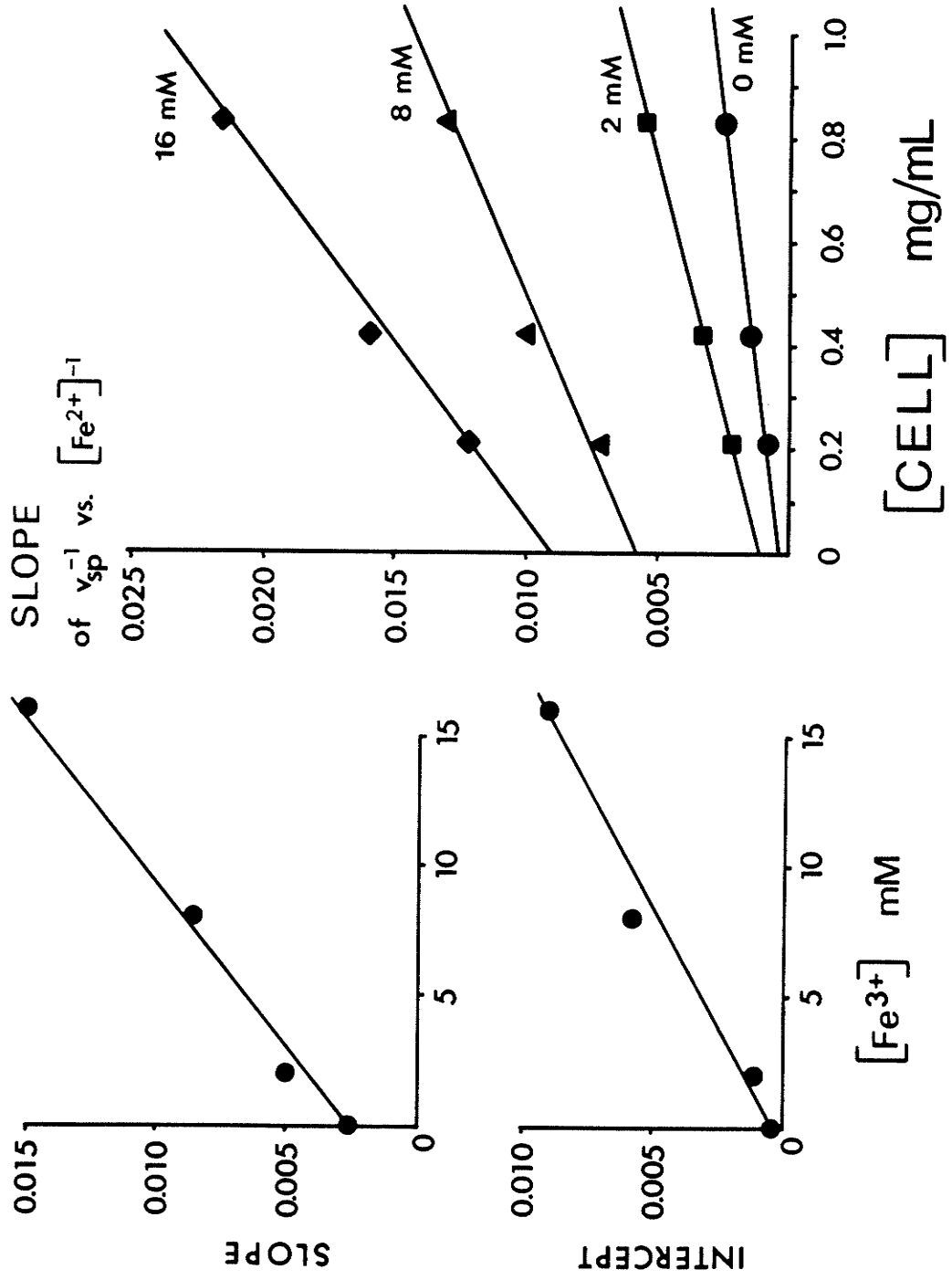
SLOPE
of v_{sp}^{-1} vs. $[Fe^{2+}]^{-1}$
16 mM
8 mM
2 mM
0 mM
0.025
0.020
0.015
0.010
0.005
0
0.2
0.4
0.6
0.8
1.0
[CELL] mg/mL
SLOPE
INTERCEPT
0.015
0.010
0.005
0.010
0.005
0
5
10
15
$[Fe^{3+}]$ mM

In the presence of Fe^{3+} as the second competitive inhibitor, the rate equation becomes:

$$v = \frac{k_3'[C][Fe^{2+}]}{[Fe^{2+}] + K_m(1 + [C]/K_i' + [Fe^{3+}]/K_{if} + [C][Fe^{3+}]/\alpha K_i' K_{if})}$$

where K_{if} is the inhibition constant for Fe^{3+} and $[Fe^{3+}]$ the concentration of Fe^{3+}.

In the double reciprocal form the equation becomes:

$$\frac{1}{v} = \frac{1}{k_3'[C]} + \frac{K_m}{k_3'[C]}(1 + \frac{[C]}{K_i'} + \frac{[Fe^{3+}]}{K_{if}} + \frac{[C][Fe^{3+}]}{\alpha K_i' K_{if}})(\frac{1}{[Fe^{3+}]})$$

The plots of $1/v$ versus $1/[Fe^{2+}]$ at fixed $[C]$ and different $[Fe^{3+}]$ should intersect on the Y-axis at $1/k_3'[C]$ with slopes increasing with $[Fe^{3+}]$, typical of competitive inhibition patterns (Fig. 5). The slope replots against $[Fe^{3+}]$ (Fig. 6) will intersect the Y-axis at $(K_m/k_3' [C] + K_m/k_3' K_i')$ and have slopes equal to $(K_m/k_3' K_{if}[C] + K_m/\alpha k_3' K_i' K_{if})$. The secondary replot of the slopes against $1/[C]$ (Fig. 6 inset) will have a slope of $K_m/k_3' K_{if}$ and an intercept on the Y-axis at $K_m/\alpha k_3' K_i' K_{if}$ and on the X-axis at $-1/\alpha K_i'$.

The plots at fixed $[Fe^{3+}]$ and various $[C]$ (Fig. 7) produced patterns different from Figure 5, the Y-intercepts and slope both decreasing with increasing $[C]$ due to the $1/[C]$ term in the rate equation. We can use the specific activity, v_{sp}, by dividing v by the cell concentration, $[C]$, to demonstrate the competitive inhibition. The rate equation then becomes:

$$\frac{1}{v_{sp}} = \frac{1}{k_3'} + \frac{K_m}{k_3'}(1 + \frac{[C]}{K_i'} + \frac{[Fe^{3+}]}{K_{if}} + \frac{[C][Fe^{3+}]}{\alpha K_i' K_{if}})(\frac{1}{[Fe^{2+}]})$$

Now the double reciprocal plots of v_{sp} versus $[Fe^{2+}]$ at fixed $[Fe^{3+}]$ should show a typical competitive inhibition by $[C]$ (Fig. 8), lines

intersecting the Y-intercept at $1/k_3'$. The slope replot against [C] (Fig. 9) will show a family of lines at different $[Fe^{3+}]$ with Y-intercepts of $(K_m/k_3' + K_m[Fe^{3+}]/k_3' K_{if})$, X-intercepts of $-K_i(1 + [Fe^{3+}]/K_{if})/(1 + [Fe^{3+}]/\alpha K_{if})$, and slopes of $(K_m/k_3' K_i' + K_m[Fe^{3+}]/\alpha k_3' K_i' K_{if})$. The secondary replot of slopes against $[Fe^{3+}]$ (Fig. 9 inset) will intersect the Y-axis at $-\alpha K_{if}$. The secondary replot of Y-intercepts (Fig. 9 inset) should intersect the Y-axis at K_m/k_3' and X-axis at $-K_{if}$.

The rate and kinetic constants obtained from these results are shown in Table 2. The value of α larger than 1 indicates that the binding of one inhibitor decreases the binding constant of the other inhibitor (59), i.e. increases the value of the apparent inhibitor constant. This is evident in Figure 6 and Figure 9 where the apparent K_i' and K_{if} values increased with increasing concentrations of the other inhibitor.

Figure 10 and Figure 11 are the Dixon plots (59) to confirm the interpretation of the results. The reciprocal of v_{sp} at $[Fe^{2+}]$ of 0.42 mM was plotted against $[Fe^{3+}]$ at three different [C] values (Fig. 10). The changing slopes indicate that the two inhibitors are not exclusive of each other in the inhibition. The lines intersect at a negative X-coordinate corresponding to αK_{if}, i.e 3.25 mM. Similar plots against [C] at four different $[Fe^{3+}]$ produced Figure 11. The four lines of different slopes intersected at the negative X-coordinate corresponding to $\alpha K_i'$, i.e. 0.66 mg wet cells per mL. These values are very close to the values expected from Table 2.

Figures 10 and 11 also show that when the specific activity (v_{sp}) is used, the inhibition by either Fe^{3+} or cell is greater when the other inhibitor concentration ([C] or $[Fe^{3+}]$) is higher, i.e. there is a

TABLE 2. Rate and kinetic constants for Fe^{2+} oxidation (II)

Constants	Values
k_3'	200 nmol O_2/minute per mg wet cells
K_m	70 μM [Fe^{2+}]
K_i'	135 μg wet cells per mL
K_{if}	640 μM [Fe^{3+}]
α	5

Figure 10. Dixon plot showing the effect of Fe^{3+} concentration on the specific activity of Fe^{2+} oxidation at three different cell concentrations (0.25, 0.50, and 1.00 mg wet cells in 1.2 mL reaction volume, as indicated). The v_{sp} values correspond to a Fe^{2+} concentration of 0.42 mM.

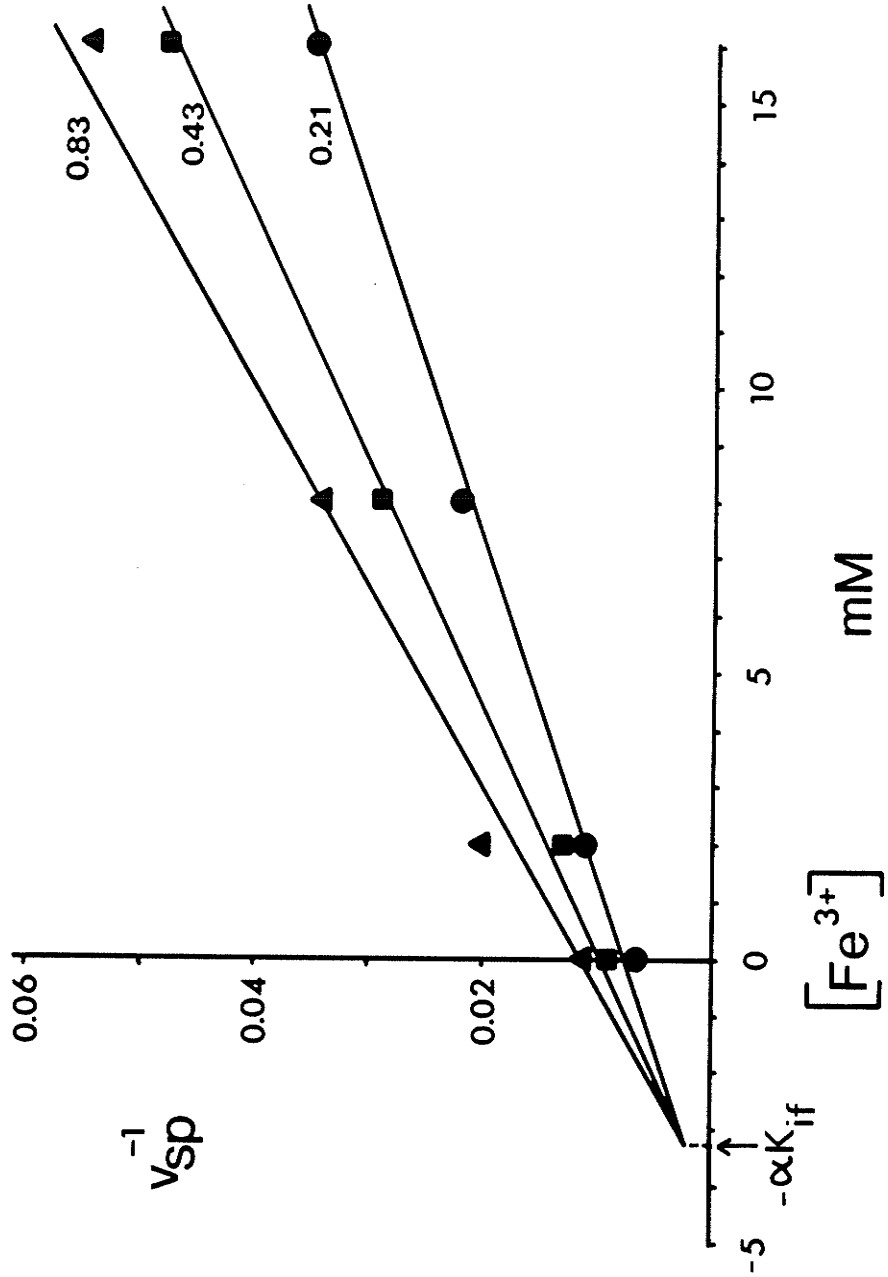
0.83
0.43
0.21
0.06
0.04
0.02
v_{sp}^{-1}
-5
$-\alpha K_{if}$
0
5
10
15
$[Fe^{3+}]$
mM

Figure 11. Dixon plot showing the effect of cell concentration on the specific activity of Fe^{2+} oxidation at the four different Fe^{3+} concentrations used (0, 2, 8, and 16 mM, as indicated). The data shown here is the same as that on Figure 10.

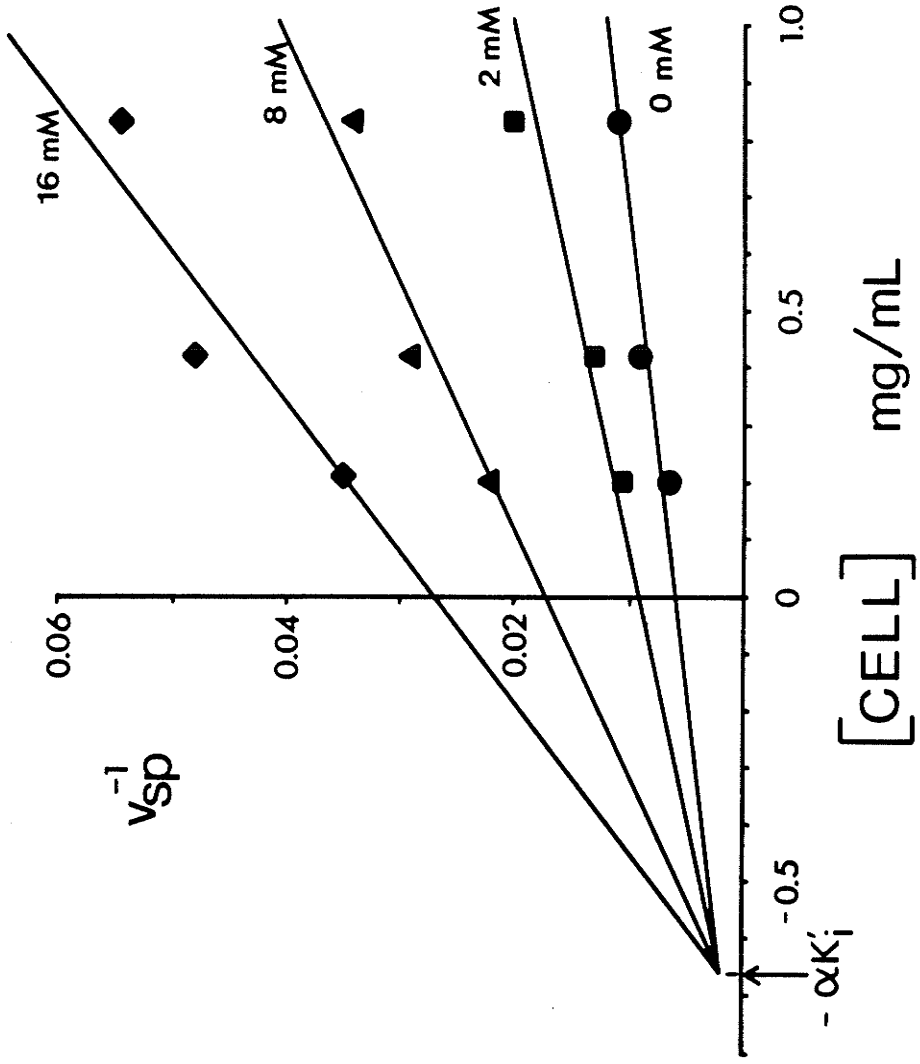
16 mM
8 mM
2 mM
0 mM
0.06
0.04
0.02
0
0.5
1.0
-0.5
v_{sp}^{-1}
[CELL] mg/mL
$-\alpha K'_i$

synergistic inhibitor effect.

Pyrite oxidation kinetics

Spontaneous solubilization of pyrite

Pyrite is not very soluble in water and the solubility product of the following reaction (52):

$$FeS_2 + H^+ \rightarrow Fe^{2+} + HS^- + S^o$$

is almost 2×10^{-19} at pH 2.3, the pH used throughout this study. The rate of Fe^{2+} solubilization from pyrite at various concentrations is shown in Figure 12. The reaction rate, v, was measured in μM Fe^{2+} produced per minute and $[FeS_2]$ in pulp density (PD). The reaction was first order with respect to pyrite with a slope (rate constant) of 3.48 μM $Fe^{2+}/[FeS_2]$ per minute. Figure 13 shows the rate of O_2 consumption during solubilization of washed pyrite. Here, v is measured in μM O_2 consumed per minute. Oxygen consumption was first order with respect to pyrite, with a rate constant of 0.40 μM $O_2/[FeS_2]$ per minute. This is much smaller than the expected value if the HS^- produced was being oxidized to S^o ($HS^- + \frac{1}{2}O_2 + H^+ \rightarrow S^o + H_2O$, with an expected rate constant of 1.74 μM $O_2/[FeS_2]$ per minute).

T. ferrooxidans and *T. thiooxidans* cells are known to adsorb on solid surfaces, even when they are killed by heat (80). Heat-killed *T. thiooxidans* cells almost stopped the Fe^{2+} release from pyrite (Fig. 12), presumably by covering the surface of pyrite particles. Intact cells also inhibited the Fe^{2+} release, although less drastically (Fig. 12). The resulting Fe^{2+} rate constants were 1.92 and 0.63 μM $Fe^{2+}/[FeS_2]$ per minute for intact and heat-killed cells, respectively. The O_2 consumption in Figure 14 indicated that *T. thiooxidans* cells were oxidizing the released sulfide portion of the unwashed pyrite beyond the S^o state according to

Figure 12. Effect of FeS_2 concentration (PD) on the rate of spontaneous dissolution of Fe^{2+}. The spontaneous solubilization rate (v) was determined as μM Fe^{2+} per minute at 30°C. Where indicated, active or heat-killed inactivated cells of *T. thiooxidans* were present at 1.56 mg wet cells per mL.

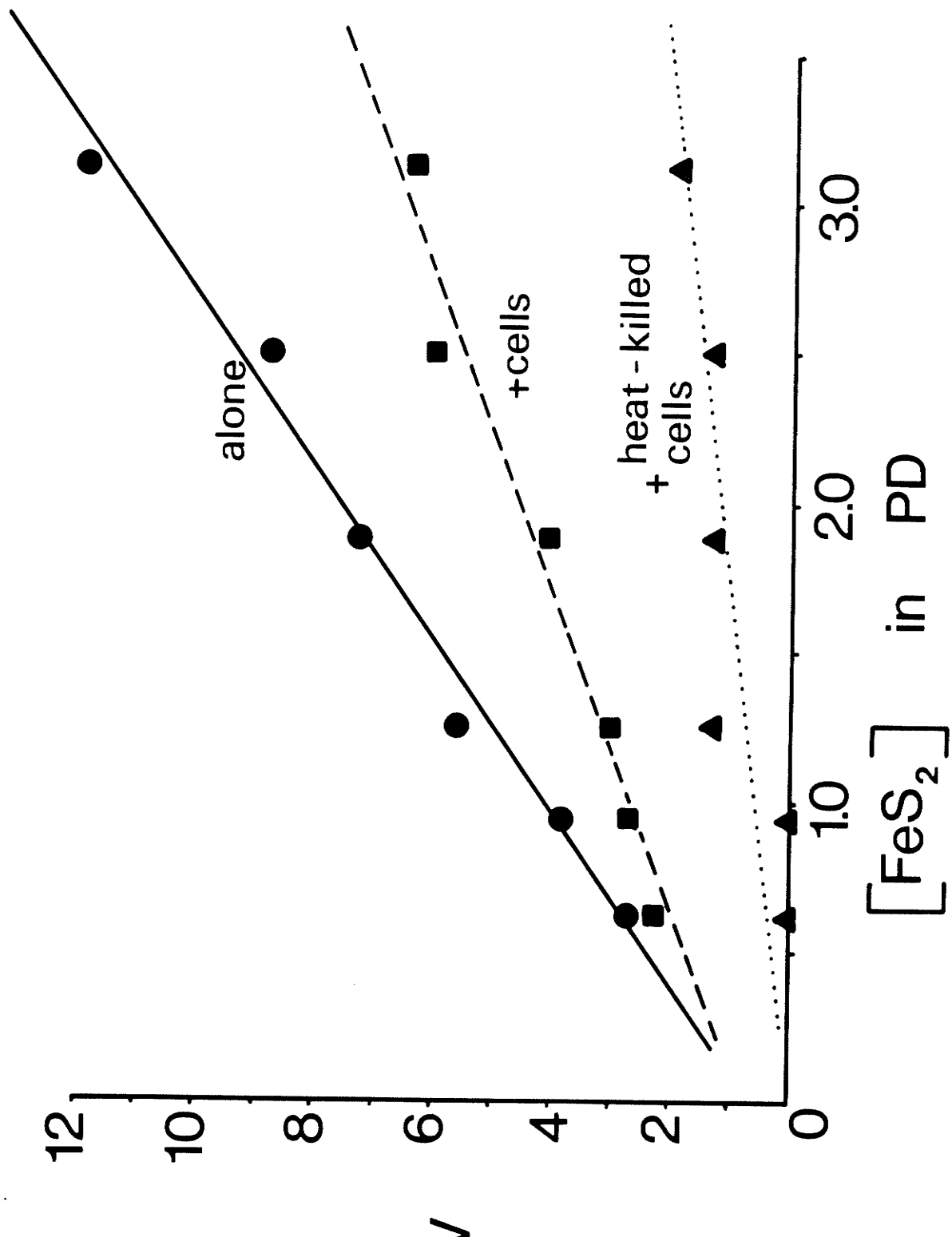
12
10
8
6
4
2
0
V
alone
+cells
heat-killed
+ cells
1.0
2.0
3.0
[FeS2] in PD

Figure 13. Effect of washed pyrite concentration (PD) on the rate of O_2 consumption. The O_2 uptake rate was determined as μM O_2 per minute at 30°C.

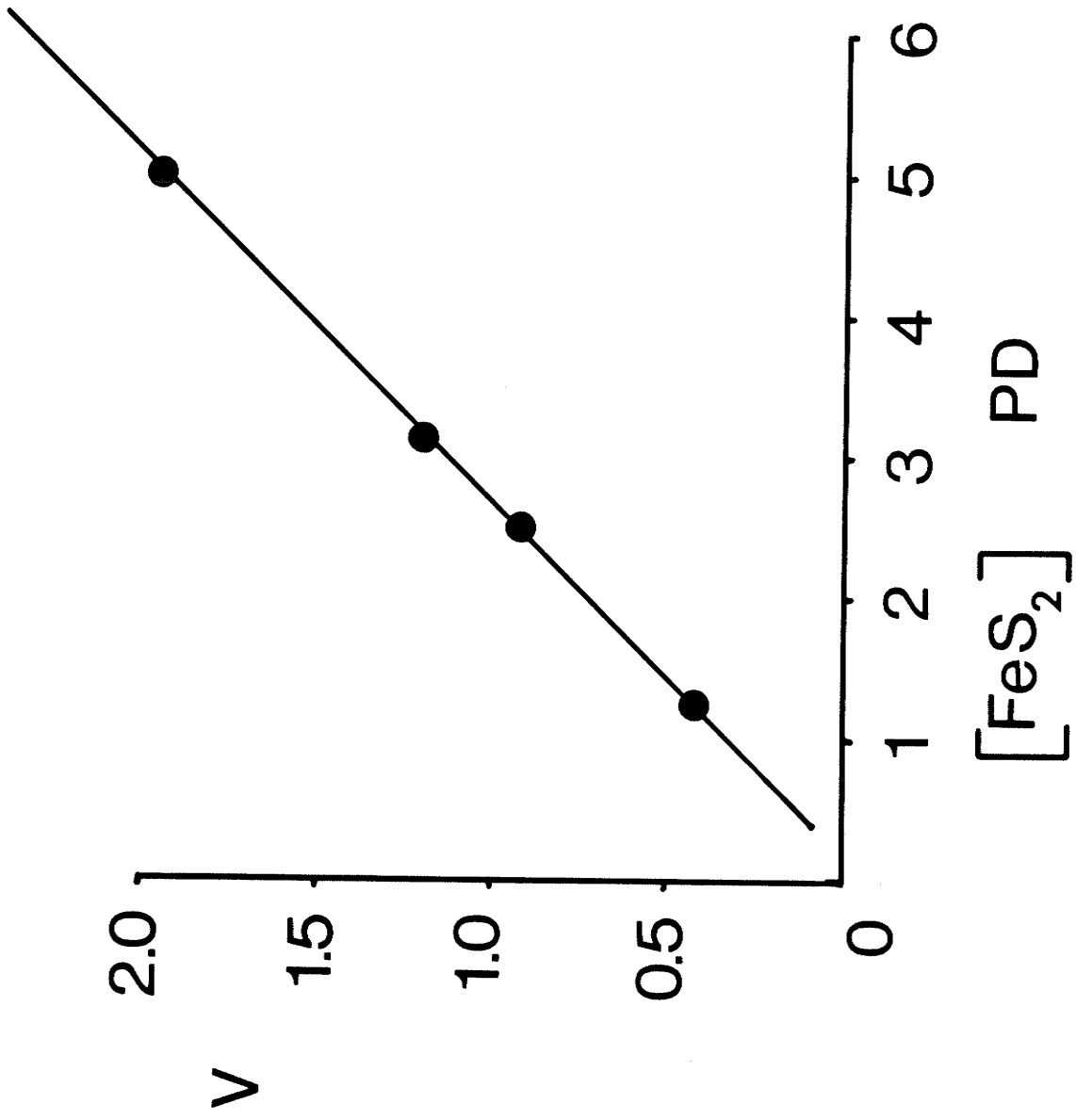
2.0
1.5
1.0
0.5
0
V
1
2
3
4
5
6
[FeS2] PD

Figure 14. Effect of unwashed pyrite concentration (PD) on the rate of O_2 consumption. The experiments were carried out as indicated in Figure 13. Where indicated, active cells of *T. thiooxidans* were present at a concentration of 1.56 mg wet cells per mL.

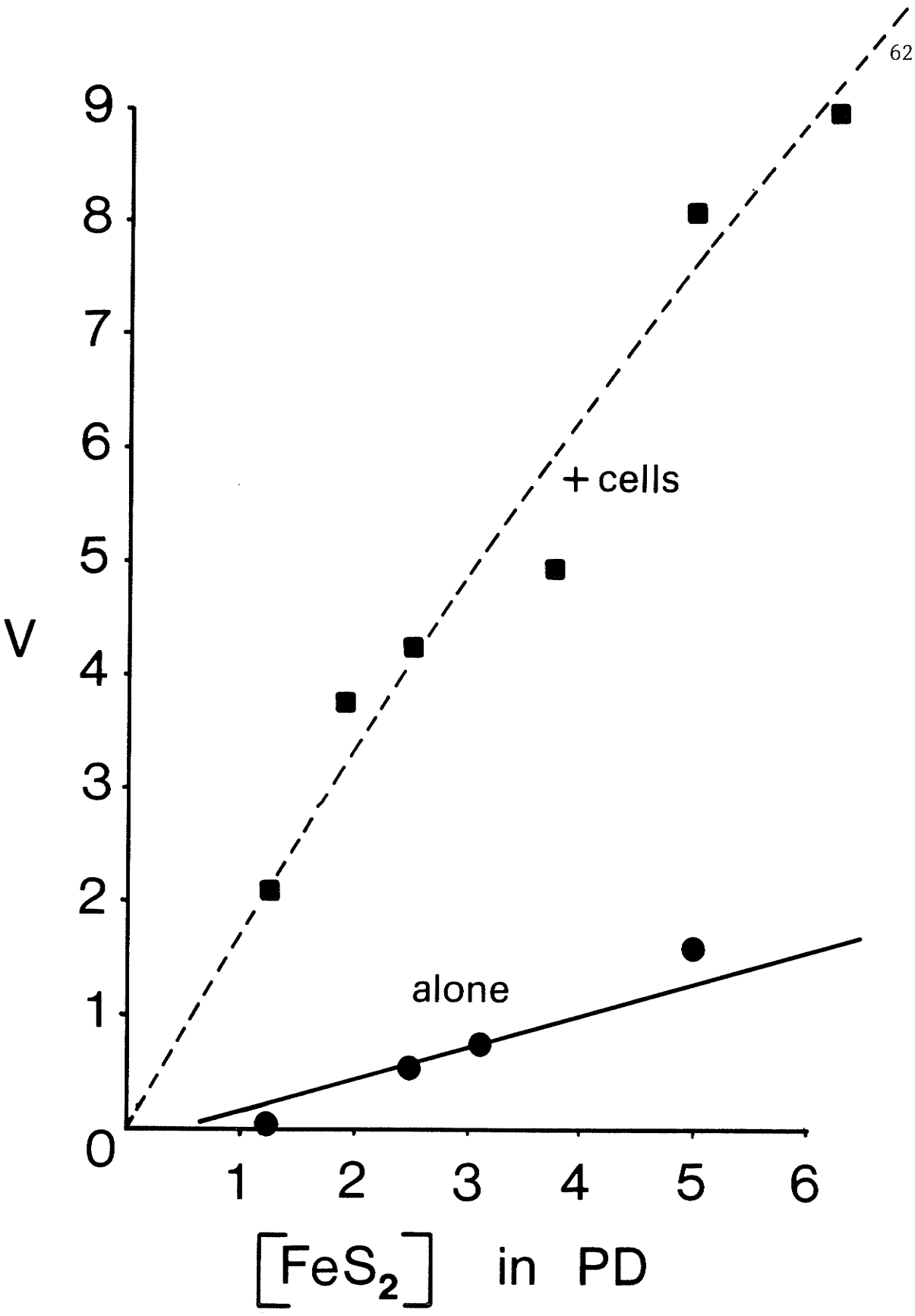
9
8
7
6
5
4
3
2
1
0
V
+ cells
alone
1
2
3
4
5
6
[FeS2] in PD

the equation:

$$HS^- + 2O_2 + H^+ \rightarrow H_2SO_4$$

At low pulp densities, the saturation velocity curve can be approximated to a rate constant of 1.74 μM $O_2/[FeS_2]$ per minute (Fig. 14) which is about twice the rate constant for the expected oxidation of HS^- to S^o (0.96 μM $O_2/[FeS_2]$ per minute) formed from pyrite in the presence of active *T. thiooxidans* cells (Fig. 12). The amount of cells used was the same for the experiments in both figures.

Indirect leaching of pyrite by ferric iron

The complete oxidation of pyrite by Fe^{3+} has been determined as:

$$FeS_2 + 8H_2O + 14Fe^{3+} \rightarrow 15Fe^{2+} + 2SO_4^{2-} + 16H^+$$

This reaction, however, requires harsh conditions and long reaction times. During the relatively mild conditions of bacterial leaching, a more plausible reaction would be (19, 37):

$$FeS_2 + 2Fe^{3+} \rightarrow 3Fe^{2+} + 2S^o$$

The reaction rate (v) was measured in mM Fe^{2+} produced per minute, having to correct for spontaneous pyrite dissolution due to the nature of the assay.

The rate of Fe^{2+} release from pyrite was determined at various concentrations of Fe^{3+} and fixed concentrations of pyrite (Fig. 15). The rate of Fe^{2+} release was linear (first order) with respect to Fe^{3+}. The effect of pyrite concentration on the rate of Fe^{2+} release at two fixed concentrations of Fe^{3+} is shown in Figure 16 (inset). The values were corrected for spontaneous dissolution by simply subtracting the corresponding values for each pulp density. The rate of Fe^{2+} formation followed typical saturation kinetics at both 10 mM and 20 mM Fe^{3+}. The

Figure 15. Effect of Fe^{3+} concentration on the rate of indirect leaching, or Fe^{3+}-mediated Fe^{2+} dissolution. The indirect leaching rate (v) was determined as mM Fe^{2+} per minute at various pulp densities of pyrite at 30°C. The lines do not go through the origin because even at $[Fe^{3+}] = 0$, there is spontaneous Fe^{3+} release occurring.

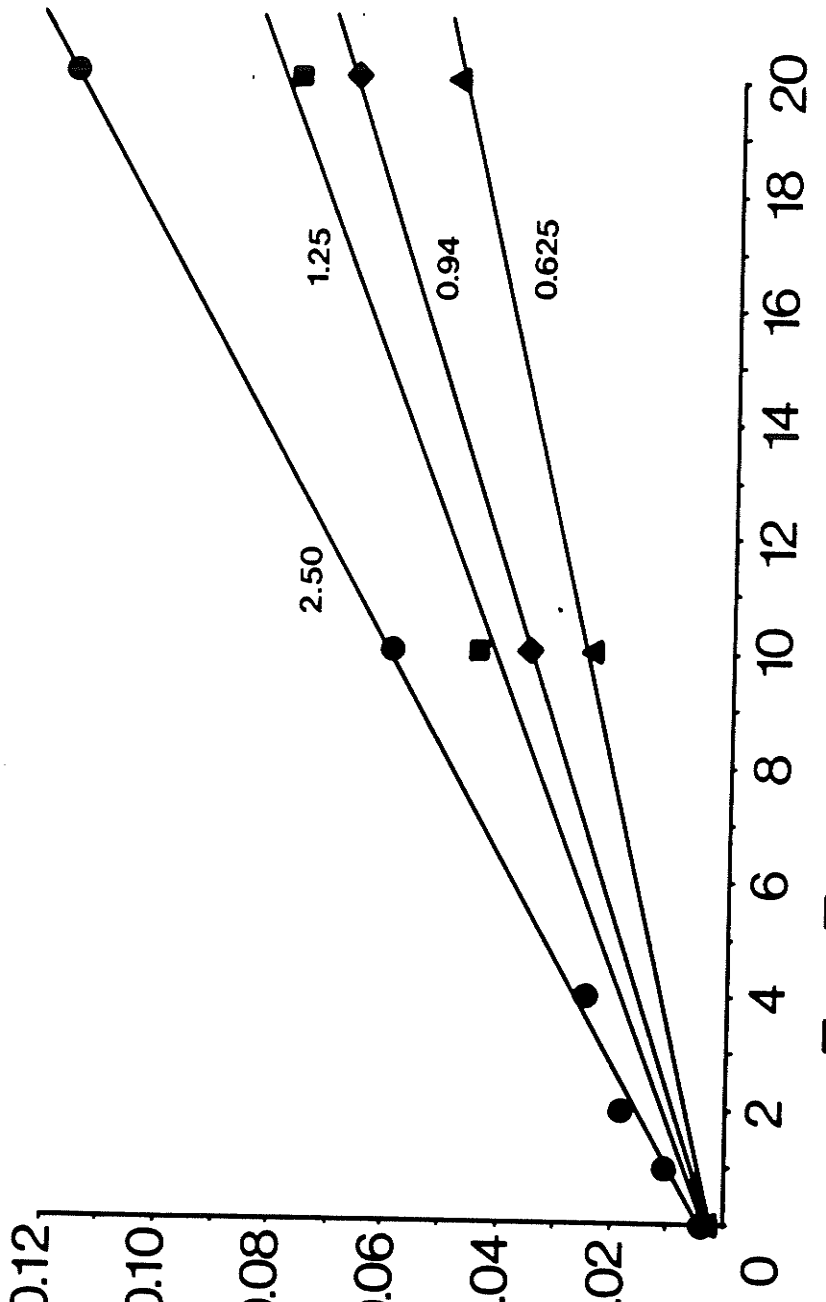
0.12
0.10
0.08
0.06
0.04
0.02
V
0
2
4
6
8
10
12
14
16
18
20
[Fe3+] in mM
2.50
1.25
0.94
0.625

Figure 16. Effect of pyrite concentration (PD) on the indirect leaching rate at two Fe^{3+} concentrations. The indirect leaching rate (v) was determined as mM Fe^{2+} per minute at the indicated mM concentrations of Fe^{3+}. The inset is the standard rate-PD plot.

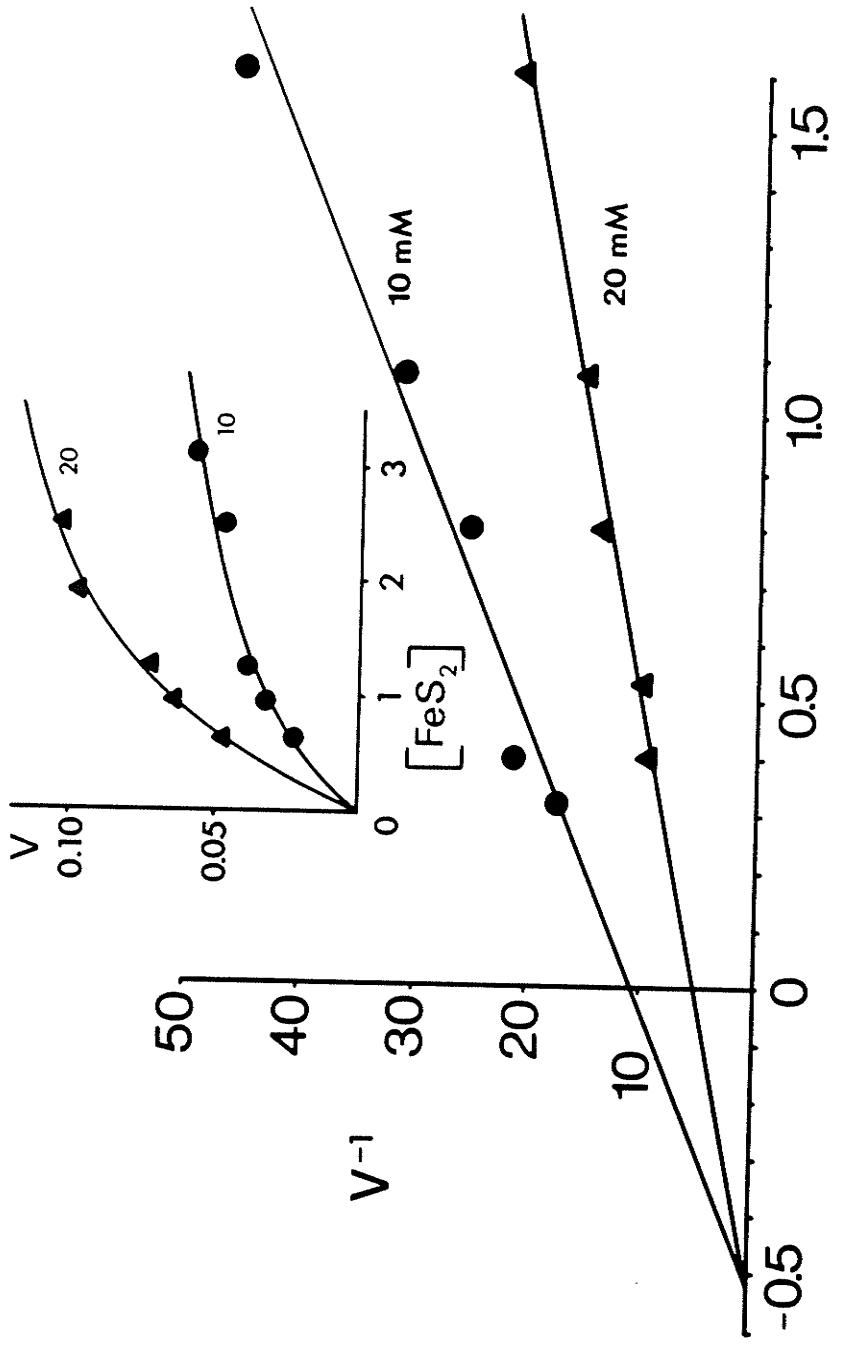
V
0.10
0.05
20
10
0
1
2
3
[FeS2]
10 mM
20 mM
V-1
50
40
30
20
10
0
-0.5
0.5
1.0
1.5
[FeS2]-1
PD-1

double reciprocal plots (43) shown in Figure 16 were linear, intersecting on the X-axis at the same point with a K_m of 1.91 PD pyrite. The results agree with the concept of pyrite as a substrate and Fe^{3+} as a catalyst (although it is also a substrate) with the formation of an FeS_2-Fe^{3+} complex as the rate-limiting step:

$$FeS_2 + Fe^{3+} \underset{k_2}{\overset{k_1}{\rightleftarrows}} FeS_2\text{-}Fe^{3+} \xrightarrow{k_3} Fe^{2+} \text{ release}$$

Under the steady-state conditions the rate of Fe^{2+} release (v) can be derived following the standard enzyme kinetics:

$$v = \frac{k_3[Fe^{3+}][FeS_2]}{K_m + [FeS_2]}$$

where $K_m = (k_2 + k_3)/k_1$. In the double reciprocal form, the equation becomes:

$$\frac{1}{v} = \frac{1}{k_3[Fe^{3+}]} + \frac{K_m}{k_3[Fe^{3+}]}\left(\frac{1}{[FeS_2]}\right)$$

Thus, plots of $1/v$ versus $1/[FeS_2]$ will show straight lines intersecting the Y-axis at $1/k_3[Fe^{3+}]$ (or $1/V_{max}$ where V_{max} is the maximal velocity) and converging on the X-axis at a point equivalent to $-1/K_m$ (Fig. 16). The k_3 value was 9.25 μM Fe^{2+} per mM Fe^{3+} per minute and was confirmed by plotting the observed rate (v) versus $[Fe^{3+}][FeS_2]/(K_m + [FeS_2])$ (Fig. 17).

Oxidation of pyrite by *T. ferrooxidans*

The rate of pyrite oxidation by *T. ferrooxidans* cells was determined by measuring the steady-state rate of O_2 consumption (μM O_2/minute) at various concentrations of cells and pyrite. The values were corrected for the slow spontaneous rates (without cells) which were less than 5% of the bacterial rates. For these experiments, both washed and unwashed pyrite

Figure 17. Determination of the constant k_3. All indirect leaching experiments are included in this figure. Reaction rate (v) was determined as mM Fe^{2+} per minute.

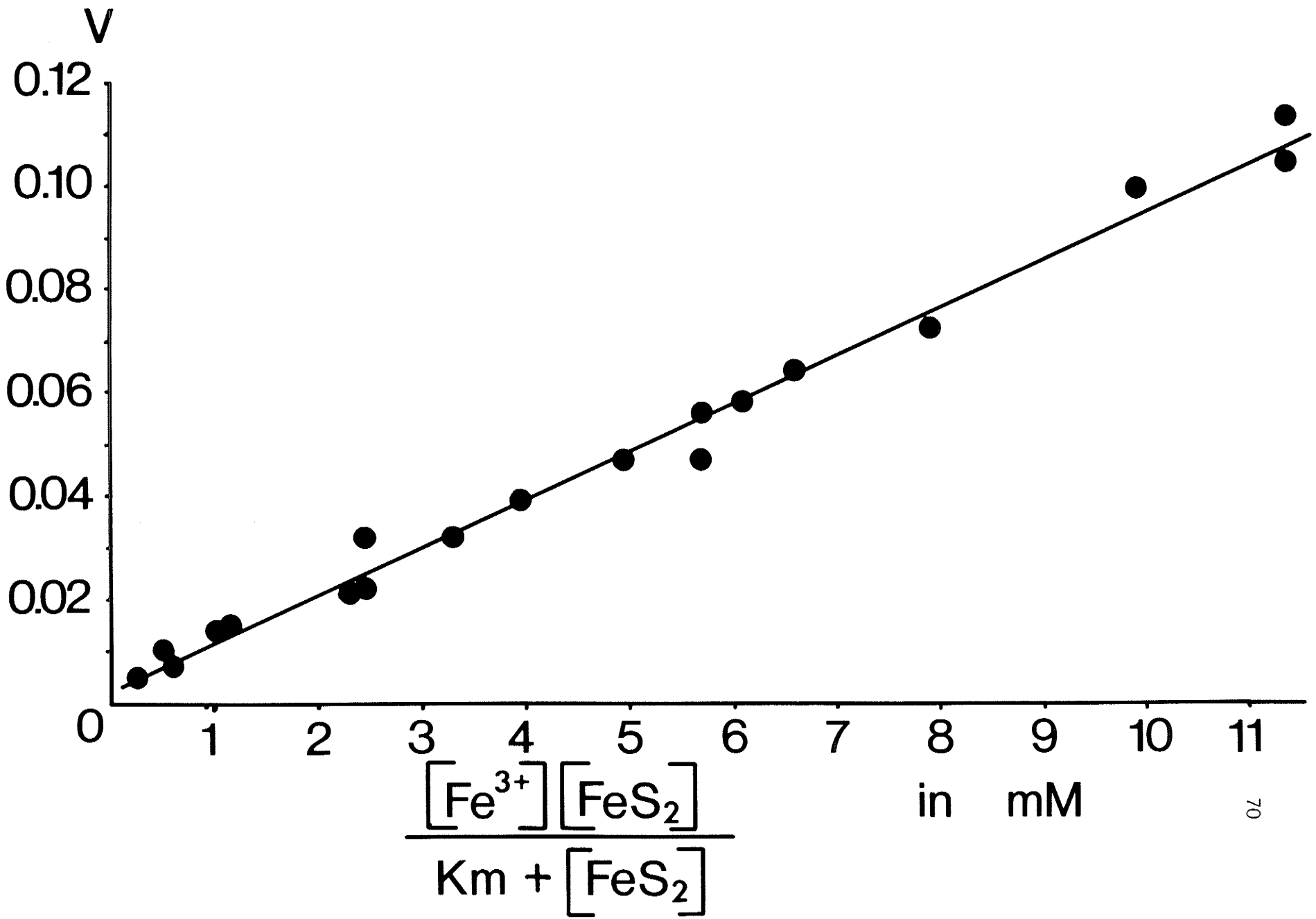
V
0.12
0.10
0.08
0.06
0.04
0.02
0
1
2
3
4
5
6
7
8
9
10
11
$\frac{[Fe^{3+}][FeS_2]}{Km + [FeS_2]}$
in mM
70

samples were used.

The rate of O_2 uptake (measured in μM O_2 per minute) during washed pyrite oxidation by *T. ferrooxidans* increased with pulp density following typical saturation kinetics as shown in Figure 18. Double reciprocal rate-pulp density plots showed a family of lines converging on the X-axis as in normal Michaelis Menten kinetics (43). Thus, the rate of pyrite oxidation by *T. ferrooxidans* can be expressed by the steady state rate equation:

$$v = \frac{k_3[C][FeS_2]}{K_m + [FeS_2]}$$

where [C] is expressed in mg wet cells per mL and $[FeS_2]$ in PD. The inverse form of the equation is:

$$\frac{1}{v} = \frac{1}{k_3[C]} + \frac{K_m}{k_3[C]}\left(\frac{1}{[FeS_2]}\right)$$

The plot of 1/v versus $1/[FeS_2]$ will show straight lines intersecting the Y-axis at $1/k_3[C]$ and converging on the X-axis at a point equivalent to $-1/K_m$ (Fig. 18). The K_m value was 2.50 PD pyrite. A replot of the inverse of the Y-intercepts (V_{max}) against [C] will give a straight line intersecting the origin and with a slope equivalent to k_3 (Fig. 18 inset). The value of k_3 was 90 μM O_2/ mg wet cells per mL per minute.

The results with unwashed pyrite gave a different pattern (Fig. 19). Here the maximum velocities were much higher and the apparent K_m values increased with increasing cell concentrations. When the O_2 uptake rate was calculated as the specific activity (v_{sp}) in μM O_2/mg wet cells per mL per minute, and replotted in the double reciprocal manner (Fig. 20), all the lines now intersected the Y-axis at the same point, characteristic of a competitive inhibition. Cell-cell competitive inhibition was

Figure 18. Effect of washed pyrite concentration (PD) on the FeS_2 oxidizing activity of various concentrations of *T. ferrooxidans* SM-4. The O_2 consumption rate (v) was determined as μM O_2 per minute at 30°C at various FeS_2 concentrations. Cell concentrations were expressed as mg wet cells per mL. The inset is a replot of the Y-intercepts to obtain the k_3 value.

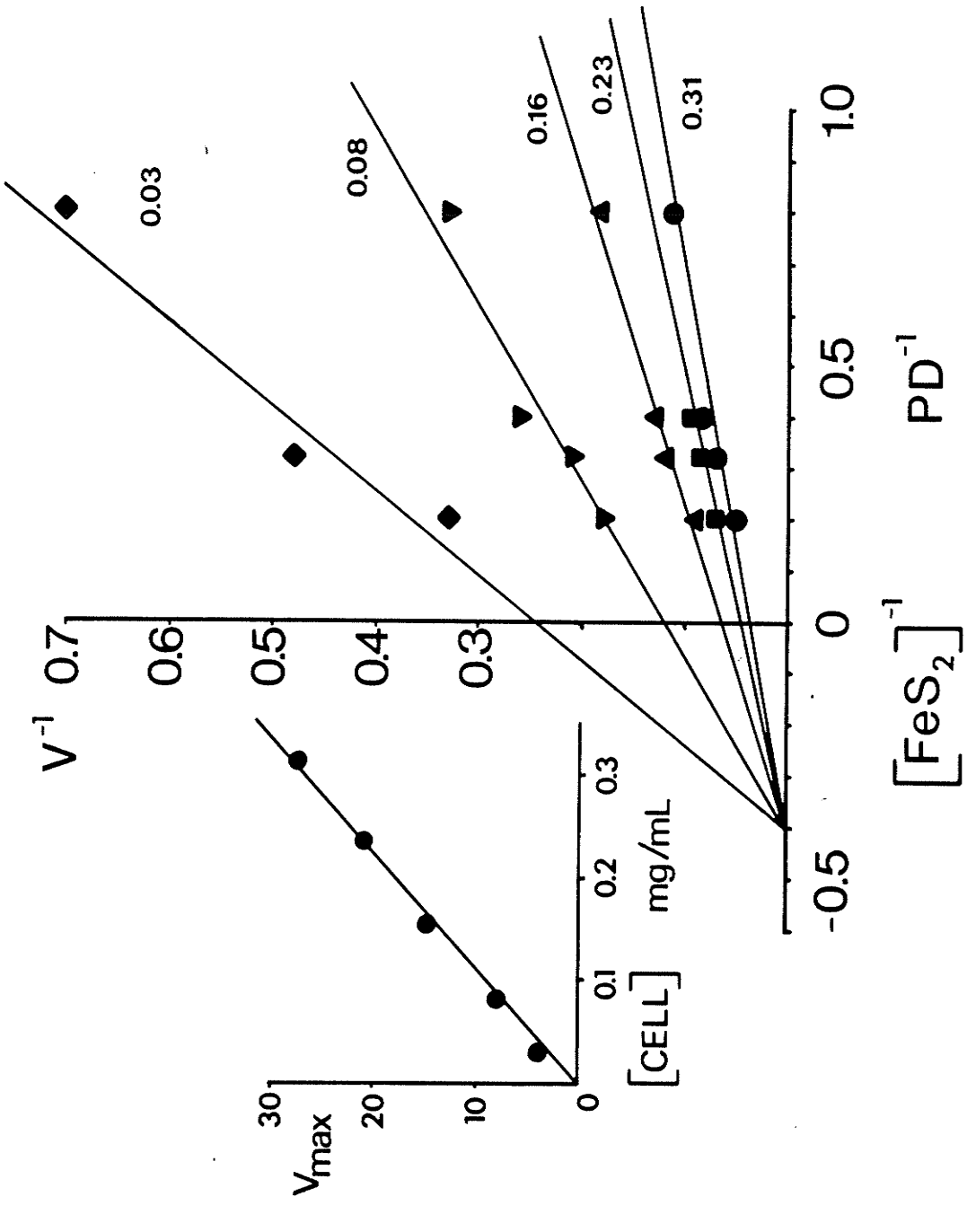
0.03
0.08
0.16
0.23
0.31
V^{-1}
0.7
0.6
0.5
0.4
0.3
-0.5
0
0.5
1.0
$[FeS_2]^{-1}$
PD^{-1}
V_{max}
30
20
10
0
0.1
0.2
0.3
[CELL] mg/mL

Figure 19. Effect of unwashed pyrite concentration (PD) on the rate of O_2 consumption by *T. ferrooxidans* SM-4. Experimental conditions were the same as those described in Figure 18.

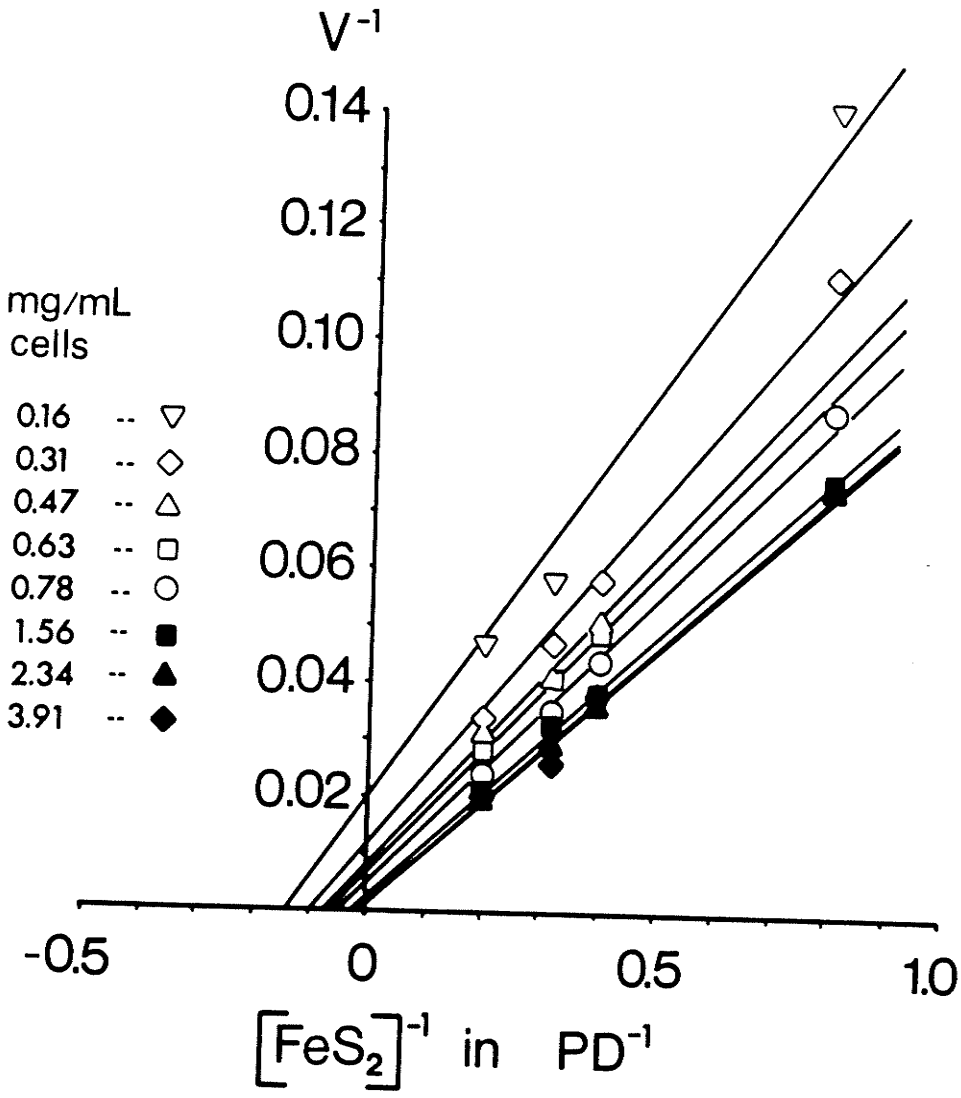
V⁻¹
0.14
0.12
0.10
0.08
0.06
0.04
0.02
mg/mL
cells
0.16 --
0.31 --
0.47 --
0.63 --
0.78 --
1.56 --
2.34 --
3.91 --
-0.5
0
0.5
1.0
[FeS2]⁻¹ in PD⁻¹

Figure 20. Competitive inhibition of unwashed pyrite oxidizing activity of *T. ferrooxidans* SM-4 cells by increasing concentrations of cells. The specific activity (v_{sp}) was calculated from the data in Figure 19 as μM O_2/mg wet cells per mL per minute.

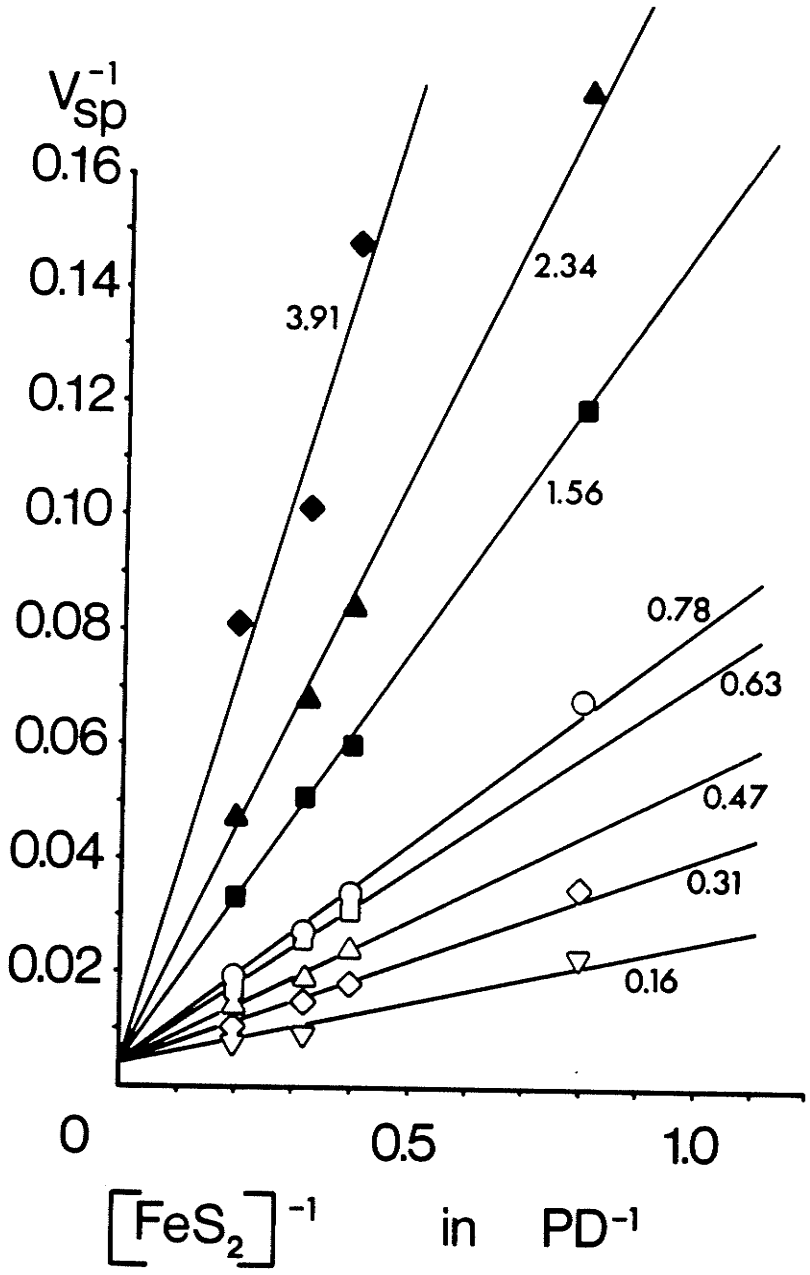
V_{sp}^{-1}
0.16
0.14
0.12
0.10
0.08
0.06
0.04
0.02
0
0.5
1.0
3.91
2.34
1.56
0.78
0.63
0.47
0.31
0.16
$[FeS_2]^{-1}$ in PD^{-1}

demonstrated earlier in the study with Fe^{2+} oxidation, the equation derived being:

$$v = \frac{k_3[C][S]}{[S] + K_m(1 + [C]/K_i')}$$

where [C] and [S] are the concentrations of cell and substrate, k_3' is k_3 times the number of enzymes per cell, and K_i' is K_i divided by the number of inhibitors per cell. If v is then divided by [C] to obtain the specific activity (v_{sp}) and the pyrite pulp density is taken as the substrate concentration:

$$v_{sp} = \frac{k_3'[FeS_2]}{[FeS_2] + K_m(1 + [C]/K_i')}$$

which in the double reciprocal form is:

$$\frac{1}{v_{sp}} = \frac{1}{k_3'} + \frac{K_m}{k_3'}(1 + \frac{[C]}{K_i'})(\frac{1}{[FeS_2]})$$

Figure 20 follows the pattern expected of the equation above. The k_3' value is obtained from the Y-intercept as 250 μM O_2/mg wet cells per mL per minute. Figure 21 is the replot of the slopes from Figure 20 versus the cell concentration. The line has a slope of $K_m/k_3' K_i'$, a Y-intercept of K_m/k_3', and an X-intercept equivalent to $-1/K_i'$. From this figure, a K_m value of 2.75 PD and a K_i' value of 0.13 mg wet cells per mL were obtained. The various rate and kinetic constants for washed and unwashed pyrite oxidation by *T. ferrooxidans* SM-4 are shown in Table 3.

With unwashed pyrite, the rate of O_2 consumption was faster during the initial 30 - 60 minutes before the linear steady-state was achieved. This was caused by an initial rapid release of Fe^{2+} from the unwashed pyrite upon contact with the liquid medium. In separate experiments it was determined that Fe^{2+} release during the 20 minutes preincubation period was 2 mM Fe^{2+} per PD pyrite. At these high concentrations, Fe^{2+} would

TABLE 3. Summary of reaction rates of pyrite oxidation by *T. ferrooxidans*

Reaction	Rate equation	Constants
Spontaneous dissolution	$v = k[FeS_2]$	$k = 3.5$ μM Fe^{2+}/min/PD
Indirect leaching	$v = \frac{k_3[Fe^{3+}][FeS_2]}{K_m + [FeS_2]}$	$k_3 = 9.25$ μM Fe^{2+}/min/mM Fe^{3+} $K_m = 1.91$ PD
T. ferrooxidans washed FeS_2	$v = \frac{k_3[C][FeS_2]}{K_m + [FeS_2]}$	$k_3 = 90$ μM O_2/min/mg cell/mL $K_m = 2.50$ PD
T. ferrooxidans unwashed FeS_2	$v = \frac{k_3[C][FeS_2]}{[FeS_2] + K_m(1 + [C]/K_i)}$	$k_3 = 250$ μM O_2/min/mg cell/mL $K_m = 2.75$ PD $K_i = 0.13$ mg cell/mL
T. ferrooxidans Fe^{2+} oxidation	$v = \frac{k_3[C][Fe^{2+}]}{[Fe^{2+}] + K_m(1 + [C]/K_i)}$	$k_3 = 125$ μM O_2/min/mg cell/mL $K_m = 0.11$ mM Fe^{2+} $K_i = 0.33$ mg cell/mL

$[FeS_2]$ = pyrite concentration in PD

$[Fe^{3+}]$ = Fe^{3+} concentration in mM

$[C]$ = cell concentration in mg wet cells per mL

$[Fe^{2+}]$ = Fe^{2+} concentration in mM

Figure 21. Replot of the slopes from Figure 20 against cell concentration. The line has a slope equivalent to $K_m/k_3' K_i'$, a Y-intercept equivalent to K_m/k_3', and an X-intercept equivalent to $-K_i'$.

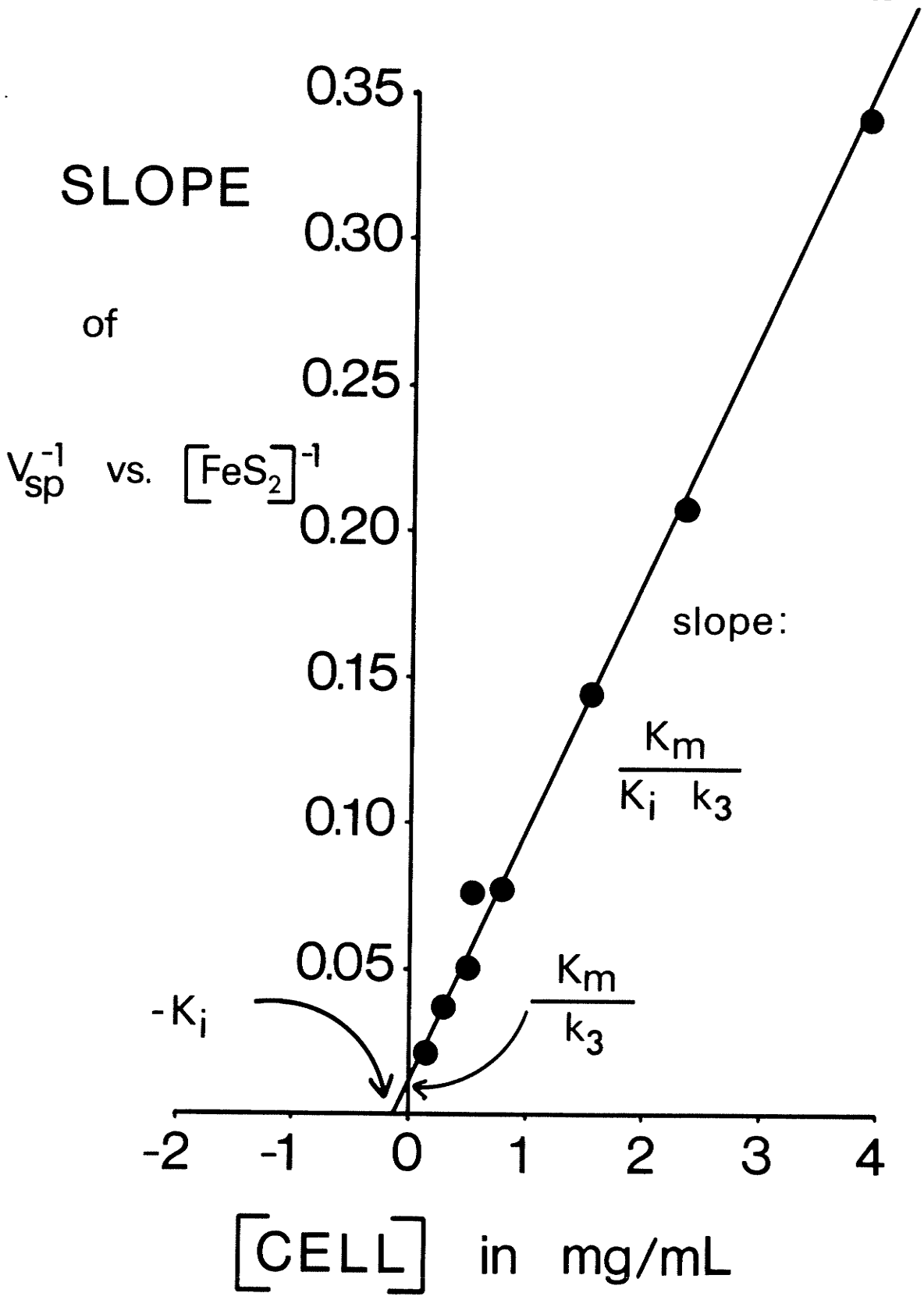
SLOPE
of
V_{sp}^{-1} vs. $[FeS_2]^{-1}$
0.35
0.30
0.25
0.20
0.15
0.10
0.05
slope:
$\frac{K_m}{K_i \ k_3}$
$\frac{K_m}{k_3}$
$-K_i$
-2
-1
0
1
2
3
4
[CELL] in mg/mL

contribute not only to the initial rapid rate of O_2 consumption, but also to the indirect leaching by the Fe^{3+} formed by bacterial oxidation. This was not the case with the washed pyrite, where no initial rapid release of Fe^{2+} occurred.

Oxidation of unwashed pyrite by *T. thiooxidans*

As with *T. ferrooxidans*, pyrite oxidation by *T. thiooxidans* was studied by measuring the steady-state rate of O_2 consumption (μM O_2 per minute) at various concentrations of cells and pyrite. The values were corrected for the spontaneous rates (without cells) which were less than 20% of the bacterial rates; O_2 uptake activity was much less with *T. thiooxidans* than with *T. ferrooxidans*. *T. thiooxidans* was only tested on the unwashed pyrite.

The rate of O_2 uptake during pyrite oxidation with *T. thiooxidans* SM-6 increased with pulp density, appearing to follow typical saturation kinetics (inset, Fig. 22). The double reciprocal plots, however, showed what seemed to be a group of lines bearing no relationship to each other (Fig. 22); the lines did not converge on the X-axis in typical Michaelis Menten fashion (43) and their slopes and K_m values did not increase or decrease with cell concentration. This changed when the O_2 uptake rate was converted to the specific activity, v_{sp}, in μM O_2/mg wet cells per mL per minute. Double reciprocal plots of v_{sp} versus PD pyrite showed a family of lines intersecting the Y-axis at the same point, typical of competitive inhibition by increasing concentrations of cells, as shown in Figure 23. Thus, the previously derived equation for cell-cell competitive inhibition could also be applied to *T. thiooxidans*:

$$v = \frac{k_3[C][FeS_2]}{[FeS_2] + K_m(1 + [C]/K_i')}$$

Figure 22. Effect of unwashed pyrite concentration (PD) on the rate of O_2 consumption by *T. thiooxidans* SM-6. The O_2 uptake rate (v) was determined as μM O_2 per minute at 30°C at various FeS_2 concentrations. Where indicated, cell concentrations are expressed as mg wet cells per mL. The inset is the standard rate-PD plot.

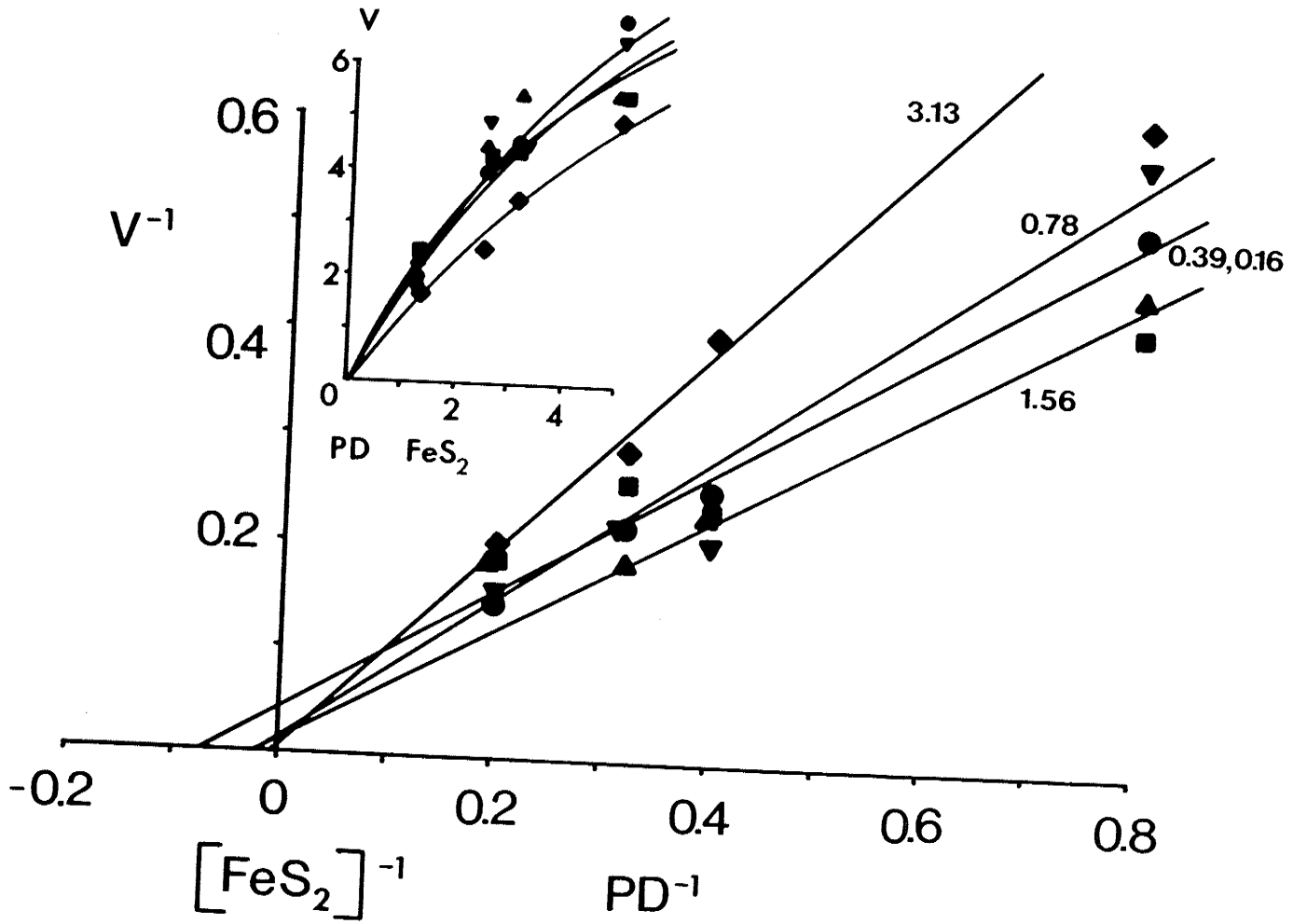
V
6
4
2
0
2
4
PD FeS2
0.6
0.4
0.2
V-1
3.13
0.78
0.39,0.16
1.56
-0.2
0
0.2
0.4
0.6
0.8
[FeS2]-1
PD-1

Figure 23. Competitive inhibition of unwashed pyrite oxidizing activity of *T. thiooxidans* SM-6 cells by increasing concentrations of cells. The specific activity (v_{sp}) was calculated from the data in Figure 22 as μM O_2/mg wet cells per mL per minute.

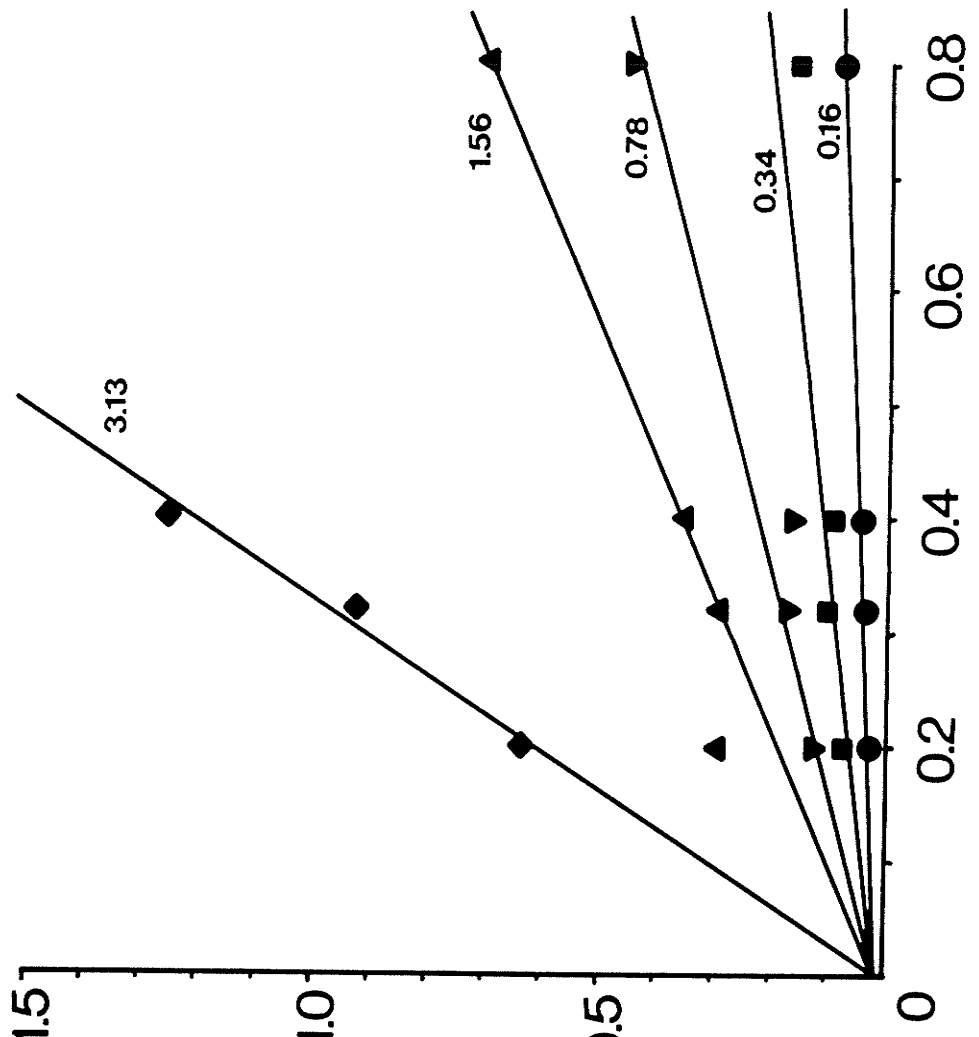
1.5
1.0
0.5
0
V_{sp}^{-1}
3.13
1.56
0.78
0.34
0.16
0.2
0.4
0.6
0.8
$[FeS_2]^{-1}$ PD^{-1}

where [C] and [FeS_2] are the concentrations of cell and pyrite, k_3' is k_3 times the number of enzymes per cell, and K_i' is K_i divided by the number of inhibitors per cell. Similarly, in terms of specific ativity:

$$v_{sp} = \frac{k_3' [FeS_2]}{[FeS_2] + K_m(1 + [C]/K_i')}$$

which in the double reciprocal plot form is:

$$\frac{1}{v_{sp}} = \frac{1}{k_3'} + \frac{K_m}{k_3'}(1 + \frac{[C]}{K_i'})(\frac{1}{[FeS_2]})$$

The equation above can describe the double reciprocal plot in Figure 23. The k_3' (obtained from the Y-intercept) had a value of 100 μM O_2/mg wet cell per mL per minute. Figure 24 is the replot of the slopes from Figure 23 versus the cell concentration. The line shown had a slope equivalent to $K_m/k_3' K_i'$, a Y-intercept of K_m/k_3', and an X-intercept equivalent to $-1/K_i'$. The K_m was similar to that of *T. ferrooxidans* with unwashed pyrite (2.81 and 2.75 PD, respectively). The K_i' value for *T. thiooxidans* SM-6 was very low at 0.05 mg wet cells per mL. The rate and kinetic constants for unwashed pyrite oxidation by *T. thiooxidans* are listed in Table 4.

The rate of O_2 consumption was faster during the initial 30 - 60 minutes before the linear steady-state was achieved. An initial rapid release of 2 mM Fe^{2+} per PD unwashed pyrite occurred during the 20 minutes preincubation period. It is quite likely that along with Fe^{2+}, a great deal (as much as 4 mM per PD unwashed pyrite) of sulfur plus sulfide was also released, providing additional substrate to *T. thiooxidans*. This high initial O_2 consumption rate observed may be due to sulfide oxidation.

Mineral-mineral interaction experiments

The interactions of chalcopyrite and sphalerite with pyrite were

Figure 24. Replot of slopes from Figure 23 against cell concentration. The line had a slope equivalent to $K_m/k_3' K_i'$, a Y-intercept equivalent to K_m/k_3', and an X-intercept equivalent to $-K_i'$.

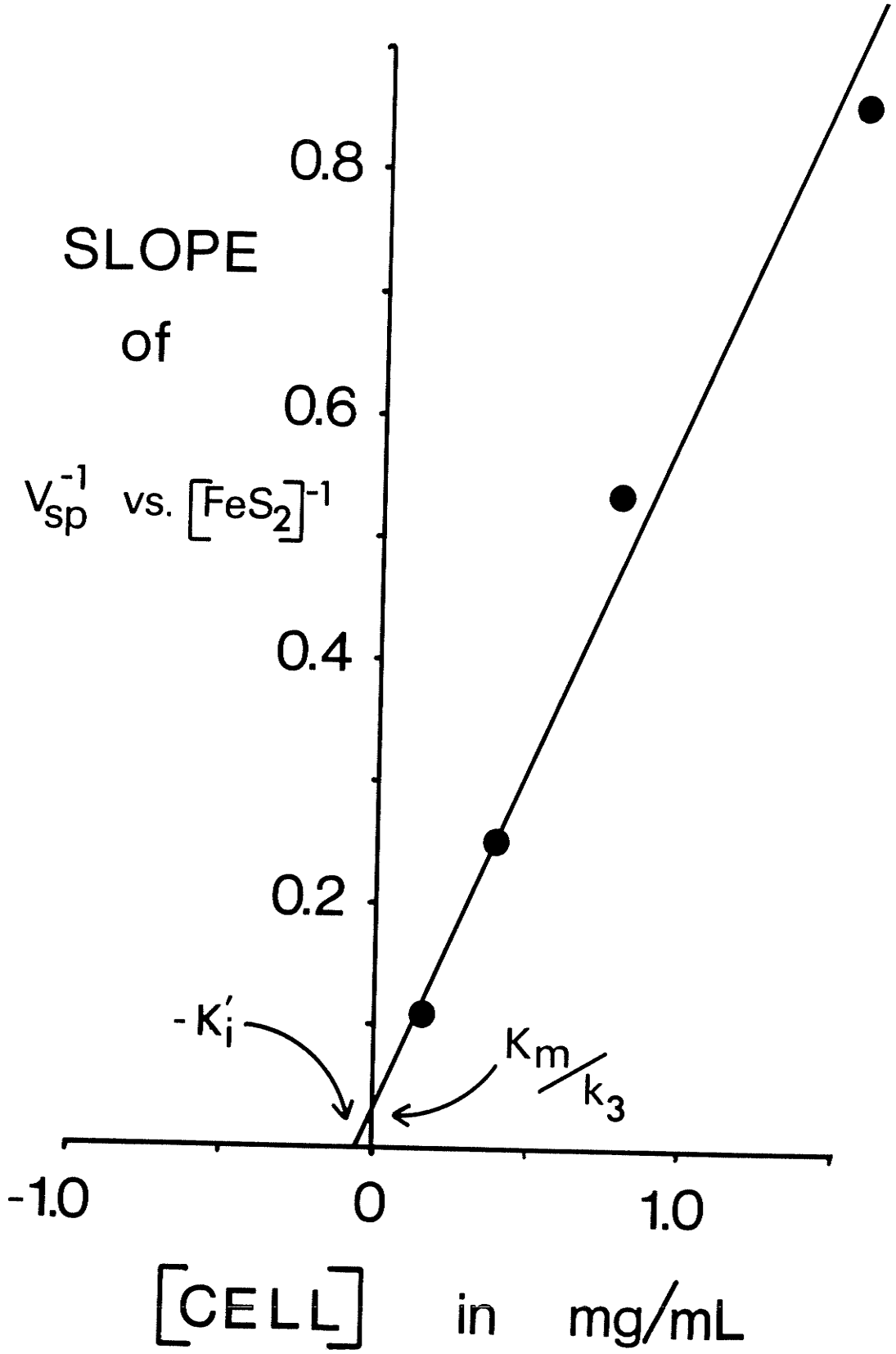
SLOPE
of
V_{sp}^{-1} vs. $[FeS_2]^{-1}$
0.8
0.6
0.4
0.2
$-K_i'$
K_m/k_3
-1.0
0
1.0
[CELL] in mg/mL

TABLE 4. Rate and kinetic constants of unwashed pyrite oxidation by *T. thiooxidans*

Constants	Values
k_3'	100 µM O_2/per minute per mg wet cells per mL
K_m	2.81 PD
K_i'	0.05 mg wet cells per mL

studied in shake-flask leaching experiments with and without inoculation with *T. ferrooxidans*, *T. thiooxidans*, or both. In addition, short-term steady-state oxidation experiments were carried out in a Warburg respirometer with resting cells of these cultures.

Shake-flask leaching studies

Chalcopyrite interaction with pyrite. The interaction of chalcopyrite with two different pyrite samples (No. 1 and No. 2) were studied in shake-flask leaching experiments for 13 days with no bacterial inoculation (chemical control) and with *T. ferrooxidans* SM-4, *T. thiooxidans* SM-6, or both (Table 5). In the absence of bacteria both pyrites increased the Cu extraction from chalcopyrite and reduced the Fe extraction. The No. 1 pyrite was much more effective in increasing the Cu extraction than the No. 2 pyrite. Thus the galvanic interaction with chalcopyrite was stronger with the No. 1 pyrite. Inoculation with *T. ferrooxidans* greatly increased the Cu extraction from chalcopyrite without increasing the Fe extraction and maintained the low pH. The introduction of *T. ferrooxidans* or No. 1 pyrite had a very similar stimulatory effect on the Cu extraction from chalcopyrite (Fig. 25). When the No. 1 pyrite and *T. ferrooxidans* were both present, there was an initial lag followed by rapid Cu leaching exceeding the leaching level by either one alone (Fig. 25). When the No. 2 pyrite and *T. ferrooxidans* were both present the Cu extraction from chalcopyrite was not much more than with *T. ferrooxidans* alone, probably because of its weaker galvanic interaction with chalcopyrite seen with the chemical control experiments above. Figure 26 compares the Cu and Fe leaching from a mixture of chalcopyrite and the No. 1 pyrite with (A) and without (B) *T. ferrooxidans* inoculation. The solubilization of Cu was

TABLE 5. Pyrite-Chalcopyrite interaction during leaching

	$CuFeS_2$ alone	$CuFeS_2$ + No. 1 FeS_2	$CuFeS_2$ + No. 2 FeS_2	No. 1 FeS_2 alone	No. 2 FeS_2 alone
A. Chemical control					
% extraction Cu	1.57	10.23	3.46	-	-
% extraction Fe	6.33	2.83	2.67	7.33	5.05
final pH	3.4	4.1	3.2	2.4	3.2
B. *T. ferrooxidans* SM-4					
% extraction Cu	11.13	14.48	12.22	-	-
% extraction Fe	6.37	22.61	32.16	29.87	49.32
final pH	2.4	2.1	2.1	2.1	2.1
C. *T. thiooxidans* SM-6					
% extraction Cu	0.82	10.32	5.80	-	-
% extraction Fe	5.53	1.68	5.08	9.47	13.07
final pH	3.2	3.0	2.2	2.1	2.1
D. Mixed culture SM-4 + SM-6					
% extraction Cu	10.41	13.57	9.86	-	-
% extraction Fe	6.45	21.52	25.15	28.09	48.37
final pH	2.4	2.1	2.3	1.9	1.9

Shake-flask leaching of -140 mesh mineral samples (5g each mineral sample/ 100 mL HP medium) for 13 days at 25°C with (10%) or without inoculum.

Figure 25. Effect of *T. ferrooxidans* SM-4 and No. 1 pyrite on the leaching of Cu from chalcopyrite. Conditions are described in Table 5.

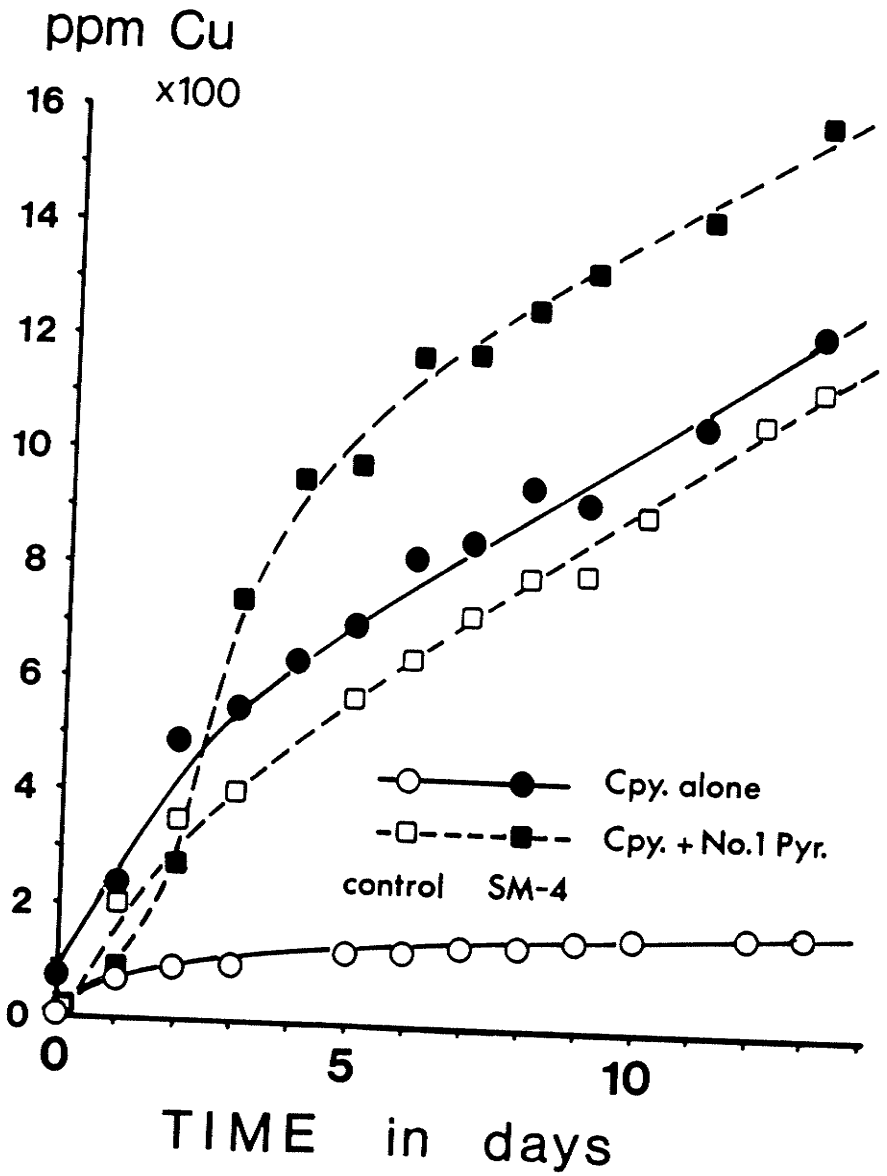
ppm Cu
x100
16
14
12
10
8
6
4
2
0
0
5
10
TIME in days
Cpy. alone
Cpy. + No.1 Pyr.
control
SM-4

Figure 26. Time-course shake-flask leaching of chalcopyrite in the presence of No. 1 pyrite with (A) and without (B) inoculation with *T. ferrooxidans* SM-4. Conditions are described in Table 5.

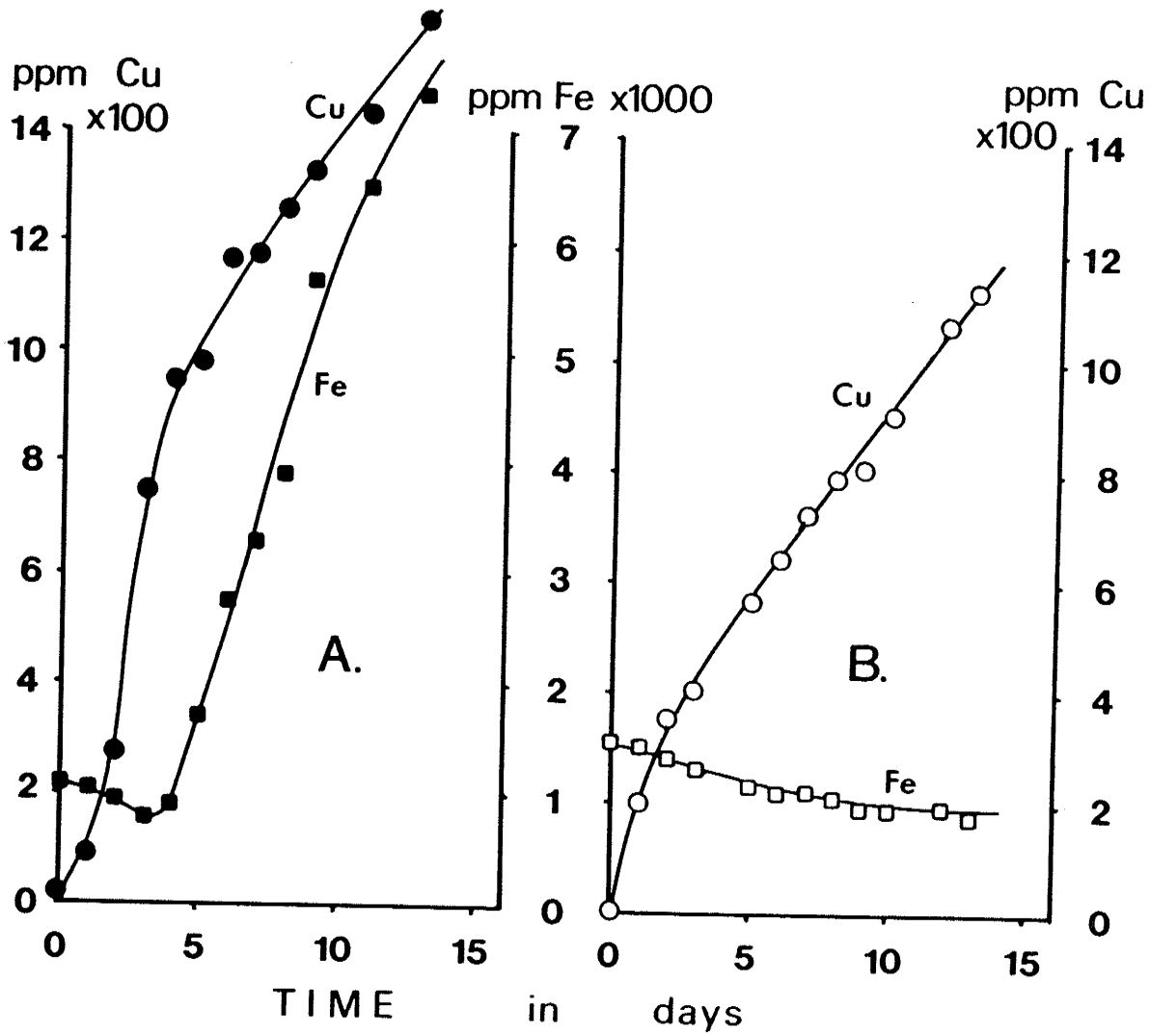
ppm Cu
x100
14
12
10
8
6
4
2
0
Cu
Fe
A.
0
5
10
15
TIME in days
ppm Fe x1000
7
6
5
4
3
2
1
0
ppm Cu
x100
14
12
10
8
6
4
2
0
Cu
Fe
B.
0
5
10
15

similar in both cases although the extent of leaching was greater with *T. ferrooxidans*. In contrast the soluble Fe decreased in the control flask (B), while it increased rapidly in the *T. ferrooxidans* flask after a lag of 3 - 4 days (A). Since the level of Fe leached was 4 to 5 times that of Cu after 10 - 13 days and the final pH was 2.1, the same as that with the pyrite alone (Table 5), *T. ferrooxidans* cells were probably growing mainly on pyrite, although the Cu extraction also increased. Both pyrite samples were leached much faster with *T. ferrooxidans* compared to the chemical control experiments (Table 5).

Leaching of chalcopyrite alone by *T. thiooxidans* SM-6 was less effective than the chemical control although the lower pH does suggest growth (Table 5). The lower Cu value may be explained by *T. thiooxidans* cells attaching to the chalcopyrite surface, blocking solubilization (see pyrite oxidation kinetic experiments). The addition of pyrite did stimulate leaching and did lower the pH, again indicating growth. This was especially true in the case of No. 2 pyrite, where both Cu and Fe extractions were significantly higher than the uninoculated control. *T. thiooxidans* cells may not be able to attack chalcopyrite but they had no trouble leaching pyrite although much more slowly than *T. ferrooxidans* cells (Table 5). The mixed culture (*T. ferrooxidans* SM-4 + *T. thiooxidans* SM-6) effectively leached chalcopyrite although not any more than the *T. ferrooxidans* culture alone. Only the No. 1 pyrite stimulated Cu extraction although Fe extraction increased with both pyrites. The extraction of Fe was still predominant over Cu, indicating preferential growth on pyrite (Table 5). The mixed culture did give the lowest pH for the pyrite flasks although the Fe extraction values were virtually the same as *T.*

ferrooxidans alone, indicating some sort of interaction taking place between *T. ferrooxidans* and *T. thiooxidans*, i.e. *T. thiooxidans* contributing to a faster sulfur or sulfide oxidation to sulfuric acid.

Sphalerite interaction with pyrite. As with chalcopyrite, sphalerite was tested for galvanic interactions with the two pyrite samples in shake-flask leaching experiments with no bacteria, the *T. ferrooxidans* isolate SM-4, the *T. thiooxidans* isolate SM-6, and a mixture of the two. These results are summarized in Table 6. In all cases (control, *T. ferrooxidans*, *T. thiooxidans*, and mixed culture), both pyrites greatly stimulated Zn extraction from sphalerite. In the chemical control experiments the No. 1 pyrite was much more effective than the No. 2 pyrite, again confirming the stronger galvanic interaction of the former with sphalerite as with chalcopyrite.

In contrast with the chalcopyrite experiments *T. thiooxidans* was effective in leaching sphalerite, increasing the Zn extraction 5 times over the chemical rate. Figure 27 shows the Zn and Fe leaching from a mixture of sphalerite and the No. 1 pyrite with (A) and without (B) *T. thiooxidans* inoculation. In both A and B the soluble Zn increased with time, but much faster in the presence of *T. thiooxidans*. The soluble Fe, on the other hand, decreased in the absence and only slightly increased in the presence of bacteria. The much higher Zn concentration achieved compared to the Fe concentration in Figure 27 indicates that sphalerite was leached preferentially over pyrite and suggests that *T. thiooxidans* cells were probably growing mainly on sphalerite.

In all sphalerite-pyrite mixtures tested (Table 6), the Fe extraction values were less than those in pyrite alone, i.e. sphalerite was

TABLE 6. Pyrite-sphalerite interaction during leaching

	ZnS alone	ZnS + No. 1 FeS_2	ZnS + No. 2 FeS_2	No. 1 FeS_2 alone	No. 2 FeS_2 alone
A. Chemical control					
% extraction Zn	1.57	12.98	5.76	-	-
% extraction Fe	-	1.17	2.05	7.33	5.05
final pH	2.5	4.1	4.1	2.4	3.2
B. *T. ferrooxidans* SM-4					
% extraction Zn	36.03	61.73	65.83	-	-
% extraction Fe	-	12.80	39.69	29.73	46.42
final pH	2.5	2.7	2.3	1.9	2.0
C. *T. thiooxidans* SM-6					
% extraction Zn	8.28	22.39	14.71	-	-
% extraction Fe	-	7.07	9.24	9.47	13.07
final pH	2.4	2.4	2.1	2.3	1.9
D. Mixed culture SM-4 + SM-6					
% extraction Zn	24.98	53.86	63.31	-	-
% extraction Fe	-	11.02	29.98	28.09	48.37
final pH	2.5	1.9	2.1	1.9	1.9

Shake-flask leaching of -140 mesh mineral samples (5g each mineral sample/ 100 mL HP medium) for 13 days at 25°C with (10%) or without inoculum.

Figure 27. Time-course shake-flask leaching of sphalerite in the presence of No. 1 pyrite with (A) and without (B) inoculation with *T. thiooxidans* SM-6. Conditions are described in Table 6.

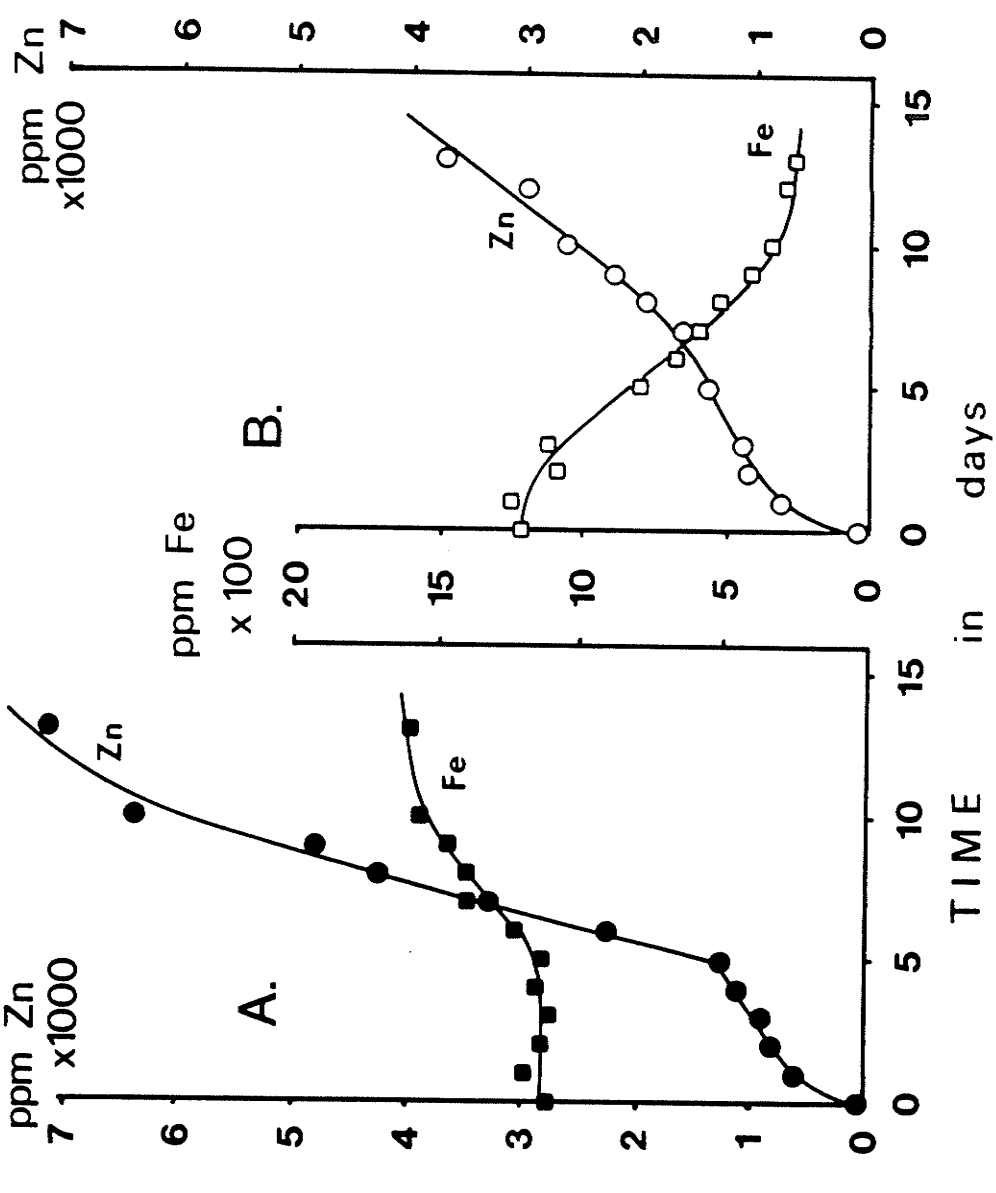
ppm Zn x1000
A.
Zn
Fe
ppm Fe x 100
B.
Zn
Fe
TIME in days

inhibiting the leaching of pyrite. These results agree with the concept that a galvanic interaction between the two minerals favours the solubilization of sphalerite. The depressed Fe extraction was smallest in the case of *T. thiooxidans* experiments, where cells were probably growing mainly on the sulfide portion of sphalerite and to a lesser degree on the pyrite sulfur-sulfide moieties. The galvanic effect may be less under those conditions.

T. ferrooxidans SM-4 was able to leach Zn from sphalerite after a lag period lasting for several days (Fig. 28), probably an adaptation period required to shift its metabolism from Fe^{2+} oxidation to the oxidation of the only substrate available: sulfide. The initiation of a logarithmic increase in Zn extraction (and probably the growth of bacteria) coincided with a temporary sudden decrease in the soluble Fe (supplied with the 10% inoculum of Fe^{2+}-grown culture). This temporary disappearence of Fe was also seen when pyrite was present (Fig. 28B), where it was followed by a rapid solubilization of Fe. This Fe leaching pattern seems to be characteristic of *T. ferrooxidans* leaching of sulfide minerals containing both sphalerite and pyrite as seen with ore leaching experiments (see Part II, Applied Studies). In some experiments (data not shown) where *T. ferrooxidans* failed to grow on sphalerite, this temporary Fe disappearence did not occur, indicating its significance. Pyrite had a positive effect in shortening the lag period required by *T. ferrooxidans* before the Zn leaching from sphalerite and also in increasing the rate of Zn extraction.

The best leaching of Zn was achieved with *T. ferrooxidans* (Table 6). In the presence of pyrite, the galvanic effect was evident, Zn extraction

Figure 28. *T. ferrooxidans* SM-4 time-course shake-flask leaching of sphalerite alone (A) and in the presence of No. 2 pyrite (B). Soluble Fe seen in (A) is from the 10% inoculum of Fe^{2+}-grown culture. Experimental conditions are described in Table 6.

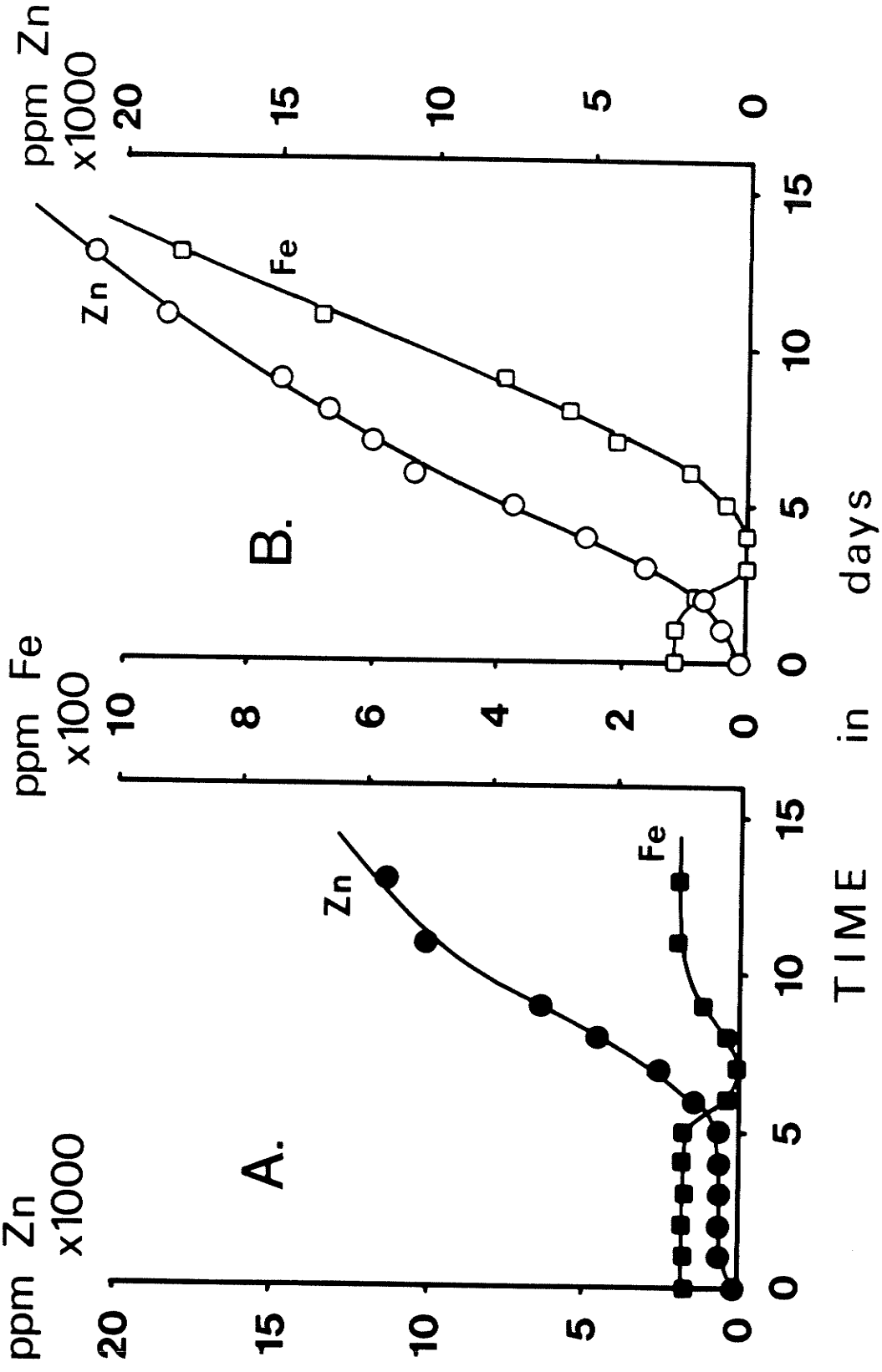
ppm Zn x1000
20
15
10
5
0
A.
Zn
Fe
ppm Fe x100
10
8
6
4
2
0
B.
ppm Zn x1000
20
15
10
5
0
Zn
Fe
0
5
10
15
TIME in days

doubling to over 60% at the expense of Fe extraction. Effective leaching of sphalerite was also seen with a mixed culture of *T. ferrooxidans* SM-4 + *T. thiooxidans* SM-6 although the metal extractions achieved were not as high as those of *T. ferrooxidans* alone (Table 6). Interestingly, however, the two pyrite samples had different effects on sphalerite leaching by the mixed culture (Fig. 29). In the presence of No. 1 pyrite, the mixed culture behaved as *T. thiooxidans* in that Zn extraction started without an adaptation period or a temporary Fe disappearence, little Fe was extracted, and a metallic sheen typical of *T. thiooxidans* could be seen on the liquid surface. In contrast, when No. 2 pyrite was present, leaching was typical of *T. ferrooxidans* in that a lag period occurred followed by a rapid Zn solubilization concurrent with a temporary Fe disappearence, an eventual high Fe extraction, and an abundance of ferric iron color and precipitate seen in the culture flask. This difference in leaching behaviour was also noticed with pyrite alone: Ferric iron color and precipitate was obvious with No. 2 pyrite but absent with No. 1 pyrite, where a metallic sheen was seen. The different pyrite samples, then, could predetermine the dominance of a particular organism in a mixed culture.

Warburg respirometer studies

Chalcopyrite oxidation. The oxidation of chalcopyrite in the presence or absence of pyrite was studied by measuring the steady-state rate of O_2 consumption (nmol O_2) for several hours with and without resting cells of *T. ferrooxidans* SM-4 and *T. thiooxidans* SM-6. The amount of Cu extracted after each experiment was also determined. The No. 1 and No. 2 pyrite samples were tested both in their untreated states and after thorough

Figure 29. Time-course shake-flask leaching of sphalerite in combination with No. 1 (A) or No. 2 (B) pyrite by a mixed culture of *T. ferrooxidans* SM-4 + *T. thiooxidans* SM-6. Conditions were as described in Table 6.

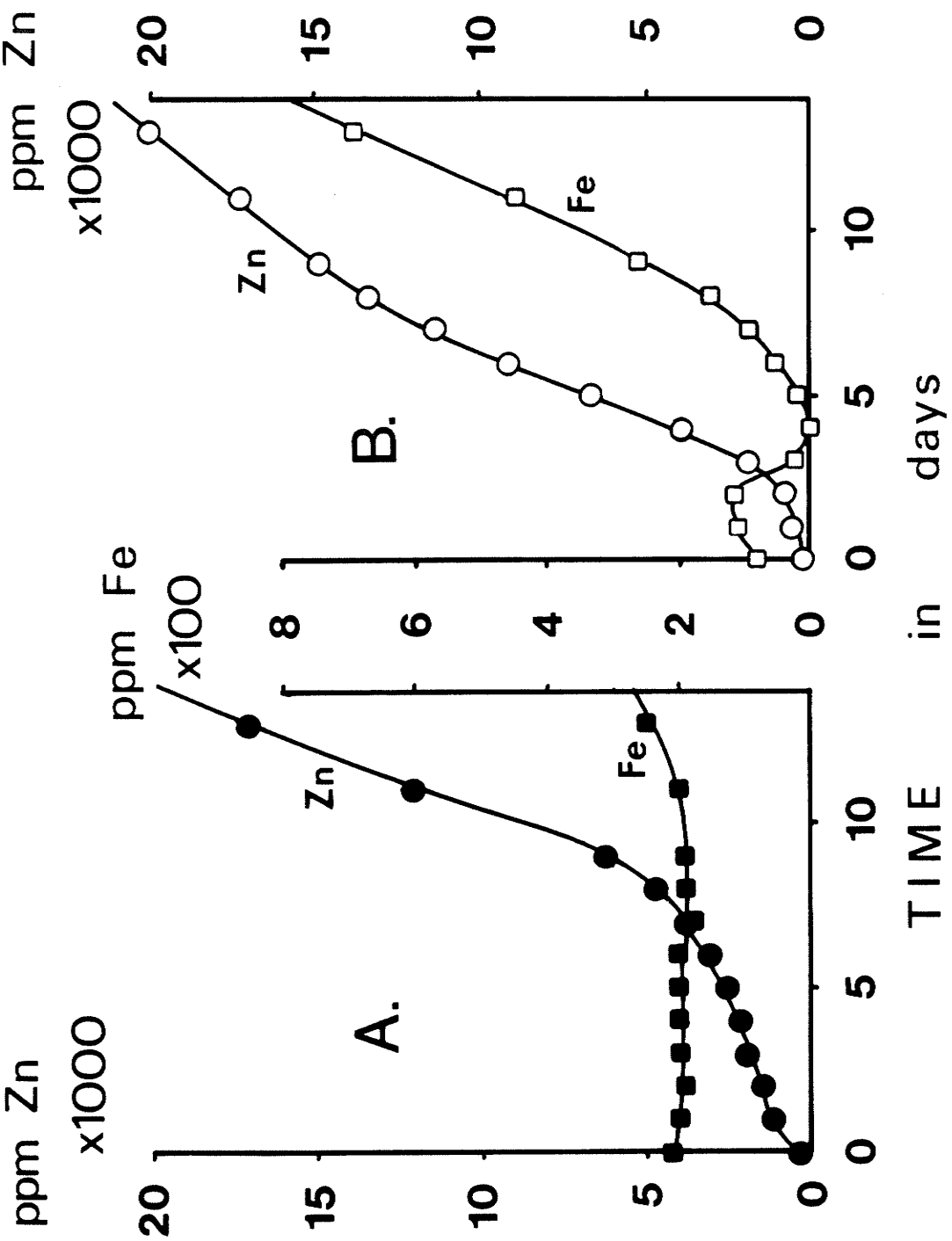
ppm Zn
x1000
20
15
10
5
0
A.
Zn
Fe
ppm Fe
x100
8
6
4
2
0
0
5
10
TIME in days
B.
Zn
Fe
ppm Zn
x1000
20
15
10
5
0
0
5
10

washing with HCl as described in Materials and Methods. This was done in order to rule out "artificial" effects by any acid soluble impurities that may have been present in the pyrite samples. The results are summarized in Table 7.

Both pyrites, untreated or HCl-washed, stimulated chemical as well as bacterial Cu extraction from chalcopyrite. Only No. 1 pyrite (both treated and untreated) stimulated the O_2 consumption of chalcopyrite (more than the sum of O_2 uptake by individual minerals) and only in the chemical and *T. thiooxidans* oxidation, except the untreated No. 2 pyrite with *T. ferrooxidans*. The O_2 uptake rate was much faster with *T. ferrooxidans* than *T. thiooxidans* in all experiments. Also in all experiments, *T. ferrooxidans* stimulated Cu extraction while *T. thiooxidans* inhibited it, probably by adhering to the mineral surface.

The O_2 uptake activity of *T. ferrooxidans* with pyrite was generally inhibited by chalcopyrite (activities less than the sum of individual minerals), except the untreated No. 2 pyrite, although the Cu extraction from chalcopyrite was always faster with pyrite. This could be due to some cells attaching to chalcopyrite, not being able to oxidize pyrite. The HCl-washed pyrite (both No. 1 and No. 2) showed the identical O_2 uptake with *T. ferrooxidans* and with or without chalcopyrite. The O_2 uptake by *T. thiooxidans* with No. 1 pyrite was stimulated by chalcopyrite as mentioned above, but that with No. 2 pyrite was inhibited by chalcopyrite. The chemical oxidation of pyrite was also stimulated by chalcopyrite only with the No. 1 pyrite. This may be due to the stronger galvanic effect exerted by No. 1 pyrite which would provide sulfide (through chalcopyrite corrosion) for either chemical or *T. thiooxidans* oxidation.

TABLE 7. Pyrite-Chalcopyrite interaction during oxidation by resting cells

	Steady-state O_2 uptake (nmol O_2/minute)			% extraction Cu		
	Chemical	SM-4	SM-6	Chemical	SM-4	SM-6
A. Untreated pyrites						
$CuFeS_2$ alone	2.2	7.7	2.9	0.35	1.71	0.29
#1 FeS_2 alone	5.0	65.0	4.6	-	-	-
#2 FeS_2 alone	4.4	109.1	13.6	-	-	-
$CuFeS_2$ + #1 FeS_2	11.4	41.7	14.2	1.52	2.97	0.68
$CuFeS_2$ + #2 FeS_2	6.7	128.8	12.1	1.11	2.29	0.74
B. HCl-washed pyrites						
$CuFeS_2$ alone	2.2	40.0	2.1	0.54	2.33	0.25
#1 FeS_2 alone	2.2	94.0	5.4	-	-	-
#2 FeS_2 alone	5.3	94.0	33.2	-	-	-
$CuFeS_2$ + #1 FeS_2	6.7	94.0	9.1	1.36	2.68	0.72
$CuFeS_2$ + #2 FeS_2	6.7	94.0	22.5	1.45	3.36	0.54

Oxidation of -140 mesh mineral samples (100 mg each mineral sample/3.2 mL reaction mixture) for several hours at 30°C in a Warburg respirometer. Extraction of Cu was determined by analysis of the reaction mixture at the end of the experiment. SM-4 and SM-6 correspond to *T. ferrooxidans* SM-4 and *T. thiooxidans* SM-6, respectively. Cells were present at a concentration of 10 mg wet cells in 3.2 mL reaction mixture.

Sphalerite oxidation. As with the chalcopyrite experiments, sphalerite oxidation in the presence or absence of pyrite was measured in nmol O_2 per minute with and without resting cells of *T. ferrooxidans* SM-4 and *T. thiooxidans* SM-6. Both untreated and HCl-washed samples of No. 1 and No. 2 pyrites were used. The solubilization of Zn was determined at the end of each experiment. Table 8 summarizes the results from the pyrite-sphalerite experiments.

Both pyrites, untreated and HCl-washed, stimulated Zn extraction and O_2 uptake activity during chemical oxidation of sphalerite, untreated pyrites slightly more than washed pyrites. As expected, more Zn solubilization was seen with the No. 1 pyrite (washed and unwashed). *T. ferrooxidans* cells on sphalerite alone displayed very low O_2 uptake activity and Zn extraction values that were less than those of the controls. The iron-grown *T. ferrooxidans* cells were probably not capable of effectively oxidizing sphalerite during the short incubation time (see adaptation periods on Fig. 28) and might have been inhibiting Zn extraction by attaching to the mineral surface. Sphalerite inhibited the oxidation of untreated and HCl-washed pyrites by *T. ferrooxidans* as seen by the reduced O_2 uptake activities. Again, this was probably due to cells attaching to sphalerite thus being unavailable for pyrite oxidation. Extraction of Zn on the other hand, increased dramatically when pyrite was available to *T. ferrooxidans* cells: the values were twice as much as the bacteria-free sphalerite-pyrite mixtures and the stimulating effect by pyrite (compared to sphalerite alone) was greater with *T. ferrooxidans*. *T. ferrooxidans* oxidation of pyrite then, enhanced the galvanic effect.

T. thiooxidans was active on sphalerite in terms of both O_2 uptake

TABLE 8. Pyrite-Sphalerite interaction during oxidation by resting cells

	Steady-state O_2 uptake (nmol O_2/minute)			% extraction Cu		
	Chemical	SM-4	SM-6	Chemical	SM-4	SM-6
A. Untreated pyrite						
ZnS alone	0.8	2.5	18.1	0.49	0.30	1.06
#1 FeS_2 alone	5.6	90.0	3.6	-	-	-
#2 FeS_2 alone	4.2	107.3	8.5	-	-	-
ZnS + #1 FeS_2	21.9	40.0	37.3	2.02	3.83	1.51
ZnS + #2 FeS_2	11.1	37.5	37.3	1.38	2.82	1.32
B. HCl-washed pyrite						
ZnS alone	0.8	1.8	21.7	0.38	0.31	1.12
#1 FeS_2 alone	3.3	103.3	6.2	-	-	-
#2 FeS_2 alone	4.3	123.3	30.7	-	-	-
ZnS + #1 FeS_2	15.3	74.5	61.5	1.47	3.20	1.80
ZnS + #2 FeS_2	6.2	100.0	38.7	0.88	2.14	1.10

Oxidation of -140 mesh mineral samples (100 mg each mineral sample/3.2 mL reaction mixture) for several hours at 30°C in a Warburg respirometer. Extraction of Cu was determined by analysis of the reaction mixture at the end of the experiment. SM-4 and SM-6 correspond to *T. ferrooxidans* SM-4 and *T. thiooxidans* SM-6, respectively. Cells were present at a concentration of 10 mg wet cells in 3.2 mL reaction mixture.

and Zn extraction. The sulfur-grown cells obviously had no trouble in oxidizing this sulfide mineral and would require no adaptation for growth in it (see Fig. 27). Both untreated pyrites stimulated O_2 uptake (activities were more than additive) and Zn extraction during sphalerite oxidation, although the extraction effect was actually less than the uninoculated controls. The HCl-washed No. 1 pyrite stimulated O_2 uptake during sphalerite oxidation but the No. 2 pyrite did not. The Zn extraction values with the washed pyrites were higher than the controls although this may be due less to galvanic effects than to a faster oxidation (higher O_2 uptake rates for *T. thiooxidans* in Table 8). Overall, it would seem that *T. thiooxidans* was minimizing or even inhibiting pyrite-sphalerite interactions. This could be happening by the removal of sulfide from sphalerite through oxidation, thus raising the electrode potential of the mineral.

DISCUSSION

The *T.ferrooxidans* mine isolate SM-4 showed an unusual cell concentration effect on the apparent K_m for Fe^{2+} in the oxidation of ferrous iron. The effect is best explained by the assumption that *T. ferrooxidans* cells competitively inhibit other *T. ferrooxidans* cells by competing with Fe^{2+} for the Fe^{2+}-binding site of the active cells. The laboratory strain ATCC 19859 did not show this effect, maintaining the same K_m value for Fe^{2+} at different cell concentrations. Thus, they did not inhibit the binding of Fe^{2+} to the Fe^{2+}-oxidizing sites at the concentrations used.

The reason for the competitive inhibition observed may lie in the unusual surface properties of *T. ferrooxidans* cells. These are believed to be covered with a ferric iron coat complex on their surface (31, 33). *T. ferrooxidans* cells are known to adsorb on solid surfaces and the adsorption is found to be inhibitory to their Fe^{2+} oxidizing activity (80). The inhibitory component could be the Fe^{3+} coat on the cell surface, since soluble Fe^{3+} competitively inhibits the Fe^{2+} oxidizing activity of *T. ferrooxidans* (39). The observed competitive inhibition by heat-inactivated cells agrees with the postulate. Heat-killed cells of *T. ferrooxidans* have been reported to adsorb on solid surfaces (80).

The difference between the laboratory strain and the mine isolate may indicate a difference in their cell surface properties. The ATCC strain has been maintained in a medium with high concentrations of soluble iron for many years while the recently isolated SM-4 strain has been living in contact with mineral surfaces such as pyrite until recently

(see Part II: Applied Studies). The former may have lost some of the adsorption properties, requiring higher concentrations of cells for inhibition than those used in this study.

We can say that there are complex interactions during Fe^{2+} oxidation by *T. ferrooxidans* among: the cells as the Fe^{2+} catalyst; Fe^{2+} as the substrate; Fe^{3+} as the product of oxidation and a competitive inhibitor of Fe^{2+} oxidation; and the cells as also a competitive inhibitor of Fe^{2+} oxidation. These interactions will all affect the rate of bacterial leaching of sulfide minerals in addition to other factors such as air supply, temperature, pH, and toxic minerals.

The results indicate that with the *T. ferrooxidans* isolate SM-4 both cells and Fe^{3+} act as competitive inhibitors of Fe^{2+} in its oxidation by cells and the inhibition is not mutually exclusive. Both inhibitors (cell and Fe^{3+}) can bind the Fe^{2+} oxidizing system simultaneously, resulting in a stronger inhibition than by each one separately due to the formation of an additional inactive form (EIX or cell-cell-Fe^{3+}). The binding of the second inhibitor (cell or Fe^{3+}), however, is inhibited by the first inhibitor (Fe^{3+} or cell) since the α value obtained is higher than 1. Therefore the apparent inhibition constants increase with increasing concentration of the other inhibitor.

During growth of *T. ferrooxidans* cells in an aqueous Fe^{2+} medium, the rate of Fe^{2+} oxidation will be governed by the Michaelis Menten equation, $v = k_3'[C]/([FeS_2] + K_m)$ (43), initially, but when the concentration of cells and Fe^{3+} increase the apparent K_m value will increase due to the competitive inhibition by cells and Fe^{3+}. The high concentration of Fe^{2+} in the normal growth medium will be essential to

overcome this effect. During leaching, this effect will be compensated by the chemical precipitation of Fe^{3+} as insoluble ferric hydroxysulfate or jarosite, removing it from solution. Further, the indirect leaching by Fe^{3+} (46, 73) will reduce the Fe^{3+} concentration, reducing the inhibitory effect.

The K_m, K_i', and K_{if} values shown in Table 2 are the minimum values and considerably smaller than those reported for apparent K_m values of 0.33 to 9.4 mM [Fe^{2+}] or higher (39, 71); for apparent K_{if} values of 1.2 to 28 mM [Fe^{3+}] (39, 71); and the K_i' value of 0.33 mg wet cells per mL for *T. ferrooxidans* SM-4 reported in Table 1. The last value was perhaps higher because of the lower activity of the cells (k_3' was 125 instead of 200 nmol O_2/minute per mg wet cells per mL for Tables 1 and 2, respectively) or simply due to the different batches of cells used.

It is interesting that the Fe^{3+} inhibition of Fe^{2+} oxidation by *T. ferrooxidans* was reported to be less pronounced at lower temperatures (41). The apparent K_{if} value dramatically increased (15 fold) when the temperature was lowered from 27°C to 5°C. Perhaps the secondary binding of inhibitor to form EIX is more dificult at lower temperatures.

During the study of pyrite oxidation by *T. ferrooxidans*, an attempt was made to understand the chemical reactions taking place alongside those carried out by bacteria. The spontaneous solubilization of pyrite was observed to be inhibited by the adsorption of active and heat-killed *T. thiooxidans* cells. Comparison of Fe^{2+} release and O_2 uptake measurements during pyrite dissolution ($FeS_2 + H^+ \rightarrow Fe^{2+} + HS^- + S^o$) indicated that most of the HS^- produced was not being oxidized by oxygen to sulfur, probably due to the very slow oxidation rate at this pH and the possible formation of polysulfides (52).

The oxidation of pyrite by ferric iron was more interesting. Ferric iron-induced Fe^{2+} release followed a typical saturation kinetics where the formation of a FeS_2-Fe^{3+} complex was the rate-limiting step, Fe^{3+} acting as a catalyst (although it is also a substrate). The nature of this FeS_2-Fe^{3+} reactive complex is both interesting and elusive. It has been proposed that the Fe^{3+} attack on pyrite is a sequential surface reaction where a sulfoxy anion is formed and dissociates from the crystal lattice (53). This theory, however, assumes that the Fe-S bond is weaker than the S-S bond when the reality is in fact the opposite (3). Another postulate is that Fe^{3+} oxidizes $-SH^{\partial-}$ surface states formed through a chemical reaction between H^+ and the sulfide surface (77). Our results do not disagree with the latter theory. The first sulfur atom (probably in the form of a $-SH^{\partial-}$ surface state) is probably removed quite easily by the first Fe^{3+} while the removal of the second sulfur atom is more difficult. The attachment of the second Fe^{3+} to the second sulfur atom could be reversible, explaining the saturation kinetics observed.

The *T. ferrooxidans* mine isolate SM-4 oxidized pyrite effectively under the experimental conditions used. The kinetics observed, however, depended on whether the pyrite sample had been washed previous to the experiment. The experiments with washed pyrite showed classical Michaelis Menten kinetics (43) whereas the experiments with the unwashed pyrite showed the cell-cell competitive inhibition effect seen with Fe^{2+} oxidation.

In contrast to the Fe^{2+} oxidation experiments, the K_m value for washed pyrite did not change with cell concentration. The *T. ferrooxidans* SM-4 cells did not competitively inhibit other cells by competing with

pyrite for the "pyrite-binding site" of active cells. The difference between Fe^{2+} oxidation and pyrite oxidation in *T. ferrooxidans* SM-4 suggests that the Fe^{2+} binding site and the pyrite binding site for the bacteria may be altogether different. The cells are probably binding to to the pyrite surface rather than oxidizing solubilized ferrous iron. Table 3 lists the rate and kinetic constants for pyrite oxidation in this study. The K_m for both indirect leaching and bacterial oxidation are similar. The rate constants (k_3 values), however, are very different: the k_3 value for the bacteria with washed pyrite was 90 μM O_2 consumed per minute per mg wet cells per mL, a value 40 times that for the indirect leaching reaction.

The interpretation of the results obtained with the unwashed pyrite sample is more difficult. Because of the rapid initial release of Fe^{2+} (probably due to other Fe-S impurities) by unwashed pyrite upon contact with the reaction mixture, the cells were encountered with 2 mM Fe^{2+} per PD pyrite at the start of the reaction. This large amount of soluble iron was rapidly oxidized by the cells (as seen by rapid initial O_2 uptake before steady-state was achieved). This means that at the start of the steady-state rate, there was at least 2 mM Fe^{3+} per PD pyrite available for indirect leaching, compared to basically zero Fe^{3+} present at the start of the steady-state rate for the washed pyrite sample (the same as the start of the reaction).

During oxidation by *T. ferrooxidans* SM-4, the apparent K_m for the unwashed pyrite increased with cell concentration, analogous to the experiments with Fe^{2+}. The K_i' seen with the unwashed pyrite is almost identical to that seen with Fe^{2+} (see Table 2). Because this effect was

not seen with washed pyrite, the bacterial oxidation of some other substrate must have been inhibited competitively by *T. ferrooxidans* cells. This other substrate could have been Fe^{2+} produced by indirect leaching, but as discussed below the rate of indirect leaching alone could not have been fast enough. It is possible that sulfur or sulfide species released in large amounts along with Fe^{2+} from the unwashed pyrite could have elicited the same effect in *T. ferrooxidans* (see experiments with *T. thiooxidans*). If *T. ferrooxidans* were oxidizing Fe^{2+} and soluble sulfur or sulfide it would help explain the 3-fold higher k_3' value seen with unwashed pyrite as opposed to washed pyrite.

Table 9 combines the pyrite and Fe^{2+} kinetic informations to determine and compare oxidation rates at different pulp densities of pyrite. Assuming cell concentrations of either 0.1 or 1.0 mg wet cells per mL, the bacterial pyrite oxidation rates (both washed and unwashed) cannot be accounted for by the oxidation of soluble Fe^{2+} produced by spontaneous pyrite dissolution plus indirect leaching . At low cell concentrations, the rates were faster with the unwashed pyrite while the opposite was true for high cell concentrations due to the cell-cell competitive inhibition effect with unwashed pyrite (Table 9). A trend is seen in Table 9 that at high enough pulp densities, the rate of pyrite oxidation at low cell concentrations could be accounted for by the amounts of soluble Fe^{2+} available by chemical processes. This, however, does not take into account inhibition of *T. ferrooxidans* cells by Fe^{3+}.

The oxidation rates of unwashed pyrite oxidation by *T. thiooxidans* SM-6 were much slower than those of *T. ferrooxidans*. According to the results obtained, this was not only due to a slower rate constant but

TABLE 9. Comparison of chemical and bacterial pyrite reactions

[FeS_2]	Spontaneous dissolution	Indirect leaching	Maximal bacterial Fe^{2+} oxidation	Bacterial pyrite oxidation		Ratio of pyrite/Fe^{2+} oxidation	
PD	μM Fe^{2+} produced/ minute	μM Fe^{2+} produced/ minute	μM O_2 consumed/ minute	μM O_2 consumed/ minute			
				mg cell/mL		mg cell/mL	
				0.1	1.0	0.1	1.0
A. Washed pyrite							
1.25	4.35	-	1.1	3.0	30.0	2.7	27.3
2.50	8.70	-	2.2	4.5	45.0	2.0	20.5
3.13	10.88	-	2.7	5.0	50.0	1.9	18.5
5.00	17.40	-	4.4	6.0	60.0	1.4	13.6
B. Unwashed pyrite							
1.25	4.35	9.15	3.4	5.5	13.6	1.6	4.0
2.50	8.70	26.22	8.7	9.0	25.8	1.1	3.0
3.23	10.88	35.88	11.7	10.4	31.4	0.9	2.7
5.00	17.40	66.9	21.1	13.3	46.8	0.6	2.2

The rates were calculated on the basis of equations shown on Table 3. For the indirect leaching rates, a negligible [Fe^{3+}] was assumed for the washed pyrite. For the unwashed pyrite, a [Fe^{3+}] of 2 mM per PD pyrite was assumed (as confirmed by rapid Fe^{2+} release). For the bacterial Fe^{2+} oxidation rates, an infinite cell concentration was assumed to oxidize an amount of Fe^{2+} equal to that produced by spontaneous dissolution plus indirect leaching.

also to a very pronounced cell-cell competitive inhibition effect (K_i' was 0.05 mg wet cells per mL).

Since sulfur species were not analyzed in this study, it is difficult to interpret the *T. thiooxidans* data. From the rapid initial release of Fe^{2+} from the unwashed pyrite, it follows that a great deal of sulfur or sulfide is also released. In other words, as much as 4 mM of sulfur/sulfide per PD pyrite would have been present at the start of the reaction (introduction of cells into the reaction mixture). Although the rapid initial O_2 uptake rates were probably due to the oxidation of soluble sulfide, it is not clear whether at steady-state *T. thiooxidans* was oxidizing released sulfur species in addition to pyrite. Because *T. thiooxidans* must come into contact with sulfur or sulfide in order to oxidize it (72), a cell-cell competitive inhibition effect could theoretically occur with both substrates (pyrite and released sulfur species).

The oxidation of sulfide minerals by bacteria is a complex process involving many non-biological reactions such as spontaneous or chemical reactions, indirect action by Fe^{3+}, and electrochemical interactions of minerals as well as bacterial action on minerals and products of non-biological reactions as described earlier.

The results in Tables 5 and 6 present some insight into the reactions associated with the oxidations of pyrite, chalcopyrite, and sphalerite (see also Historical on Part II, Applied Studies). Chemical control experiments of a single mineral showed that the spontaneous chemical dissolutions of these three minerals were slow. The solubilization rates of Cu or Zn dramatically increased when pyrites were present with

chalcopyrite or sphalerite clearly due to the electrochemical interactions favouring the oxidation of the mineral with the lowest electrode potential (EP). The EP values according to Karavaiko (35) are: 0.6, 0.5, and 0.23 Volts for pyrite, chalcopyrite, and sphalerite. Thus in the presence of pyrite, chalcopyrite and sphalerite will be oxidized by the anodic half-reactions: $CuFeS_2 \rightarrow Cu^{2+} + Fe^{2+} + 2S^o + 4e-$ and $ZnS \rightarrow Zn^{2+} + S^o + 2e-$. The cathodic half-reaction on the pyrite surface will reduce O_2: $O_2 + 4H^+ + 4e- \rightarrow 2H_2O$. As expected from the lower EP value the galvanic effect was stronger with sphalerite than chalcopyrite. Of the two pyrites tested, the No. 1 pyrite sample showed a much stronger effect, suggesting a possibly higher EP value, although not determined in this study. The results of short-term resting cell experiments (Tables 7 and 8) also support the stronger effect by No. 1 pyrite both in the oxidation and the metal solubilization.

The inoculation with *T. ferrooxidans* SM-4 led to a dramatic increase in the solubilization of Cu from chalcopyrite, Fe from pyrite, or Zn from sphalerite (Tables 5 and 6), although the last required an adaptation period (Fig. 28). Clearly the Fe^{2+} oxidation by *T. ferrooxidans* coupled to the indirect leaching by Fe^{3+} must have played a major role here. *T. thiooxidans* SM-6, however, increased only the solubilization of Zn from sphalerite and to a lesser extent Fe from pyrite, but inhibited the Cu extraction from chalcopyrite. The oxidation experiments in Tables 7 and 8 also showed that *T. thiooxidans* cells oxidized sphalerite and some pyrite (No. 2), but not chalcopyrite.

When pyrite was present the Cu solubilization from chalcopyrite was was further stimulated by *T. ferrooxidans*, but the rate was not much more

than that from chalcopyrite with *T. ferrooxidans* (Tables 5 and 6). *T. thiooxidans* did not enhance the Cu solubilization from chalcopyrite with pyrite. The Zn extraction from sphalerite in the presence of pyrite, on the other hand, was stimulated considerably by inoculation with *T. ferrooxidans* or *T. thiooxidans* (more with *T. ferrooxidans*). The rates were close to the sums of the chemical control rates of ZnS plus pyrite (galvanic interaction) and the bacterial leaching rates from ZnS alone.

In all these leaching experiments with chalcopyrite it is interesting that the extraction of Cu and Fe did not follow the stoichiometry expected of $CuFeS_2$ (Table 5). In the chemical control or with the *T. thiooxidans* inoculation Fe was solubilized faster than Cu, while with the *T. ferrooxidans* or *T. ferrooxidans* plus *T. thiooxidans* inoculation Cu was solubilized faster than Fe. These results suggest that when $CuFeS_2$ was solubilized, Cu or Fe released sometimes formed insoluble precipitates or minerals. On the study of bacterial leaching of chalcopyrite with and without pyrite or pyrrhotite (FeS), Ahonen et al. (2) reported a positive effect of pyrite on Cu leaching, but a depressing effect of pyrrhotite. They suggested a possible formation of covelite (CuS) as the cause. The lower yield of soluble Cu in Table 5 may be caused by a similar mechanism. The lower yield of soluble Fe with *T. ferrooxidans* may be related to the Fe^{3+} state of Fe which may form insoluble ferric hydroxide or jarosite.

PART II

APPLIED STUDIES

Part of this work is available elsewhere:

Hector M. Lizama and Isamu Suzuki. Bacterial Leaching of a Sulfide Ore by *Thiobacillus ferrooxidans* and *Thiobacillus thiooxidans*: I. Shake Flask Studies. Biotechnology and Bioengineering. 1988, Vol. 32, pp. 110-116.

I. Suzuki, H. Lizama, J.K. Oh, and P.D. Tackaberry. Complex Sulphide Base Metal Leaching and Economics. Biominet Proceedings SP87-10, CANMET, Ottawa. Ed. R.G.L. McCready. 1987. pp. 57-73.

Isamu Suzuki, Hector M. Lizama, and Jae Key Oh. Bacterial Leaching of a Complex Sulphide Ore. Biominet Proceedings SP86-9E, CANMET, Ottawa. Ed. R.G.L. McCready. 1986. pp. 127-146

Hector M. Lizama and Isamu Suzuki. Bacterial Leaching of a Sulfide Ore by *Thiobacillus ferrooxidans* and *Thiobacillus thiooxidans* Part II: Column Leaching Studies. Hydrometallurgy. 1989, Vol. 22 (in press).

INTRODUCTION

A bacterial leaching pre-feasibility study for the ore remnants of the Flin Flon mine of Hudson Bay Mining and Smelting Co., Ltd. was carried out under the auspices of the Canada-Manitoba Mineral Development Agreement. The study was carried out using indigenous strains of *T. ferrooxidans* and *T. thiooxidans* isolated from the mine itself. These bacterial isolates as well as laboratory strains of *T. ferrooxidans* and *T. thiooxidans* were tested for growth on a finely-ground mixed sulfide ore containing pyrite, chalcopyrite, and sphalerite. Successful strains which showed good bacterial leaching ability were further tested on percolating columns with coarser-ground ore. In these experiments, ore was used alone or in combination with sand, smelter slag, or tailings to simulate the conditions encountered in the back-filled stopes of the Flin Flon mine. The results suggested that *T. ferrooxidans* and *T. thiooxidans* leach sulfide ores by different mechanisms and opened up a possibility of preferential leaching of Cu or Zn by choice of organism and leaching conditions.

From the column leaching experiments, a mixed culture of *T. ferrooxidans* and *T. thiooxidans* was selected for further experiments to test the effect of ore particle size on the leaching rates. A relationship could then be established which could be used to predict *in-situ* bacterial leaching activity in the back-filled stopes of the Flin Flon mine. In order to confirm this, a large-scale column leaching experiment using 1.8 tons of ore (particle size 6 to 8 inches in diameter) was carried out for several months.

HISTORICAL

The role of bacteria in leaching

The solubilization of Cu from ores was carried out for several centuries before the involvement of bacteria was established (6, 47). With time, the use of microorganisms for the extraction of valuable metals from sulfide ores has increased in importance. To date, bacterial leaching has been mostly confined to the production of Cu and U (13, 47), although it could be expanded to cover all sulfide minerals.

Most leaching studies to date have concentrated on *T. ferrooxidans*, this being mainly due to the production of ferric sulfate by this organism. However, it has been shown that the presence of other thiobacilli in addition to *T. ferrooxidans*, particularly the acidophile *T. thiooxidans*, results in enhanced leaching (12). Indeed, the oxidation of sulfur has been shown to be extremely important in leaching operations. Sulfur deposition on the mineral surface has been known to slow down or even stop the leaching process (12). Thus, *T. thiooxidans* is indispensable for exposing the mineral surface for further leaching by oxidizing the sulfur to sulfuric acid (12). At the same time, the production of sulfuric acid prevents the total precipitation of Fe^{3+} and permits the proton-dependent growth of *T. ferrooxidans* (38).

The mechanism of bacterial action on the sulfide mineral is still not completely understood. Bacteria are thought to attack the sulfide mineral both directly and indirectly by the production of Fe^{3+} and H_2SO_4 (35, 46). Experiments with synthetically prepared sulfide minerals showed that bacteria successfully solubilized metal in the absence of iron (30,

74), although extraction could be doubled in its presence. Scanning electron micrographs showed bacterial attachment to sulfide mineral surfaces in the presence of nutrients (7, 9, 46). Attachment appeared to be specific to the sulfide moiety of the mineral, causing pitting and corrosion of the mineral surface.

Through their unique metabolism, mineral leaching bacteria have proven to be great catalysts in the extraction of metals. Because they are living systems, however, bacterial activity depends on a number of physical and environmental factors. Bacterial leaching was found to be optimal between the temperatures of 25°C and 45°C (38, 46). The limits of bacterial oxidation occurred at 10°C and 55°C although chemical oxidation does occur above 55°C (46). The optimum pH for the oxidation of Fe^{2+}, FeS_2, $CuFeS_2$, and ZnS by *T. ferrooxidans* was found to be between 1.0 and 2.5 even though the bacteria can be active at slightly higher pH (46, 60).

T. ferrooxidans and *T. thiooxidans* are strict aerobes and thus require oxygen for activity. The greatest number of sulfur and iron oxidizing thiobacilli were always found at the surface of leaching dumps (30, 36). The availability of substrate is also important, the largest bacterial populations always being associated with finely ground ore (30). This is because more surface area of sulfide mineral is exposed with smaller particles. If the ore particle size was decreased too much, however, the surface area of the gangue (waste rock) also increased to the point of diluting the substrate (20, 46). Among the nutritional requirements of *T. ferrooxidans* and *T. thiooxidans* were the mineral salts of NH_4, SO_4^{2-}, K^+, PO_4^-, Mg^{2+}, and Ca^{2+}. Some of these and other trace elements were usually supplied by impurities in the ore (46). The carbon

source requirements were fulfilled by CO_2 from the atmosphere (18, 26, 46).

The bacterial leaching process could be inhibited by a number of factors. *T. ferrooxidans* was greatly resistant to high concentrations of Cu, Zn, Ni, Co, Mn, and Al although inhibited by the anions of As, Se, and Te (30, 48, 78). Silver and mercury have been found to be toxic for *T. ferrooxidans* and *T. thiooxidans* at μM concentrations (30). Leaching could also be slowed down or stopped altogether by the deposition of $CaSO_4$ (from calcium carbonate in the ore reacting with H_2SO_4), ferric precipitates, and elemental sulfur on the mineral surface (12). The sulfur oxidation and the production of acid to keep Fe^{3+} in solution are important to reduce the last two problems.

Chemical reactions involved in bacterial leaching

The oxidation of pyrite by *T. ferrooxidans* is generally expressed by the following reactions (47):

$$2FeS_2 + 7O_2 + 2H_2O \xrightarrow{\text{bacteria}} 2\ FeSO_4 + 2H_2SO_4$$

$$FeS_2 + Fe_2(SO_4)_3 \rightarrow 3FeSO_4 + 2S$$

$$4FeSO_4 + O_2 + 2H_2SO_4 \xrightarrow{\text{bacteria}} 2Fe_2(SO_4)_3 + 2H_2O$$

$$2S + 3O_2 + 2H_2O \xrightarrow{\text{bacteria}} 2H_2SO_4$$

All the reactions are oxidative and equivalent to the overall chemical oxidation reaction of pyrite:

$$2FeS_2 + 7\tfrac{1}{2}O_2 + H_2O \rightarrow Fe_2(SO_4)_3 + H_2SO_4$$

T. ferrooxidans then, is really acting as a microbial catalyst, lowering the activation energy of the reaction and greatly accelerating it (47). *T. thiooxidans* would only be able to catalyze the first and last of the

reactions mentioned above.

Chalcopyrite is the most common copper-containing sulfide mineral although it is also the most difficult to oxidize (35, 38). Its oxidation by *T. ferrooxidans* can be described by the reactions (47):

$$2CuFeS_2 + 8\tfrac{1}{2}O_2 + H_2SO_4 \xrightarrow{\text{bacteria}} 2CuSO_4 + Fe_2(SO_4)_3 + H_2O$$

$$CuFeS_2 + 2Fe_2(SO_4)_3 \rightarrow CuSO_4 + 5FeSO_4 + 2S$$

in addition to the oxidation of $FeSO_4$ and S shown for the pyrite oxidation. Detailed studies of chalcopyrite oxidation by *T. thiooxidans* have not been carried out but the bacterium probably attacks the sulfide moiety or the elemental sulfur formed by the reaction with Fe^{3+}.

The zinc-containing mineral sphalerite can be oxidized by both *T. ferrooxidans* and *T. thiooxidans* (35). Its oxidation can be expressed by the reaction:

$$ZnS + 2O_2 \rightarrow ZnSO_4$$

T. thiooxidans was more effective at leaching sphalerite than *T. ferrooxidans* (35), probably because the former was more effective at sulfide oxidation. The presence of Fe^{3+} has been known to intensify leaching of sphalerite by *T. ferrooxidans* (35).

As shown in the above reactions, Fe^{3+} is a powerful oxidant (30) and participates in the solubilization of probably all sulfide minerals. At the same time, Fe^{3+} plays a very important role in maintaining an acid pH. In response to a rise in pH, ferric sulfate undergoes a series of hydrolytic reactions in which complex ferric hydroxides are formed, regenerating acid (75). The ferric hydroxide salts precipitate as jarosite:

$$3Fe^{3+} + 3H_2O + 2SO_4^{2-} + A \rightarrow A[Fe(SO_4)\cdot 2Fe(OH)_3] + 3H^+$$

where A = H_3O^+, NH_4, K^+, Na^+, etc.

Electrochemistry of bacterial leaching

Studies on the chemical oxidation of sulfide minerals showed that their rate of oxidation depended on their solubility product (76). In the presence of acid, the polar chemical bonds were weakened by the bonding of H^+ to S atoms in the sulfide lattice, forming weakly-attached $-SH^{\partial-}$ groups. These $-SH^{\partial-}$ groups could then escape into solution as H_2S through further H^+ addition (76).

From this, it was postulated that bacterial action consisted of removing the rate-limiting $-SH^{\partial-}$ groups from the sulfide surface by way of an, as yet undiscovered, complex molecular carrier (76). The production of an extracellular "film" by *T. ferrooxidans* cells forming corrosive pits while growing on synthetic pyrite has been documented (57). It could not be established whether the liquid in the film was either aqueous or completely organic but was thought to be removing or dissolving sulfur from the pyrite surface. In leaching studies, bacterial activity was found to be dependent on the solubility product of the sulfide mineral and its conductivity (77), whether that be electron (n-type) or hole (p-type). Sulfide mineral of the p-type with its low concentration of electrons contained a higher proportion of broken bonds; as a result, the breakage of bonds by H^+ was less significant and dissolution was facilitated (77).

When Fe^{3+} was present, there was less need to break chemical bonds by H^+ interaction (76). This was because Fe^{3+} was able to oxidize $-SH^{\partial-}$ directly, releasing H^+ and colloidal sulfur. Thus, the presence of Fe^{3+} is of great importance from an electrochemical point of view. The Fe^{3+}/

Fe^{2+} couple provides a high redox potential (Eh) to drive sulfide mineral oxidation. The indirect leaching mechanism is highly dependent on the Eh of the medium which is a measure of its oxidizing ability (46); the greater the difference between the Eh and the EP (electrode potential) of the sulfide mineral, the greater the leaching. During leaching, the Eh rarely increases as high as the Fe^{3+}/Fe^{2+} couple (+747 mV at 25°C) because of precipitation of oxidized iron. Recorded Eh values during oxidation of sulfide minerals have been between +340 and +540 mV (46).

Sulfide minerals will interact electrochemically with each other in aqueous medium, forming galvanic currents (50). When two sulfide minerals interact this way, a galvanic current will flow through the solution from the mineral with the highest EP value to the mineral with the lowest EP value (35, 56). Thus, the mineral with the lower potential in the electromotive series will corrode more rapidly (35, 50). For example, when pyrite (EP = 0.63 V) is in contact with chalcopyrite (EP = 0.52 V), chalcopyrite will corrode more rapidly than pyrite which is essentially passified (50):

CHALCOPYRITE: $CuFeS_2 \rightarrow Cu^{2+} + Fe^{2+} + 2S^o + 4e-$ (acts as anode)

PYRITE: $O_2 + 4H^+ + 4e- \rightarrow 2H_2O$ (acts as cathode)

This type of galvanic interaction was maintained by *T. ferrooxidans* which oxidized the formed ferrous iron to ferric and elemental sulfur to sulfuric acid (50), maintaining the surface of the minerals exposed. Thus, both bacterial action and galvanic interactions have been shown to have significant effects on leaching.

MATERIALS AND METHODS

Materials

All chemicals and reagents used were of reagent grade and obtained commercially. Elemental sulfur was obtained from British Drug Houses, Ltd., Toronto. All soluble salts, including ferrous sulfate, were obtained from Fisher Scientific Co., Fairlawn, N.J., U.S.A., Sulfuric acid (concentrated, 96% by weight, 36 N) was also obtained from Fisher Scientific Co. All reagents and media were prepared using glass-distilled water.

Ore

All ore samples were provided by Hudson Bay Mining and Smelting Co., Ltd. from the Flin Flon mine. They consisted of mixed sulfide ore samples containing Cu, Zn, Fe, and S and the minerals chalcopyrite ($CuFeS_2$), sphalerite (ZnS), pyrite (FeS_2), and pyrrhotite (FeS) in various amounts. The characteristics of the various ore samples used are summarized in Tables 1 and 2. Included among the impurities found in the ore samples were carbonates ($CaCO_3$ and $MgCO_3$) and diorite.

Slag

Smelter slag for the preliminary column experiments was provided to us by Hudson Bay Mining and Smelting Co., Ltd. The slag came from the Flin Flon smelter and had a particle size of -3/4". It was composed of 0.46% Cu, 1.58% Zn, 34.8% Fe, and 37.4% SiO_2 according to elemental analysis provided with the sample.

Tailings

A sample of tailings was gathered from one of the back-filled stopes

in the South Main section of the Flin Flon mine. The tailings sample had a very fine particle size and seemed to contain a great deal of ferric precipitate by its red-brown color. No elemental analysis for the tailings sample was available.

Sand

The sand used in the small and large scale column experiments was silica sand 20 - 40 mesh obtained from Winnipeg Supply Co., Winnipeg.

Methods

Isolation and growth of microorganisms

Water samples from various locations at the South Main Shaft of the Flin Flon mine were collected and used to inoculate bacterial medium. The laboratory strains of *T. ferrooxidans* used were the ATCC strains 13661 and 19859. The *T. thiooxidans* laboratory strain used was ATCC 8085. In the case of iron-grown cells (*T. ferrooxidans*), a 10 mL inoculum (either water sample or previous culture) was added to 90 mL of the iron medium in a 250 mL Erlenmeyer flask. These flask cultures were grown at 25°C on a gyrotary shaker at 150 rpm. Sulfur grown cells (*T. thiooxidans*) were grown stationary at 28°C either in 250 mL Erlenmeyer flasks with 90 mL Starkey's medium plus 10 mL of water sample or in 2.7 L Fernbach flasks with 900 mL Starkey's medium plus 100 mL previous culture.

Media

The iron medium (49) used for the growth of *T. ferrooxidans* contained 0.1 g K_2HPO_4, 0.4 g $(NH_4)_2SO_4$, 0.4 g $MgSO_4 \cdot 7H_2O$, and 33.3 g $FeSO_4 \cdot 7H_2O$ per liter and adjusted to pH 2.3 with H_2SO_4. The medium used for *T. thiooxidans* was Starkey's No. 1 medium (62): 0.3 g $(NH_4)_2SO_4$, 3.5 g KH_2PO_4, 18 mg $FeSO_4 \cdot 7H_2O$, 0.5 g $MgSO_4 \cdot 7H_2O$, and 0.25 g $CaCl_2$ per liter.

Powdered elemental sulfur was spread evenly on the surface after inoculation (69). The media used for the leaching experiments were either HP (high phosphate) or LP (low phosphate) medium. The HP medium was the iron medium without ferrous sulfate while the LP medium contained 35 mg K_2HPO_4, 66 mg $(NH_4)_2SO_4$, and 123 mg $MgSO_4 \cdot 7H_2O$ per liter and was adjusted to pH 2.3 with H_2SO_4.

Sterility

Aseptic technique was used throughout isolation, culture maintenance, and shake-flask studies. Growth media were sterile. Sulfur, ore, sand, smelter slag, and tailings were not sterilized. Sterile technique was unfeasible and not used in column studies.

Shake-flask leaching experiments

These experiments were carried out in 250 mL Erlenmeyer flasks containing 90 mL of HP or LP medium plus 10 mL inoculum of *T. ferrooxidans* or *T. thiooxidans* or both and 10 g of -200 mesh ore to make a 10% slurry. The flasks were incubated at 25°C on a rotary shaker at 150 rpm for several days. In some experiments, it was necessary to supplement the ore flasks with daily addition of 10 N H_2SO_4 during the first four days. Periodically, 5 mL samples of slurry were collected aseptically and frozen in order to halt bacterial activity. The samples were thawed, filtered through Whatman No. 1 filter paper, and centrifuged at 13000 x g for 10 minutes. The clear samples were then analyzed for Cu, Zn, and Fe by atomic absorption spectrophotometry at the Manitoba Provincial Soil Testing Laboratory.

Small column apparatus

The percolating column set-up (49) is illustrated in Figure 1. The

column itself was made of acrylic plastic, with an inside diameter of 7.5 cm and a height of 59 cm. It had a perforated acrylic base 3 cm from the bottom to hold the crushed ore, thus making a separate bottom reservoir from which liquid was led by gravity to a 1 L Erlenmeyer flask which served as a culture reservoir. The culture flask contained 550 mL of medium which was circulated to the top of the column by a Gilson Miniplus 2 peristaltic pump. The tubing used was Tygon tubing® (Norton). Aeration was provided by a glass sparger in the culture reservoir; there were air outlets both at the top of the culture flask and at the top of the column. The bed volume was between 2 and 2.5 L and that of the bottom reservoir about 150 mL. The column contained between 3 and 4 Kg of material. This was usually (unless specified) a 50% mixture of ore and sand.

Packing of the small columns

Prior to loading the small columns, the material (ore or ore-containing) was agglomerated by mixing and tumbling in the presence of a small volume of concentrated sulfuric acid (4 to 8 mL). This was done in order to prevent plugging and channeling. After loading, the packed column was washed with 2 to 3 volumes of distilled water.

Large column apparatus

The pilot-scale percolating column set-up is illustrated in Figure 2. The column itself was made of polyvynyl chloride (PVC), manufactured by Scepter Manufacturing Co., Ltd., Edmonton. The column had an inside diameter of 55 cm and a height of 4.5 m (15 feet), with a wall and base thickness of 1". It was assembled in three 5-foot sections with flanges at each junction. The junctions were made watertight by $\frac{1}{4}$"-thick rubber gaskets and secured by 22 two-inch bolts. The column had a removable

perforated plate ($\frac{1}{4}$" PVC with 12 evenly-distributed 1"-diameter holes) 10 cm from the top for distribution of incoming liquid. At the bottom, there were three outlet ball-type 3/4" valves on each side at 4", 8", and 12" from the bottom. The column was topped off by a fitted lid (PVC, $\frac{1}{4}$" thick) with a center perforation (3/4" threaded) for incoming tubing and a second perforation for an air outlet.

The column was built on top of a supporting steel-timber base. Three 8" x 8" x 10' steel beams were laid parallel 6" apart with an overlying 3' x 3' wooden base consisting of 24 2" x 4" x 3' spruce pieces. This was overlayed by a 1"-thick layer of foam.

Inside the bottom of the column, a layer 8" deep was made of broken granite rock, the interstitial spaces filled with glass marbles, and overlayed with a water-permeable plastic fabric. This bottom layer served both as a bed support and a filter for small particles. The bed volume proper was about 1000 L ($1m^3$), containing a mixture of ore and sand.

During operation, all bottom outlet valves were kept closed, save one at 4" from the bottom. From this valve, liquid flowed by gravity to a 20 L collecting tank. From here, liquid was pumped by a peristaltic pump (Gilson Miniplus 2) to a 50 L (Nalgene) culture carboy where aeration and acid adjustment took place. A second peristaltic pump carried the now aerated and acidified leaching solution by a $\frac{1}{4}$" PVC non-flexible tubing up 15 feet to the top of the column where a perforated tubing (Tygon 2.4 mm I.D.) distributed it evenly over the surface. An aquarium air pump supplied air by way of two glass spargers in the culture carboy and one in the collecting tank. The pH of the medium in the culture carboy was kept constant at 2.5 by a Radiometer titrator type TTT11b connected with

a Radiometer pH meter type PHM28 with 10 N H_2SO_4 which was fed by gravity through a magnetic valve. In case of overflow from the culture carboy, an overflow line was installed from the neck of the carboy to a second carboy 8" below.

Packing of the large column

Ore was packed in the column in bundles of about 40 Kg each in polyethylene netting ($3\frac{1}{2}$" squares) tied with polyethylene sideline cord. Sand was poured along with the ore. Before packing, the sand was wetted with tap water, then lowered in buckets inside the column where it was evenly spread out. Layers of water-permeable plastic fabric (Geotextiles) were placed at strategic places for uniform distribution of the percolating liquid: between the column bed and the 8" granite layer at the bottom of the column; at the 1st stage/2nd stage and 2nd stage/3rd stage junctions; at the top of the column bed, underneath the top perforated plate, and; overlying the top perforated plate.

TABLE 1. Chemical make-up of ore samples

Ore sample	Particle size	Metal content				
		Cu	Zn	Fe	S	others
High-grade I	-200 mesh & 3/4"	4.9	12.5	30.0	37.5	15.1
High-grade II	3/4"	3.7	10.2	29.0	34.6	22.5
Low-grade	3/4"	0.8	8.0	30.5	34.3	26.4
Fraction 1	$\frac{1}{4}$" - $\frac{1}{2}$"	9.6	12.8	28.0	34.2	15.4
2	$\frac{1}{2}$" - 1"	9.3	16.2	26.9	33.9	13.7
3	1" - $1\frac{1}{2}$"	9.1	11.4	27.6	33.4	18.5
4	$1\frac{1}{2}$" - 2"	8.1	12.3	27.5	33.3	18.8
Large column	6" - 8"	2.1	3.4	23.0	20.9	50.6

Values given as % weight.

TABLE 2. Mineral make-up of ore samples

Ore sample	Particle size	Mineral content				
		$CuFeS_2$	ZnS	FeS_2	FeS	impurities
High-grade I	-200 mesh & 3/4"	14.2	18.6	51.0	3.0	15.1
High-grade II	3/4"	10.7	15.2	52.0	2.6	22.5
Low grade	3/4"	2.3	12.2	54.6	7.0	26.4
Fraction 1	$\frac{1}{4}$" - $\frac{1}{2}$"	27.7	19.1	25.9	11.9	15.4
2	$\frac{1}{2}$" - 1"	26.9	24.2	21.5	13.7	13.7
3	1" - $1\frac{1}{2}$"	26.3	17.0	27.4	10.8	18.5
4	$1\frac{1}{2}$" - 2"	23.4	18.3	27.5	12.0	18.8
Large column	6" - 8"	6.1	5.1	18.6	19.6	50.6

Values given as % weight.

Figure 1. Small-scale column leaching experiment set-up. The culture reservoir held 550 mL of leaching solution which was kept recirculating. The bed volume was between 2 and 2.5 L and that of the bottom reservoir about 150 mL. Aeration was provided by a glass sparger.

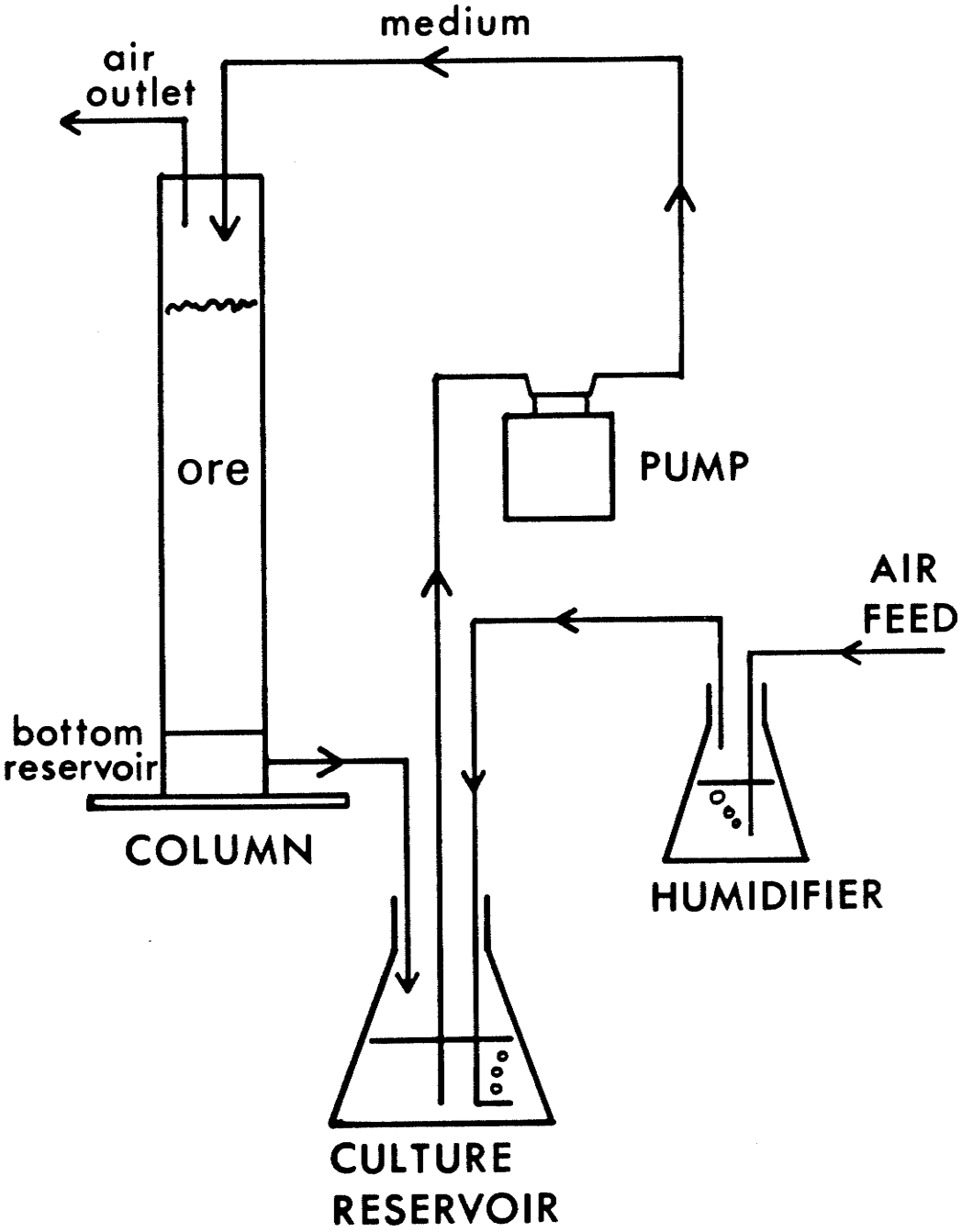
medium
air
outlet
ore
PUMP
AIR
FEED
bottom
reservoir
COLUMN
HUMIDIFIER
CULTURE
RESERVOIR

Figure 2. Large-scale column leaching experiment set-up. The culture carboy and the collecting tank contained about 50 L of leaching solution which was kept recirculating. The column bed volume was about 1000 L. Acid was added in the form of 10 N H_2SO_4 to keep the pH of the system at 2.5. Aeration was provided by two glass spargers in the culture carboy and one in the collecting tank.

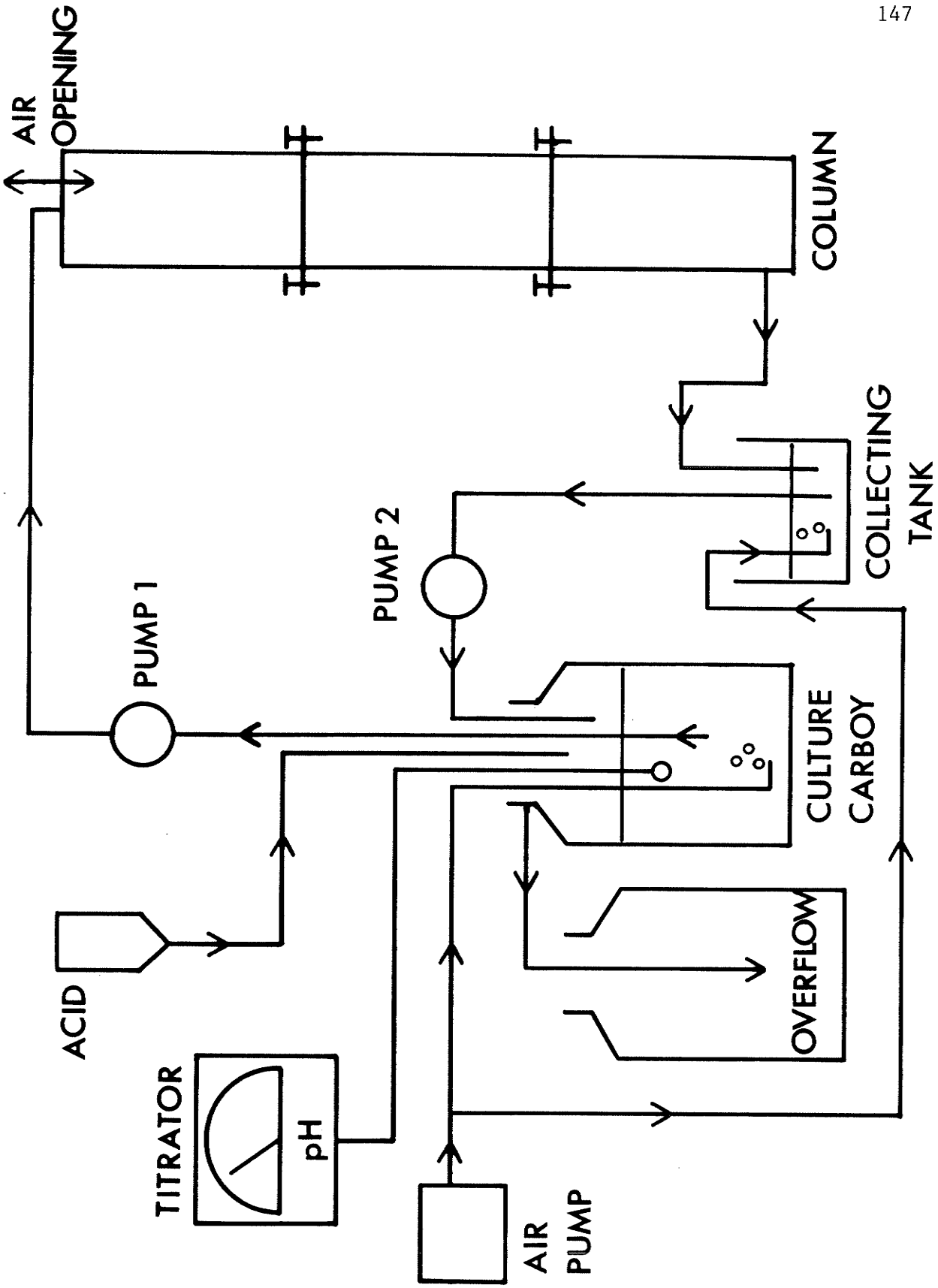
AIR OPENING
COLUMN
COLLECTING TANK
PUMP 2
PUMP 1
CULTURE CARBOY
OVERFLOW
ACID
TITRATOR
pH
AIR PUMP

RESULTS

Shake-flask leaching experiments

In these set of experiments, a basic study was carried out on the bacterial leaching of Cu and Zn from the finely ground ore (-200 mesh).

Leaching by iron-grown isolates

T. ferrooxidans isolates grown on Fe^{2+} were not able to leach metals from the -200 mesh No. 1 high grade ore in the LP medium. At this low phosphate concentration (0.2 mM), a 10% ore slurry raised the pH to 5.0 from 2.3 during shaking probably due to the calcium carbonate present as calcite. This rise in pH stopped the growth of the organism. In the initial experiments, the HP medium (0.6 mM phosphate) with its better buffering capacity had to be used. Only four of the isolates (SM-1, 2, 4, and 5) were capable of growing on the ore, maintaining the acid pH. The control (no bacterial inoculum), SM-3, and the laboratory strains ATCC 13661 and 19859 failed either to leach metals or maintain the acid pH.

Figure 3 illustrates a typical time-course leaching experiment with the bacterial isolate SM-1. With all the successful isolates, Cu began to be extracted first, followed next by Zn and last by Fe. The isolates showed a lag of 4 - 5 days before commencement of leaching even though the Fe^{3+} initially present in the inoculum must have caused some solubilization. Apparently, a period of adaptation was required in all successful isolates before growth on the ore. As can be seen from Figure 3 and Table 3, Zn was extracted much more so than Cu. The Cu/Zn % extraction ratios were on the order of 0.1 after 18 days. This indicates that ZnS was solubilized preferentially over $CuFeS_2$, although it was the

Figure 3. Time-course of shake-flask leaching by iron-grown SM-1 in HP medium. Conditions are described in Table 3.

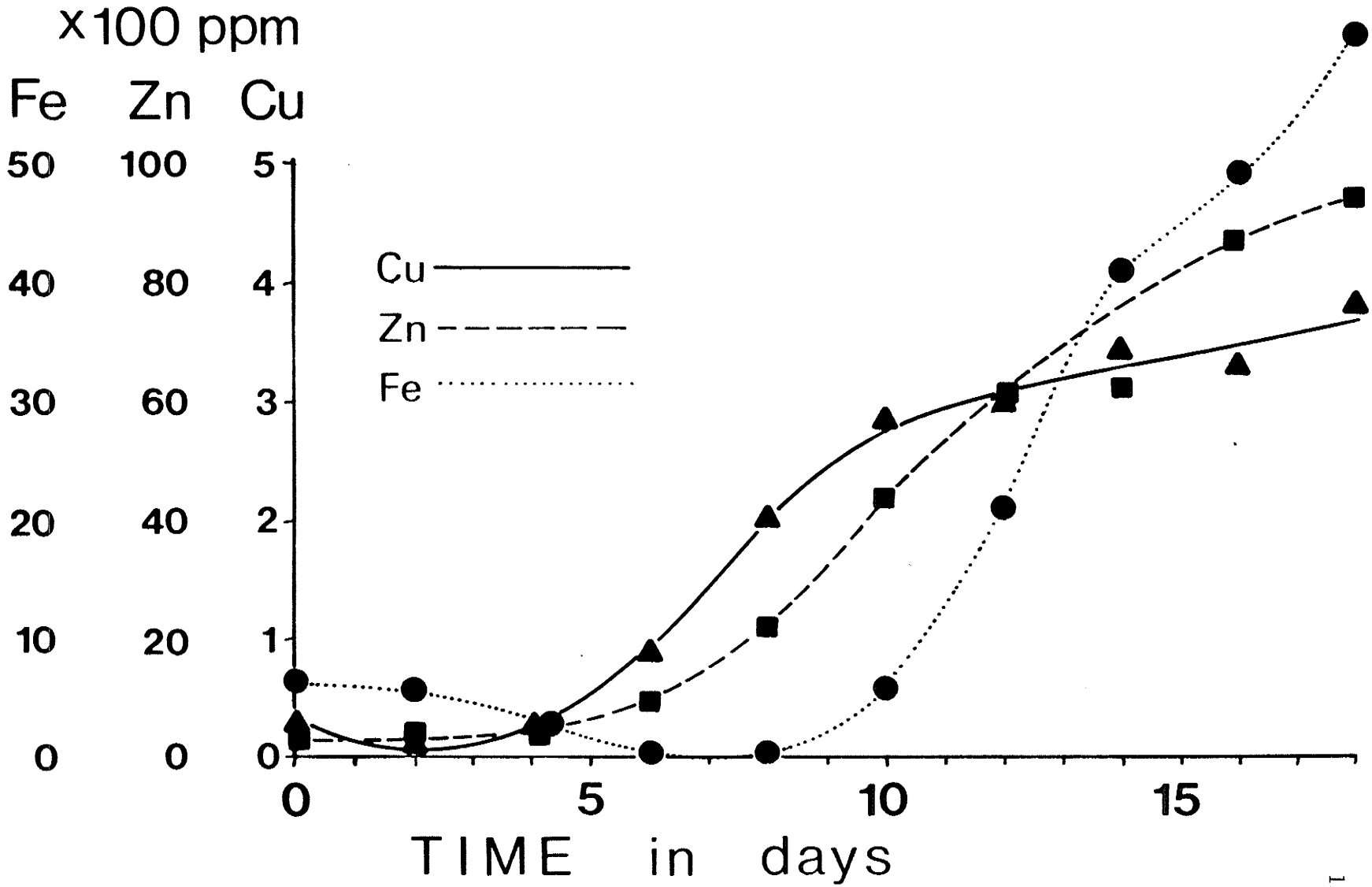
x100 ppm
Fe
Zn
Cu
50
40
30
20
10
0
100
80
60
40
20
0
5
4
3
2
1
0
Cu
Zn
Fe
0
5
10
15
TIME in days

TABLE 3. Shake-flask ore leaching by iron-grown isolates

Bacterial strains	Extraction achieved (%)			Cu/Zn % extraction ratio	Final pH
	Cu	Zn	Fe		
SM-1	7.8	76.2	20.7	0.10	2.1
SM-2	7.3	67.7	22.0	0.11	2.1
SM-3	0.8	13.8	0.0	-	4.4
SM-4	10.0	68.8	19.8	0.15	2.0
SM-5	7.8	72.6	10.3	0.11	2.4
ATCC 13661	0.9	13.4	0.0	-	4.6
ATCC 19859	0.9	10.7	0.0	-	4.7
Control	0.0	8.9	0.0	-	4.8

Shake-flask leaching of -200 mesh ore (10 g/100 mL HP medium) for 18 days at 25°C with 10% inoculum of iron-grown bacteria (except control).

latter that seemed to be leached first (Fig. 3)

Leaching by sulfur-grown isolates

Leaching of the ore by the sulfur-grown bacterial strains is shown in Table 4. No leaching was seen with the uninoculated control or with the *T. thiooxidans* laboratory strain ATCC 8085 and the pH remained high. The *T. thiooxidans* isolates SM-6 and SM-7 grown on the Starkey's medium were quite effective at leaching the ore in the LP medium. The acidic pH (1.0) and high phosphate concentration in the inoculum probably helped to counteract the alkalinity of the ore to some extent during the first few days. Figure 4 shows the time course leaching profile of SM-6. There was an initial lag lasting 1 - 4 days (depending on the isolate and the experiment) when no metals were extracted; at the end of this lag, extraction began simultaneously for all three metals, although the rate of solubilization was lower than that with *T. ferrooxidans*. This lag coincided with a slight rise in pH from 2.3 to 3.1. The pH then went down to 2.5 as the organisms were able to grow on the ore and produce sulfuric acid. As seen in Figure 4 and Table 4, Zn was again extracted much more extensively than Cu or Fe, but the Cu/Zn % extraction ratios were constant and twice the values obtained with iron-grown cells. The iron extraction rate was much slower (only 10%) with *T. thiooxidans*, which is not capable of oxidizing iron.

Leaching by ore-adapted cells

The effect of ore adaptation on the leaching activities of the isolates was examined (Table 5). For this experiment, the *T. ferrooxidans* isolates SM-1, SM-4, and SM-5, and the *T. thiooxidans* isolate SM-6 were used both in the HP and LP media. The *T. ferrooxidans* isolates required

TABLE 4. Shake-flask ore leaching by sulfur-grown isolates

Bacterial strains	Extraction achieved (%)			Cu/Zn % extraction ratio	Final pH
	Cu	Zn	Fe		
SM-6	3.9	15.8	1.9	0.25	2.5
SM-7	4.5	18.6	2.3	0.24	2.4
ATCC 8085	0.9	8.8	0.0	-	4.5
Control	0.0	3.2	0.0	-	5.2

Shake-flask leaching of -200 mesh ore (10 g/100 mL LP medium). The leaching by the isolates SM-6 and SM-7 was monitored for 14 days while the ATCC strain and the control were only monitored for 9 days. All experiments were carried out at 25°C. Except for the control, a 10% inoculum of sulfur-grown bacteria was used in each case.

Figure 4. Time-course of shake-flask leaching by sulfur-grown SM-6 in LP medium. Conditions are described in Table 4.

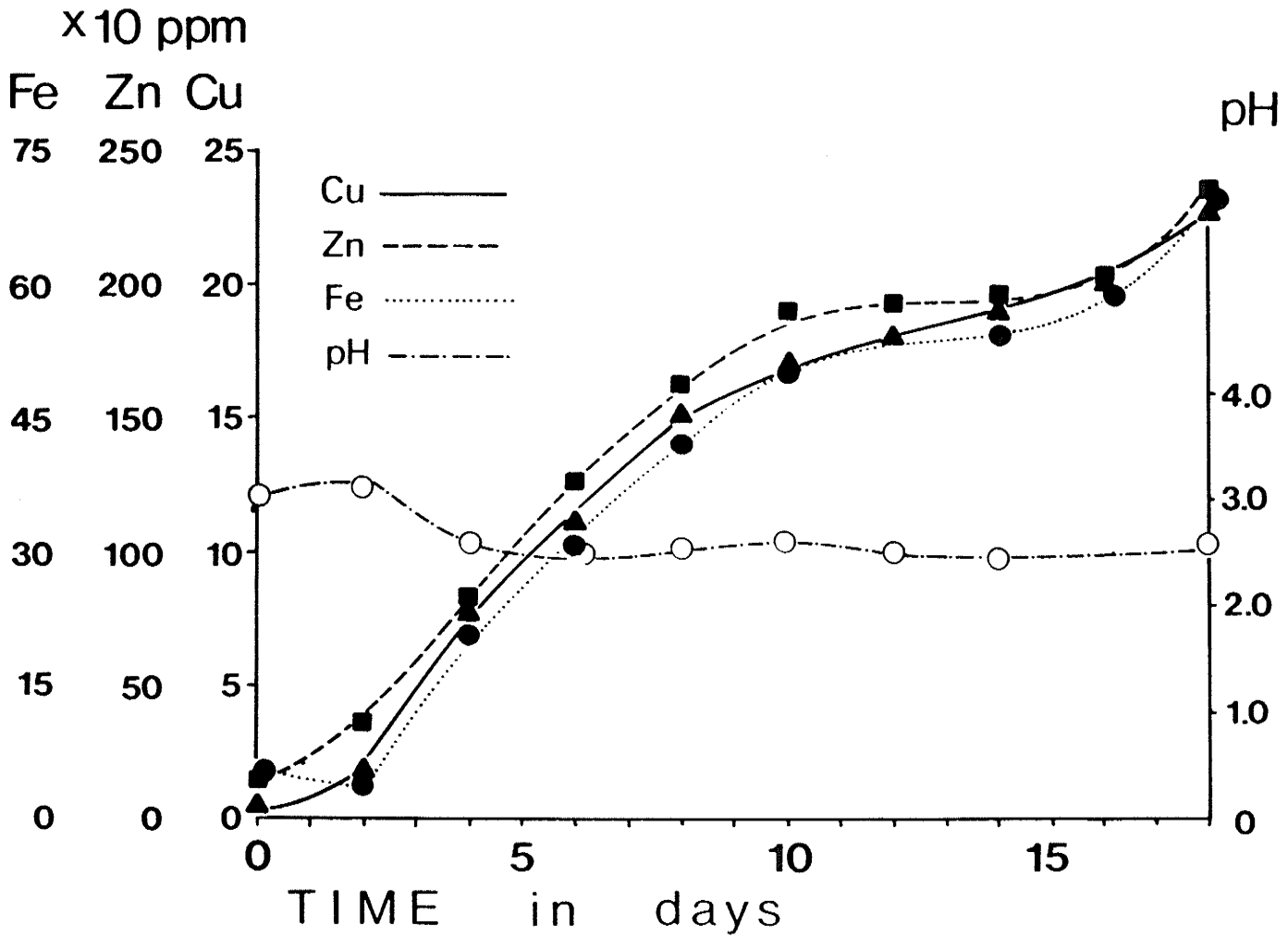
x 10 ppm
Fe Zn Cu
pH
75 250 25
60 200 20
45 150 15
30 100 10
15 50 5
0 0 0
Cu
Zn
Fe
pH
4.0
3.0
2.0
1.0
0
0 5 10 15
TIME in days

TABLE 5. Shake-flask ore leaching by ore-adapted isolates

Bacterial strain	Extraction achieved (%)			Cu/Zn % extraction ratio	Final pH
	Cu	Zn	Fe		
A. In LP medium					
SM-1	7.1	97.9	8.9	0.07	3.1
SM-4	6.3	99.8	10.3	0.06	2.7
SM-5	5.9	77.1	13.3	0.08	2.9
SM-6	8.3	25.0	4.1	0.34	2.8
B. In HP medium					
SM-1	7.6	82.4	18.9	0.09	2.1
SM-4	8.3	99.2	20.0	0.12	2.1
SM-5	8.8	77.4	23.2	0.11	2.0
SM-6	10.4	82.6	12.7	0.13	1.9

Shake-flask leaching of -200 mesh ore (10 g/100 mL LP or HP medium) for 16 days at 25°C with 10% inoculum from ore-grown cells (previous leaching experiment flasks in LP or HP medium after removal of ore by filtration).

the addition of acid for the first 4 days when growing on the LP medium. The time course leaching experiments in both media are illustrated for *T. ferrooxidans* SM-1 (Fig. 5) and *T. thiooxidans* SM-6 (Fig. 6).

The ore-adapted *T. ferrooxidans* isolates showed, as expected, shortened lag periods before Cu and Zn extraction (Fig. 5) compared to the non-adapted isolates (Fig. 3). The extraction was particularly fast in the LP medium during the first half of the experimental period. The solubilization of Fe still required long lag periods, and Cu extraction started generally before Zn extraction, as with the non-adapted cells. The Fe solubilization was lower in the LP medium than in the HP medium, perhaps because of the higher pH reached in the LP medium precipitating the ferric iron. The Cu/Zn % extraction ratios were low in spite of adaptation , lower in the LP medium than in the HP medium indicating a preferential solubilization of Zn over Cu (Table 5).

The ore-adapted *T. thiooxidans* isolate SM-6 showed a slow leaching phase for Cu, Zn, and Fe during the first half of the experimental period (Fig. 6), similar to non-adapted cells (Fig. 4), but a dramatic increase during the second half in the extraction of Cu (both LP and HP media), Zn (only in HP medium), and Fe (only in HP medium). As a result, the Cu/Zn % extraction ratio increased in the LP medium to a high value of 0.34, while it was only 0.13 in the HP medium (Table 5). The Zn and Fe extraction in the HP medium reached a high level comparable to that with *T. ferrooxidans* strains (Fig. 6, Table 5).

In general, *T. ferrooxidans* seems to favour the extraction of Zn over Cu (lower Cu/Zn % extraction ratio), and *T. thiooxidans* seems to accomplish a more balanced solubilization of both Cu and Zn (higher Cu/Zn

Figure 5. Time-course of shake-flask leaching by ore-adapted SM-1 in LP or HP medium. Conditions are described in Table 5.

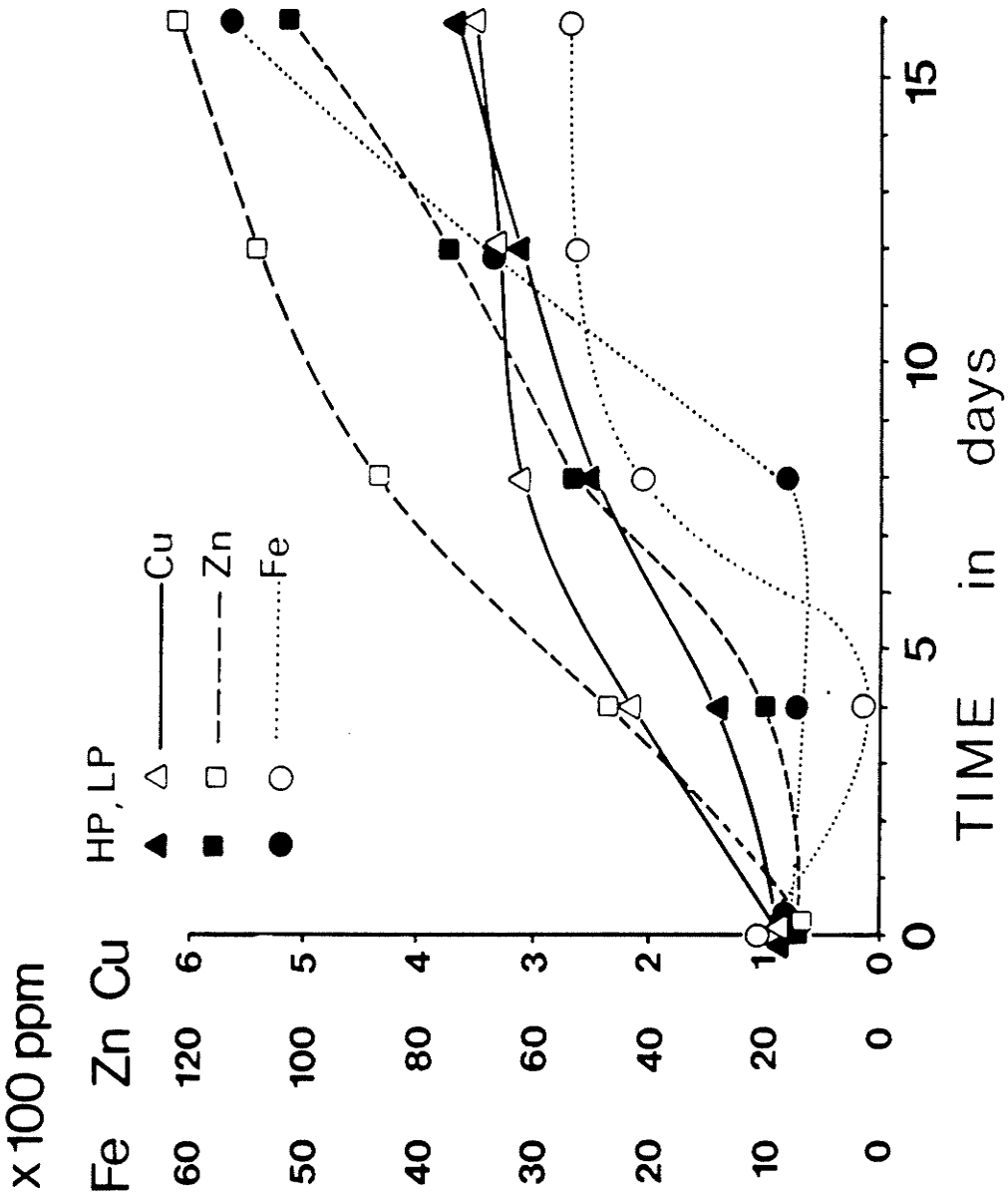
x 100 ppm
Fe Zn Cu
60 120 6
50 100 5
40 80 4
30 60 3
20 40 2
10 20 1
0 0 0
HP, LP
Cu
Zn
Fe
0 5 10 15
TIME in days

Figure 6. Time-course of shake-flask leaching by ore-adapted SM-6 in LP or HP medium. Conditions are described in Table 5.

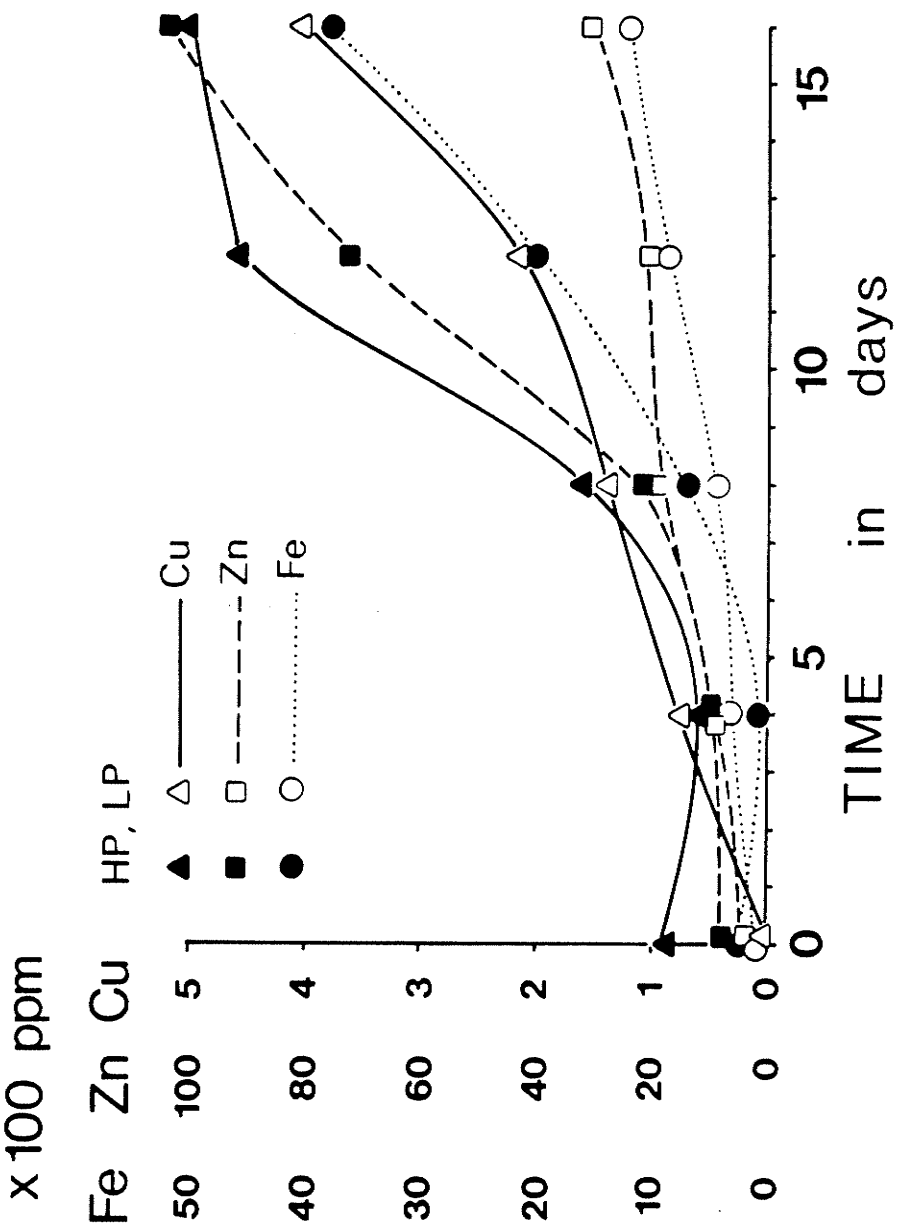
x 100 ppm
Fe Zn Cu
50 100 5
40 80 4
30 60 3
20 40 2
10 20 1
0 0 0
HP, LP
Cu
Zn
Fe
0
5
10
15
TIME in days

% extraction ratio).

Leaching by mixed cultures

Having established the leaching properties of the individual *T. ferrooxidans* and *T. thiooxidans* bacterial strains, experiments were carried out using mixed cultures of the *T. ferrooxidans* strains SM-1, SM-2, SM-4, and SM-5 with the *T. thiooxidans* strain SM-6 in both LP and HP media. The results are summarized in Table 6 and Figure 7. Although there were variations among the mixed cultures, growth on the LP medium was characterized by high Cu/Zn % extraction ratios throughout the experimental period, while in the HP medium the ratios decreased with time, favouring the extraction of more Zn than Cu. The leaching of Fe was more extensive in the HP medium than in the LP medium. In other words, the cultures behaved as *T. thiooxidans* when grown on LP medium and *T. ferrooxidans* when grown on the HP medium. The morphological aspects of the cultures corroborated this observation. In the LP medium, the cultures showed a great deal of metallic sheen on the liquid surface and no ferric iron production, typical of *T. thiooxidans*. In the HP medium, the cultures showed no metallic sheen and a great deal of ferric iron production, typical of *T. ferrooxidans*. At the same time, typical ordered patterns of metal leaching where Cu is extracted first, followed by Zn and Fe, are observed in the HP medium, while in the LP medium, all metal leaching begins to be extracted simultaneously. It appears, then, that the LP medium favours *T. thiooxidans* growth, while the HP medium favours *T. ferrooxidans* growth. Whether this is due to buffering effects, nutrient effects, or some other effects, is not clear.

TABLE 6. Shake-flask ore leaching by mixed cultures

Bacterial strains	Extraction achieved (%)			Cu/Zn % extraction ratio	Final pH
	Cu	Zn	Fe		
A. In LP medium					
SM-1 + SM-6	10.0	64.0	9.7	0.16	1.9
SM-2 + SM-6	8.8	96.3	12.9	0.09	2.1
SM-4 + SM-6	8.2	41.6	8.4	0.20	2.3
SM-5 + SM-6	10.6	50.6	9.2	0.21	2.1
B. In HP medium					
SM-1 + SM-6	9.8	76.8	26.5	0.12	1.9
SM-2 + SM-6	8.4	76.8	23.1	0.11	2.0
SM-4 + SM-6	9.4	86.7	22.4	0.11	2.1
SM-5 + SM-6	10.2	88.6	22.7	0.12	1.9

Shake-flask leaching of -200 mesh ore (10 g/100 mL LP or HP medium) for 16 days at 25°C with 5% each of *T. ferrooxidans* and *T. thiooxidans* inoculum from ore-grown cells in respective medium after removal of ore by filtration.

Figure 7. Time-course of shake-flask leaching by a mixed culture of ore-adapted SM-1 and SM-6. Conditions are described in Table 6.

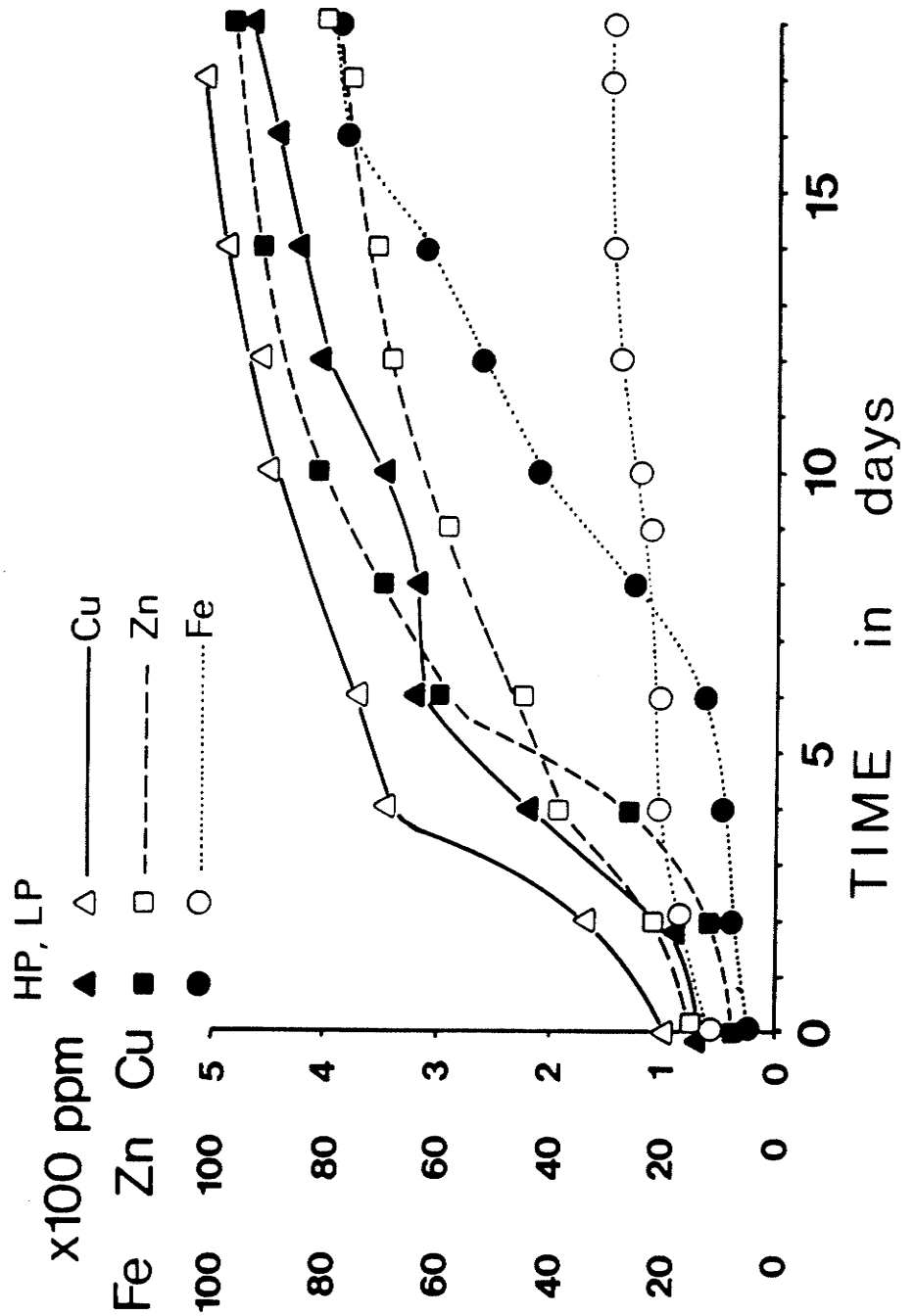
HP, LP
Cu
Zn
Fe
x100 ppm
Fe Zn Cu
100 100 5
80 80 4
60 60 3
40 40 2
20 20 1
0 0 0
0
5
10
15
TIME in days

Small-scale column leaching experiments

Our ore-leaching study was extended to the use of laboratory-scale percolating columns with coarser ore (-3/4" particle size). In these experiments, the isolates used were those which grew successfully on the -200 mesh ore in the shake-flask experiments.

Preliminary experiments

In the first of these preliminary column leaching experiments, three columns were packed with ore alone, ore plus smelter slag, and ore plus tailings in 50% weight mixtures as described in Materials and Methods. The columns were inoculated with the *T. ferrooxidans* isolate SM-4. The results are summarized in Table 7. Leaching of Cu and Zn progressed well in the ore and ore + slag columns, with much higher Cu/Zn % extraction ratios than in the shake-flask experiments. No leaching occurred in the ore + tailings column. For all columns, it was necessary to periodically add acid in the form of 10 N H_2SO_4 to the culture flask in order to maintain the pH under 2.5. The column with the ore alone consumed the least ammount of acid although the leaching rates were not as high as with the ore + slag column, indicating a beneficial effect by the slag. The ore + tailings column had the highest acid consumption. The column effluents had a pH of 3.5 except in the ore + tailings column where the effluent came out at pH 5.3. The high column pH was obviously detrimental to the growth of bacteria in this column, resulting in no metal leaching from the ore in the tailings column.

Since the shake-flask experiments showed that *T. thiooxidans* isolates maintained an acid pH in LP medium without addition of sulfuric acid, the effect of inoculation with sulfur-grown SM-6 was studied on the ore and

TABLE 7. Preliminary column experiments with *T. ferrooxidans* isolate SM-4

	Columns		
	1 ore alone	2 ore + slag	3 ore + tailings
Duration (d)	47	47	47
Cu % extraction/30d	0.52	1.27	0
Zn % extraction/30d	0.80	1.87	0
Cu/Zn % ratio	0.65	0.68	-
g acid/Kg ore/30d	1.48	2.95	4.26

Column leaching experiments were carried out as described in Materials and Methods using LP medium. The ore sample used was the No. 1 high-grade ore sample ground to -3/4". The flow rate used was 0.057 mL per cm^2 per minute. Acid used was in the form of 10 N H_2SO_4 (density of 36 N/96% = 1.84 g/mL).

ore + tailings columns. The results are shown in Table 8. A major effect of *T. thiooxidans* addition was to increase the extraction of Cu while decreasing that of Zn, approaching equal percentage extractions of Cu and Zn. In the ore + tailings column there was still no leaching except for a trace of Zn. The acid requirement was not reduced. The use of HP medium in the shake-flask experiments had a beneficial effect on the maintenance of acid pH. The phosphate concentration was therefore increased to 0.6 mM (HP) from 0.2 mM (LP). The results are also shown in Table 8. There was no marked difference in metal extraction from that with LP medium. There was still practically no leaching in the tailings column. The higher phosphate content of the medium did, however, lower the acid requirements for both ore and ore + tailings columns. The time-course leaching for the column with ore alone under the various conditions is illustrated in Figure 8.

Leaching by single cultures

Six separate leach columns containing a 50% mixture of ore plus sand were set up as described in the Materials and Methods. Three of these columns contained high grade ore while the other three contained low grade ore. The columns were inoculated with various *T. ferrooxidans and T. thiooxidans* isolates. For all columns, the LP medium was used as the circulating leaching solution which was kept percolating from one to two months. The results from these experiments are shown in Table 9 and Figures 9 and 10.

The results indicate an efficient leaching of both Cu and Zn by all bacterial strains tested from both the high grade ore and the low grade ore. The percentage extraction rates for Cu and Zn from the low grade ore

TABLE 8. Preliminary column experiments with the mixed culture SM-6 + SM-4

	Columns			
	1 ore alone		2 ore + tailings	
	LP	HP	LP	HP
Duration (d)	30	28	30	28
Cu % extraction/30d	0.56	0.52	0	0
Zn % extraction/30d	0.72	0.68	0.05	0
Cu/Zn % ratio	0.78	0.76	-	-
g acid/Kg ore/30d	1.88	1.13	5.33	4.83

Column leaching experiments were carried out as described in Materials and Methods. All columns had previously been exposed to leaching with SM-4 for 47 days (see previous Table) prior to replacement of medium and inoculation with sulfur-grown SM-6. At the end of 30 days leaching the medium was replaced with HP medium and leaching was continued. The flow rate was 0.057 mL per cm^2 per minute, as before. Acid was added in the form of 10 N H_2SO_4.

Figure 8. Time course of ore column leaching. Ore (4 Kg) was packed in a small column as described in Materials and Methods and was percolated with LP medium inoculated with iron-grown SM-4 at 25°C (Experiment I). After 47 days, the medium in the flask was replaced with 500 mL fresh LP medium and reinoculated with sulfur-grown SM-6 culture. Leaching was continued for another 30 days (Experiment II). In Experiment III, the medium was again replaced, increasing the phosphate concentration to 0.6 mM (HP) and leaching was continued. In all the experiments, the pH was maintained below 2.5 by daily addition of 10 N H_2SO_4 to the culture flask.

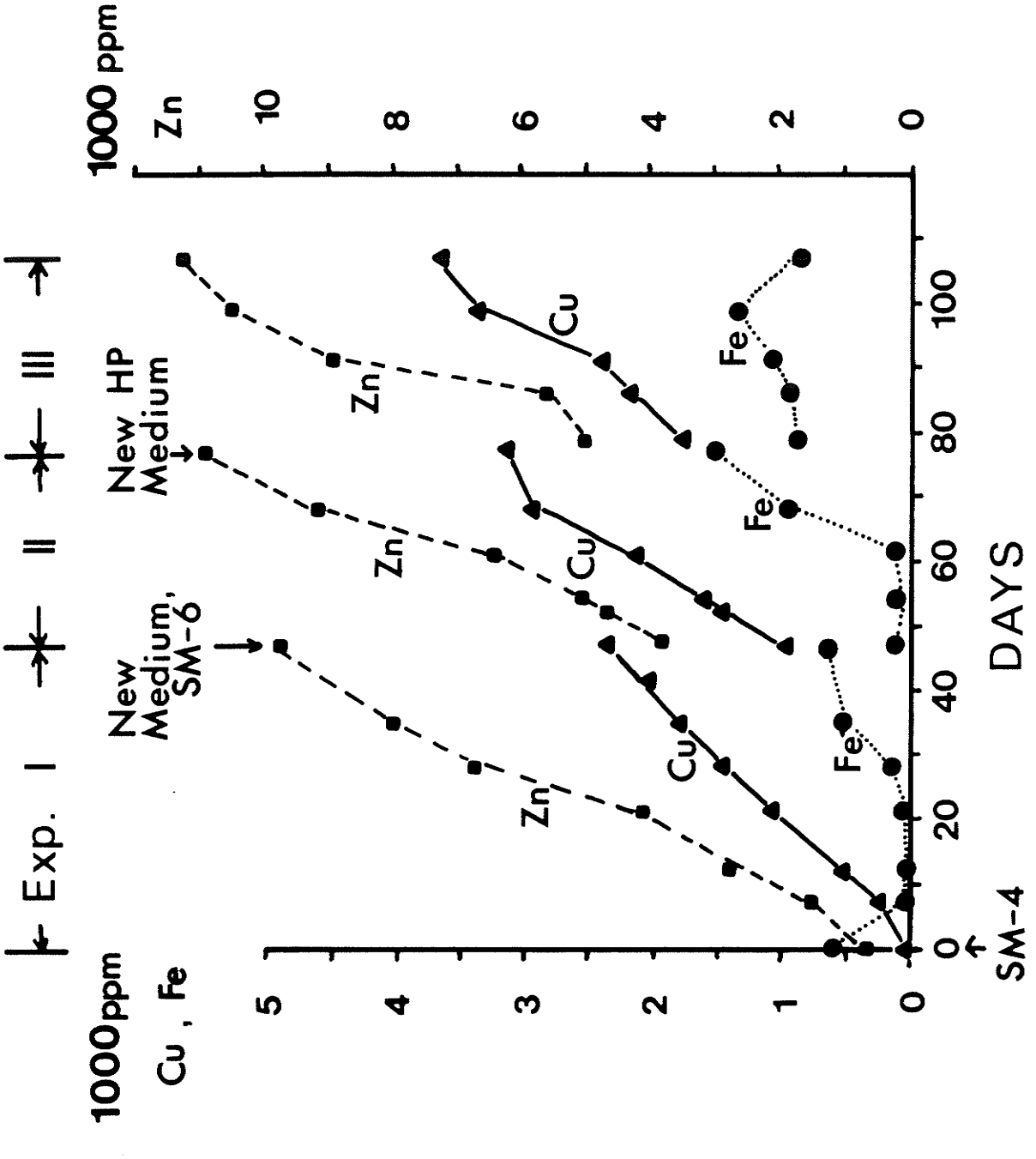
Exp. I
II
III
1000ppm
Cu , Fe
1000 ppm
Zn
New Medium, SM-6
New HP Medium
Zn
Cu
Fe
SM-4
DAYS
0
20
40
60
80
100
1
2
3
4
5
6
8
10

TABLE 9. Leaching by pure cultures

	Columns			
	T. ferrooxidans		*T. thiooxidans*	
	SM-4	SM-5	SM-6	SM-7
A. High grade ore				
Duration (d)	47	52	43	ND
Cu % extraction/30d	0.61	1.07	1.04	-
Zn % extraction/30d	1.87	3.24	2.53	-
Cu/Zn % ratio	0.33	0.33	0.41	-
g acid/Kg ore/30d	4.0	4.1	4.2	-
B. Low grade ore				
Duration (d)	56	ND	53	49
Cu % extraction/30d	2.52	-	3.18	2.83
Zn % extraction/30d	3.49	-	3.95	2.55
Cu/Zn % ratio	0.72	-	0.81	1.11
g acid/Kg ore/30d	4.8	-	7.8	6.8

Column leaching experiments were carried out as described in Materials and Methods using LP medium. High grade ore used was sample No. 1 for SM-4 and sample No. 2 for SM-5 and SM-6. Acid: 96% sulfuric acid (density = 1.84 g/mL). Concentration was reduced to 10 N for addition.

ND : not done

Figure 9. Column leaching of high grade ore by SM-5 (A) and SM-6 (B) in LP medium. The ore used was the No. 2 high grade ore sample. Ore was mixed with sand in a 50% weight mixture as described in Materials and Methods.

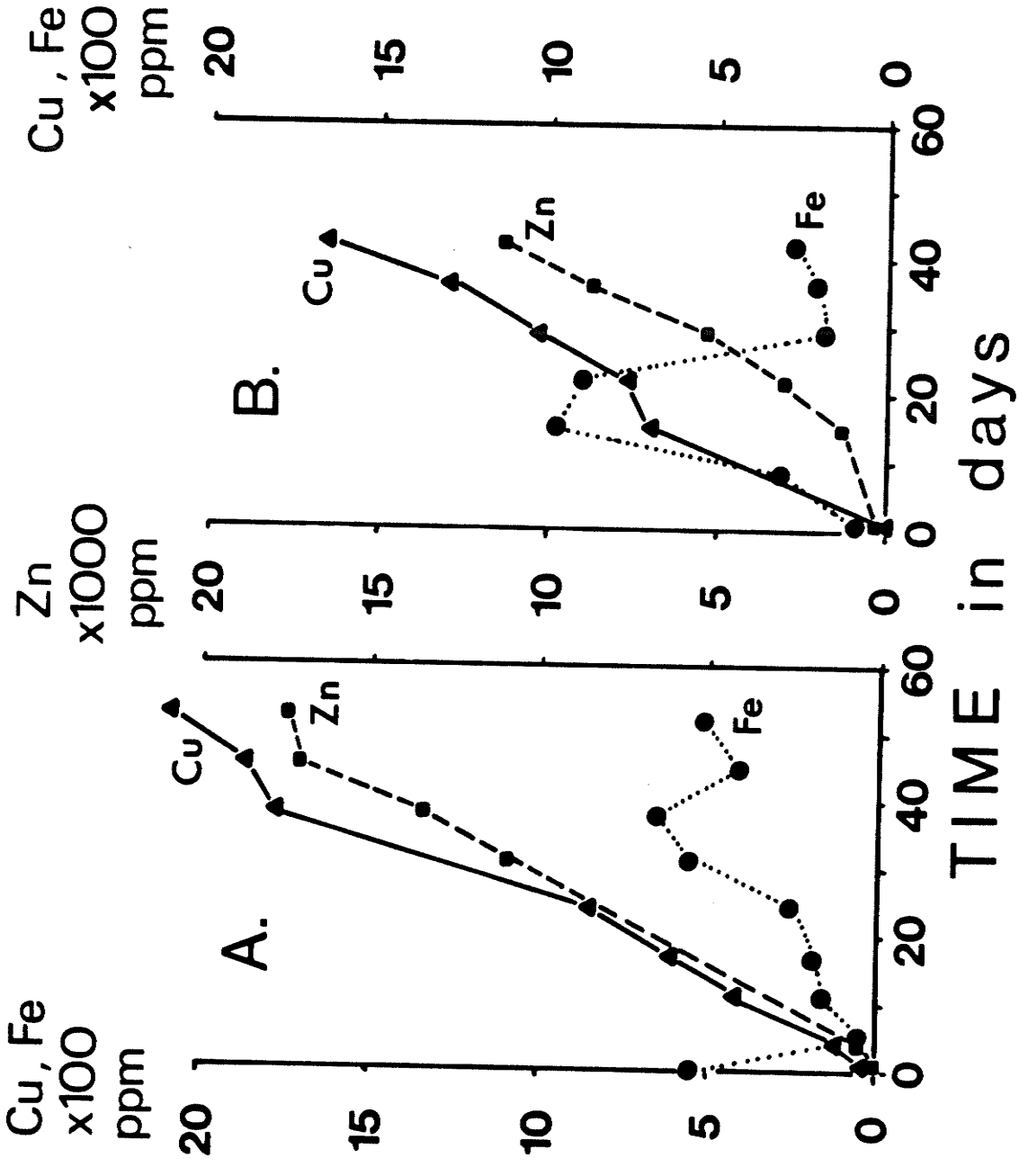
Cu, Fe
x100
ppm
Zn
x1000
ppm
Cu, Fe
x100
ppm
A.
B.
Cu
Zn
Fe
0
5
10
15
20
0
20
40
60
TIME in days

Figure 10. Column leaching of low grade ore by SM-4 (A) and SM-7 (B) in LP medium. Ore was mixed with sand in a 50% weight mixture as described in Materials and Methods.

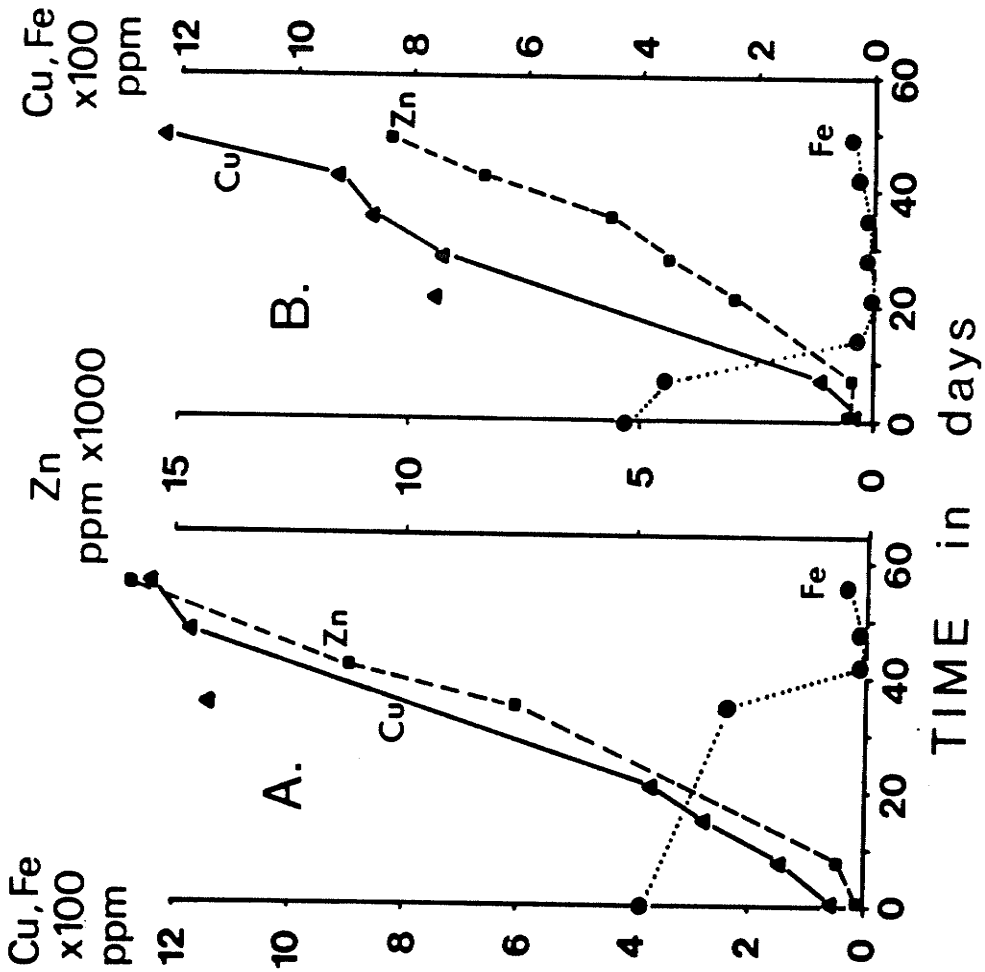
Cu, Fe
x100
ppm
Zn
ppm x1000
A.
B.
Cu
Zn
Fe
TIME in days
0
2
4
6
8
10
12
5
15
20
40
60

were much higher than those from the high grade ore (4 and 2 times by SM-4 and 3 and 1.5 times by SM-6 for Cu and Zn, respectively). The Cu/Zn % extraction ratios were higher (0.72 - 1.11) with the low grade ore than with the high grade ore (0.33 - 0.41). The ratios were higher with *T. thiooxidans* than with *T. ferrooxidans* in agreement with shake-flask experiments, but the low value of 0.33 in column leaching with *T. ferrooxidans* was still higher than the values obtained in shake-flasks (0.1 - 0.2).

It was necessary to add acid almost daily to maintain the pH below 2.5 as in the shake-flask leaching. The acid requirement was higher with the low grade ore. This was probably due to the higher gangue content (24%) compared to the high grade ore samples (15.1% and 22.5%) or the higher pyrrhotite content (7.0% compared to 3.0% and 2.6%) which is known to consume acid (2). *T. thiooxidans* which is expected to produce sulfuric acid from sulfides did not reduce the acid requirement. The level of soluble iron remained low in Figures 9 and 10, but ferric iron precipitate (ferric hydroxide or jarosite) was pronounced in columns with *T. ferrooxidans*. This precipitation can release sulfuric acid (73). Columns with *T. thiooxidans* showed little iron precipitation since the organism cannot oxidize ferrous iron to ferric iron. There was, however, some soluble iron release during the leaching (Fig. 9B) presumably as ferrous iron which eventually dissappeared possibly by chemical oxidation and precipitation.

Leaching of high grade ore by mixed cultures

The effect of mixed cultures of *T. ferrooxidans* and *T. thiooxidans* was studied on high grade ore leaching (Table 10 and Figure 11). Columns

TABLE 10. Leaching of high grade ore by mixed cultures

	Columns		
	SM-(4 + 6)	SM-(5 + 6)	SM-(1 + 6)
A. LP medium			
Duration (d)	30	36	29
Cu % extraction/30d	1.30	1.26	1.73
Zn % extraction/30d	1.42	4.27	5.27
Cu/Zn % ratio	0.92	0.30	0.33
g acid/Kg ore/30d	5.2	4.2	4.2
B. HP medium			
Duration (d)	28	34	39
Cu % extraction/30d	1.07	1.19	1.61
Zn % extraction/30d	1.54	3.95	4.54
Cu/Zn % ratio	0.69	0.30	0.35
g acid/Kg ore/30d	3.5	3.2	2.7

Column leaching experiments were carried out as described in Materials and Methods using LP or HP medium. High grade ore used was sample No. 1 for SM-4 + SM-6 column and sample No.2 for SM-5 + SM-6 and SM-1 + SM-6 columns. Acid: 96% sulfuric acid (density = 1.84 g/mL). Concentration was reduced to 10 N for addition.

Figure 11. Column leaching of high grade ore by SM-5 + SM-6 mixed culture. (A) LP medium; (B) HP medium. The No. 2 high grade ore sample was used.

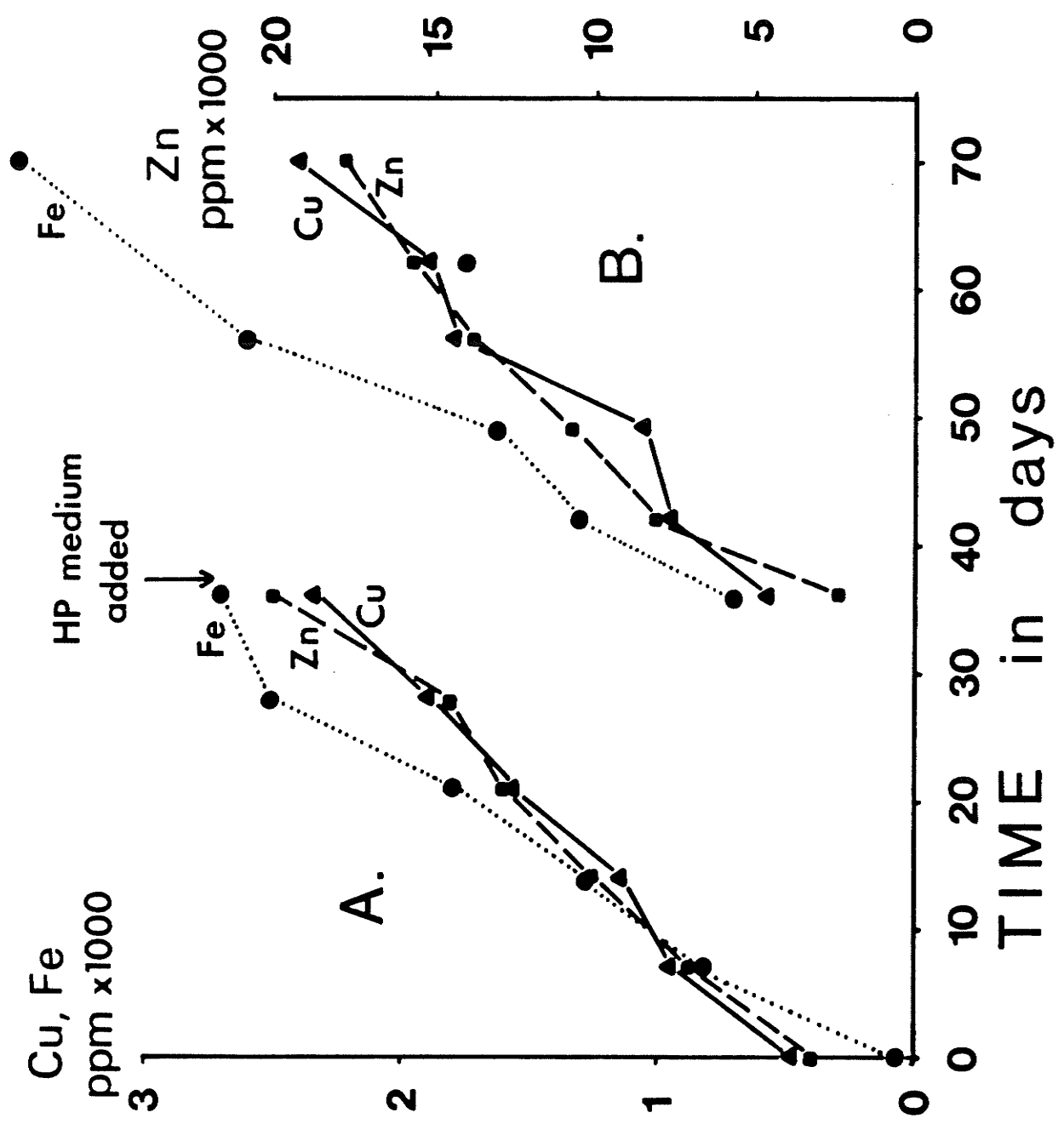
Cu, Fe
ppm x1000
3
2
1
0
Zn
ppm x1000
20
15
10
5
0
HP medium
added
Fe
Zn
Cu
A.
B.
Fe
Cu
Zn
0
10
20
30
40
50
60
70
TIME in days

from experiments in Table 9A were used for this purpose after replacing the culture reservoirs with fresh LP medium plus 50 mL fresh bacterial culture of different strain. *T. thiooxidans* SM-6 was inoculated into the SM-4 and SM-5 columns (both *T. ferrooxidans*) to constitute the SM-4 + SM-6 and SM-5 + SM-6 columns. *T. ferrooxidans* SM-1 was inoculated into the SM-6 column to form the SM-1 + SM-6 column.

The addition of SM-6 culture to the SM-4 and SM-5 columns (Table 10A) increased the Cu extraction rate, particularly in the SM-4 column (0.61 → 1.30 %/30d) increasing the Cu/Zn % extraction ratio from 0.33 to 0.92. The addition of SM-1 to the SM-6 column increased both the Cu and Zn extraction rate considerably (1.04 → 1.73 % Cu and 2.53 → 5.27 % Zn /30d). The Cu/Zn % extraction ratio was reduced from 0.41 to 0.33, a typical value for *T. ferrooxidans* alone (Table 9). The acid consumption was relatively unchanged by mixed cultures. The production of soluble iron increased (Fig. 11A) in parallel with Cu and Zn in contrast with single cultures (Figures 9 and 10).

The effect of medium was studied by replacing the leaching solution in the culture reservoir with HP medium. In the shake-flask experiments the LP medium favoured *T. thiooxidans* and the HP medium *T. ferrooxidans* in the mixed cultures. The concentration of soluble iron increased as expected from *T. ferrooxidans* activities (Fig. 11B). The Cu and Zn extraction rates showed a slight decrease in almost all the columns (Table 10B). In the SM-4 + SM-6 column the Cu/Zn % extraction ratio decreased from 0.92 to 0.69 as expected from the dominance of *T. ferrooxidans*, while the ratio did not change in other columns. The acid requirement was reduced as expected due to the higher buffering capacity

of the HP medium.

Leaching of low grade ore by mixed cultures

The effect of mixed cultures of *T. ferrooxidans* and *T. thiooxidans* was then studied on the leaching of low grade ore (Table 11 and Figure 12). The columns from experiments in Table 9B were used after replacing the medium in the culture reservoir with fresh LP medium plus 50 mL fresh bacterial cultures: SM-6 to the SM-4 column (SM-4 + SM-6), SM-5 to the SM-6 column (SM-5 + SM-6), and SM-4 to the SM-7 column (SM-4 + SM-7).

The addition of SM-6 culture to the SM-4 column (Table 11A) doubled the Zn extraction rate (3.49 → 7.28 %/30d), while the Cu extraction rate increased only slightly, resulting in a decrease in the Cu/Zn % extraction ratio (0.72 → 0.40). The addition of SM-5 and SM-4 to the SM-6 column and SM-7 column, respectively, had unexpectedly different effects. SM-5 decreased sharply both the Cu and Zn extraction rates of the SM-6 column (3.18 → 1.08 % Cu and 3.95 → 1.38 % Zn/30d), while SM-4 increased greatly both the rates of the SM-7 column (2.83 → 5.57 % Cu and 2.55 → 7.93 % Zn/30d). These results may indicate that SM-5 and SM-6 are not compatible in the low grade ore column and that SM-5 is inhibiting the ore leaching by SM-6, while SM-4 is compatible with both SM-6 and SM-7, particularly with SM-7 where the leaching rates increased with the mixed culture. It is, however, noted that SM-6 improved the metal leaching rates of the high grade ore column with SM-5 (Table 10). The Cu/Zn % extraction ratio of the SM-7 column was reduced by the SM-4 culture (1.11 → 0.70) due to a higher increase (3 times) in the Zn extraction rate than in the Cu extraction rate (2 times). The soluble iron concentration also showed a modest increase (Figure 10B and 12A). The acid requirement decreased in

TABLE 11. Leaching of low grade ore by mixed cultures

	Columns		
	SM-(4 + 6)	SM-(5 + 6)	SM-(4 + 7)
A. LP medium			
Duration (d)	36	30	29
Cu % extraction/30d	2.93	1.08	5.57
Zn % extraction/30d	7.28	1.38	7.93
Cu/Zn % ratio	0.40	0.79	0.70
g acid/Kg ore/30d	4.2	5.6	4.2
B. HP medium			
Duration (d)	28	28	34
Cu % extraction/30d	3.42	1.35	4.41
Zn % extraction/30d	7.64	2.42	9.52
Cu/Zn % ratio	0.45	0.56	0.46
g acid/Kg ore/30d	2.8	5.1	2.9

Column leaching experiments were carried out as described in Materials and Methods using LP or HP medium. Acid: 96% sulfuric acid (density = 1.84 g/mL). Concentration was reduced to 10 N for addition.

Figure 12. Column leaching of low grade ore by SM-4 + SM-7 mixed culture. (A) LP medium; (B) HP medium.

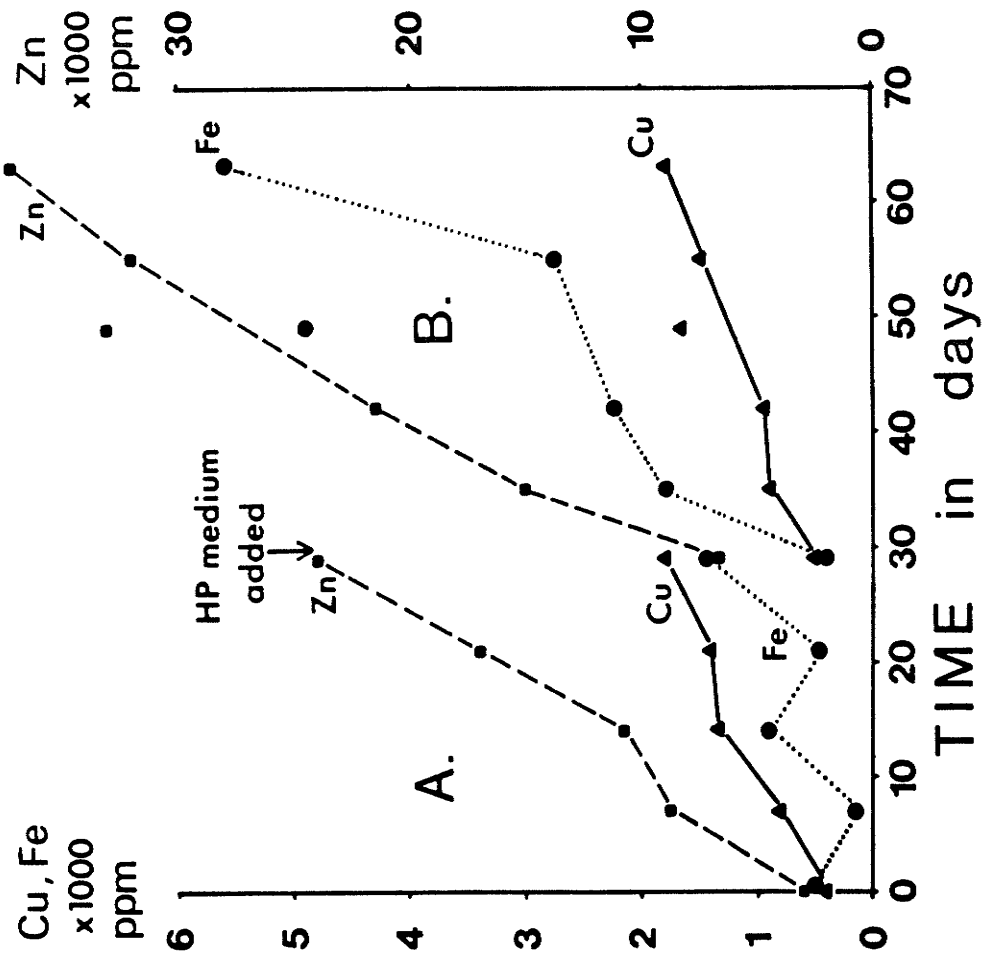
Cu, Fe
x1000
ppm
Zn
x1000
ppm
A.
B.
HP medium
added
Zn
Cu
Fe
Zn
Fe
Cu
TIME in days

all three columns by mixed cultures.

When the leaching medium was changed to HP medium the results in Table 11B and Figure 12B were obtained. In contrast to the results with the high grade ore (Table 10), the Cu and Zn extraction rates generally increased in the HP medium compared to the rates in the LP medium. The Cu/Zn % extraction ratio decreased as expected, except in the SM-4 + SM-6 column. The acid requirement was reduced in the columns, particularly in the SM-4 + SM-6 and the SM-4 + SM-7 columns, the two fastest leaching columns of all the columns studied in this work. The soluble iron production increased (Fig. 12B) in the HP medium as expected.

Ore surface area experiments

The small columns were used to test the effect of ore particle size on the leaching rates. For this purpose, 50% mixtures of sand plus ore of different particle sizes were leached by a mixed culture of *T. ferrooxidans* SM-4 plus *T. thiooxidans* SM-7. Four different size fractions were used: (1) $\frac{1}{4}$" - $\frac{1}{2}$"; (2) $\frac{1}{2}$" - 1"; (3) 1" - $1\frac{1}{2}$"; (4) $1\frac{1}{2}$" - 2". No fines were present in any of the samples. The available surface area of ore in each column was calculated using average specific gravities of minerals (8). The particulars for each column are listed in Table 12. The columns were run under standard conditions (using a flow rate of 0.057 mL/cm^2 per minute) for more than two months in order to establish active bacterial populations.

Four experiments of roughly one month duration each were carried out using different flow rates. The results from these experiments are summarized in Table 13. The extraction rates were lower than the previous experiments with the same bacterial cultures and acid consumption was

TABLE 12. Characteristics of ore size fractions

	Columns			
	1	2	3	4
Size fraction	$\frac{1}{4}$" - $\frac{1}{2}$"	$\frac{1}{2}$" - 1"	1" - $1\frac{1}{2}$"	$1\frac{1}{2}$" - 2"
Average diameter (mm)	9.6	19.0	31.8	44.4
Kg ore used	1.7	1.7	1.7	1.7
Average specific gravity (g/cm^3)	4.25	4.24	4.22	4.22
Total surface area (cm^2)	2498	1270	763	557

Surface areas were calculated by assuming spheres with diameters equal to the average particle sizes of the fractions. The theoretical number of spheres per 1.7 Kg ore were calculated using the average specific gravity of each ore fraction.

TABLE 13. Ore surface area experiments

	Columns			
	1	2	3	4
Surface area (cm^2)	2498	1270	763	557
A. Flow rate = 0.031 mL/cm^2 per minute				
Cu % extraction/30d	0.85	0.58	0.33	0.35
Zn % extraction/30d	1.04	0.56	0.53	0.45
Cu/Zn % ratio	0.82	1.04	0.62	0.78
g acid/Kg ore/30d	3.73	2.95	1.87	1.87
B. Flow rate = 0.057 mL/cm^2 per minute				
Cu % extraction/30d	0.97	0.66	0.41	0.45
Zn % extraction/30d	1.53	0.64	0.48	0.36
Cu/Zn % ratio	0.63	1.03	0.85	1.25
g acid/Kg ore/30d	2.95	2.64	2.18	1.87
C. Flow rate = 0.096 mL/cm^2 per minute				
Cu % extraction/30d	0.76	0.62	0.43	0.37
Zn % extraction/30d	1.90	0.82	0.47	0.41
Cu/Zn % ratio	0.40	0.76	0.91	0.90
g acid/Kg ore/30d	2.03	1.75	1.17	0.75
D. Flow rate = 0.125 mL/cm^2 per minute				
Cu % extraction/30d	0.95	0.55	0.53	0.37
Zn % extraction/30d	1.52	0.51	0.42	0.21
Cu/Zn % ratio	0.63	1.08	1.26	1.76
g acid/Kg ore/30d	0.02	0.02	0.02	0.02

Column leaching experiments were carried out as described in Materials and Methods using HP medium. The ore samples are described in Tables 1, 2, and 12. The mixed culture SM-4 + SM-7 was used.

higher. This was probably due to the different ore samples used. Both Cu and Zn extraction rates tended to increase with the surface area of ore available to the bacteria. This is to be expected, since the mineral surface is in fact the substrate used by the microorganisms (5, 82). Figure 13 illustrates the results obtained using a flow rate of 0.031 mL/cm^2 per minute and shows a linear relationship between metal extraction and surface area. This also indicates that the Cu/Zn % extraction ratios remained fairly constant with surface area for the particle sizes used. Monthly acid consumption also increased linearly with surface area (Fig. 13 inset). Similar relationships for both metal extraction and acid consumption were seen at the other flow rates.

The extraction rates were also found to increase linearly with the inverse of particle size (Fig. 14). This can be explained in terms of the relationship between mass and surface area. If we assume that ore particles have overall spherical shapes, then:

Surface area (S.A.) = $4\pi r^2$ where r = radius

Volume (V) = $4/3\pi r^3$

and particle volume is interconvertible with particle mass by way of the particle's specific gravity. A spherical ore particle with a particle size equivalent to 2nr will have a mass proportional to $(nr)^3$ while a smaller particle of the same ore with a particle size of 2r will only have a mass proportional to r^3. Thus, it will require n^3 number of the smaller particles to make up an equivalent mass of one large particle. Now, if we compare the total surface area of equivalent ammounts (by weight) of the two different ore samples:

Total S.A. (large) = 1 particle x $4\pi(nr)^2$/particle = $4n^2\pi r^2$

Figure 13. Effect of ore surface area available on the leaching rates for Cu and Zn. Data obtained from Table 13. Inset is the effect of ore surface area on the acid consumption (data also obtained from Table 13). Column leaching experiments were carried out with ore fractions listed in Table 12 mixed with sand and using the SM-4 + SM-7 mixed culture at a flow rate of 0.031 mL/cm^2 per minute. Minimum surface area refers to the surface area of a single spherical solid particle of ore with a mass of 1.7 Kg and a specific gravity of 4.23 g/cm^3 (average value derived from the mineral content data, Table 2). This theoretical ore particle would have a volume of 402 cm^3, a surface area of 263 cm^2, and radius of 45.8 mm (particle size or diameter of 91.6 mm).

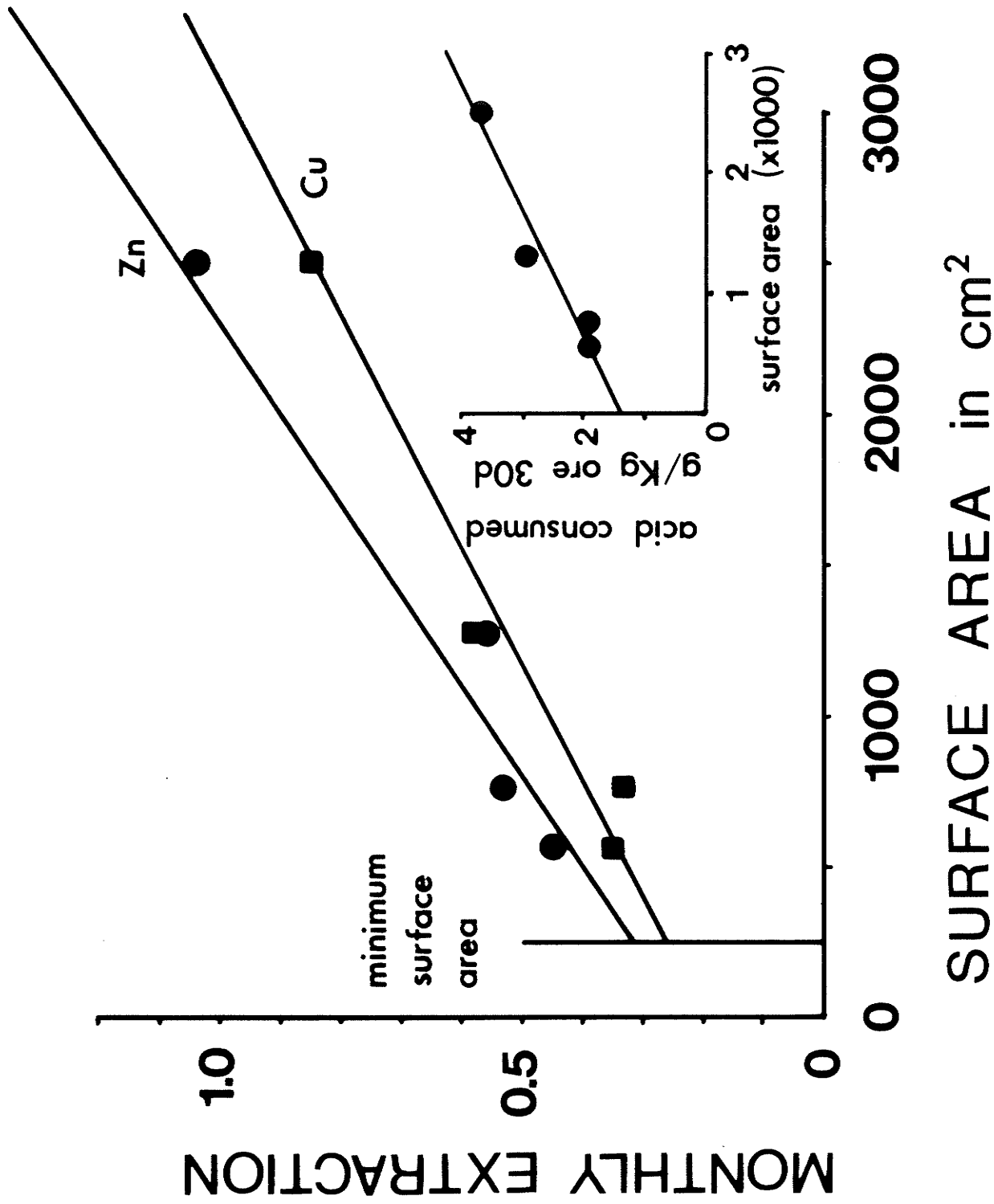
MONTHLY EXTRACTION
1.0
0.5
0
0
1000
2000
3000
SURFACE AREA in cm²
Zn
Cu
minimum surface area
acid consumed g/Kg ore 30d
4
2
0
0
1
2
3
surface area (x1000)

Figure 14. Effect of ore particle size on the leaching rates for Cu and Zn. Conditions were the same as in Figure 13.

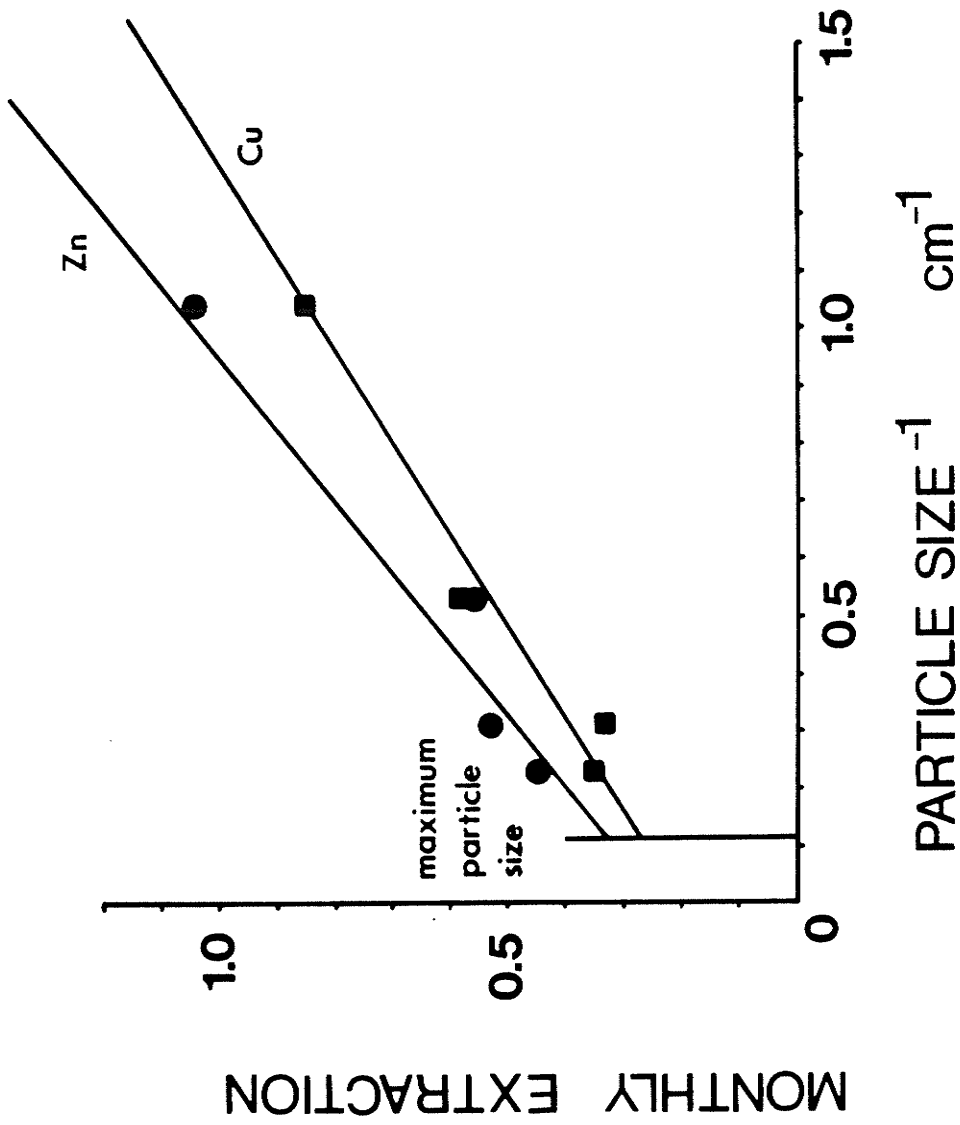
MONTHLY EXTRACTION
1.0
0.5
0
0.5
1.0
1.5
PARTICLE SIZE^{-1} cm^{-1}
Zn
Cu
maximum particle size

Total S.A. (small) = n^3 particles x $4\pi r^2$/particle = $4n^3\pi r^2$

The surface area ratio of the small particle sized ore to the large particle sized ore will be $n^3/n^2 = n$ (see Fig. 18 for example). As a result, the increase in surface area will be directly proportional to the decrease in r, or particle size. Hence, leaching rate (which increases with surface area) will increase with decreasing particle size (1/r).

Flow rate had an ambiguous effect on the leaching rates as seen in Figures 15 and 16. The leaching rates increased with increasing flow rate up to a maximum value, then decreased. The maximum leaching rates for Cu, irrespective of surface area, occurred at flow rates of 0.060 to 0.070 mL/cm^2 per minute. With Zn leaching, the flow rates at which maximum extraction occurred tended to increase with increasing ore surface area. Extraction maxima for Zn occurred at approximate flow rates of 0.050, 0.050, 0.085, and 0.095 mL/cm^2 per minute for columns 4, 3, 2, and 1, respectively. Flow rate had a clear effect on the acid consumption by the system. In all cases, acid requirement for leaching decreased with increasing flow rate. At a flow rate of 0.125 mL/cm^2 per minute (the fastest flow rate used), the acid consumption for all four columns was virtually zero (Table 13). This can only be explained by increased acid production by bacteria at higher flow rates.

Large-scale column experiment

A large-scale column leaching experiment with large-size ore particles (6" to 8" diameter) was carried out. The column had an inside diameter of 55 cm and a height of 4.5 m, containing 1.8 tons of ore and 650 Kg of sand. A mixed culture of *T. ferrooxidans* SM-4 and *T. thiooxidans* SM-7 was used.

Figure 15. Effect of flow rate on the leaching rates of Cu. Data was obtained from Table 13. The monthly extraction rates are expressed in % extraction per 30 days.

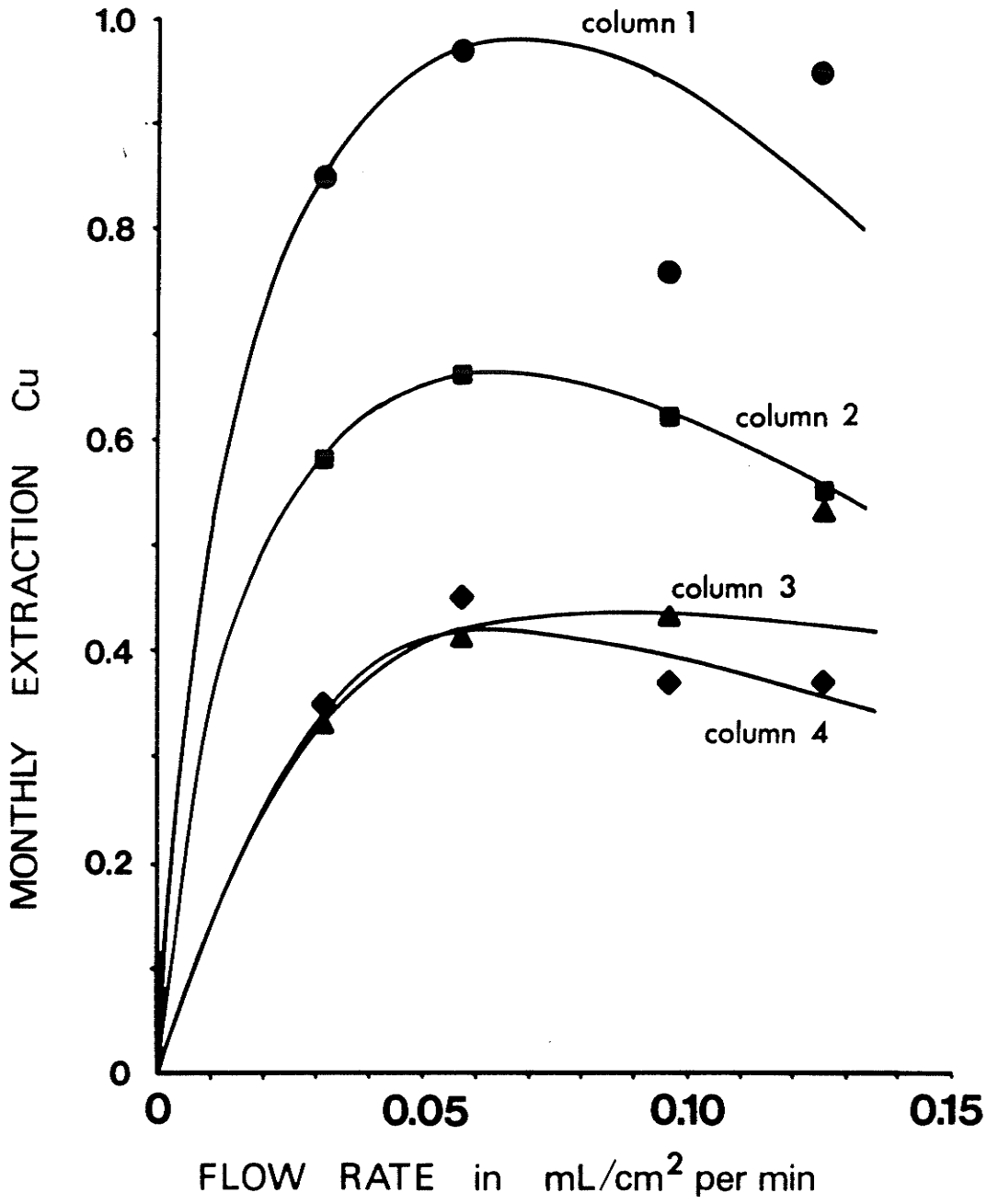
1.0
0.8
0.6
0.4
0.2
0
MONTHLY EXTRACTION Cu
column 1
column 2
column 3
column 4
0
0.05
0.10
0.15
FLOW RATE in mL/cm2 per min

Figure 16. Effect of flow rate on the leaching rates of Zn. Data was obtained from Table 13. The monthly extraction rates are expressed in % extraction per 30 days.

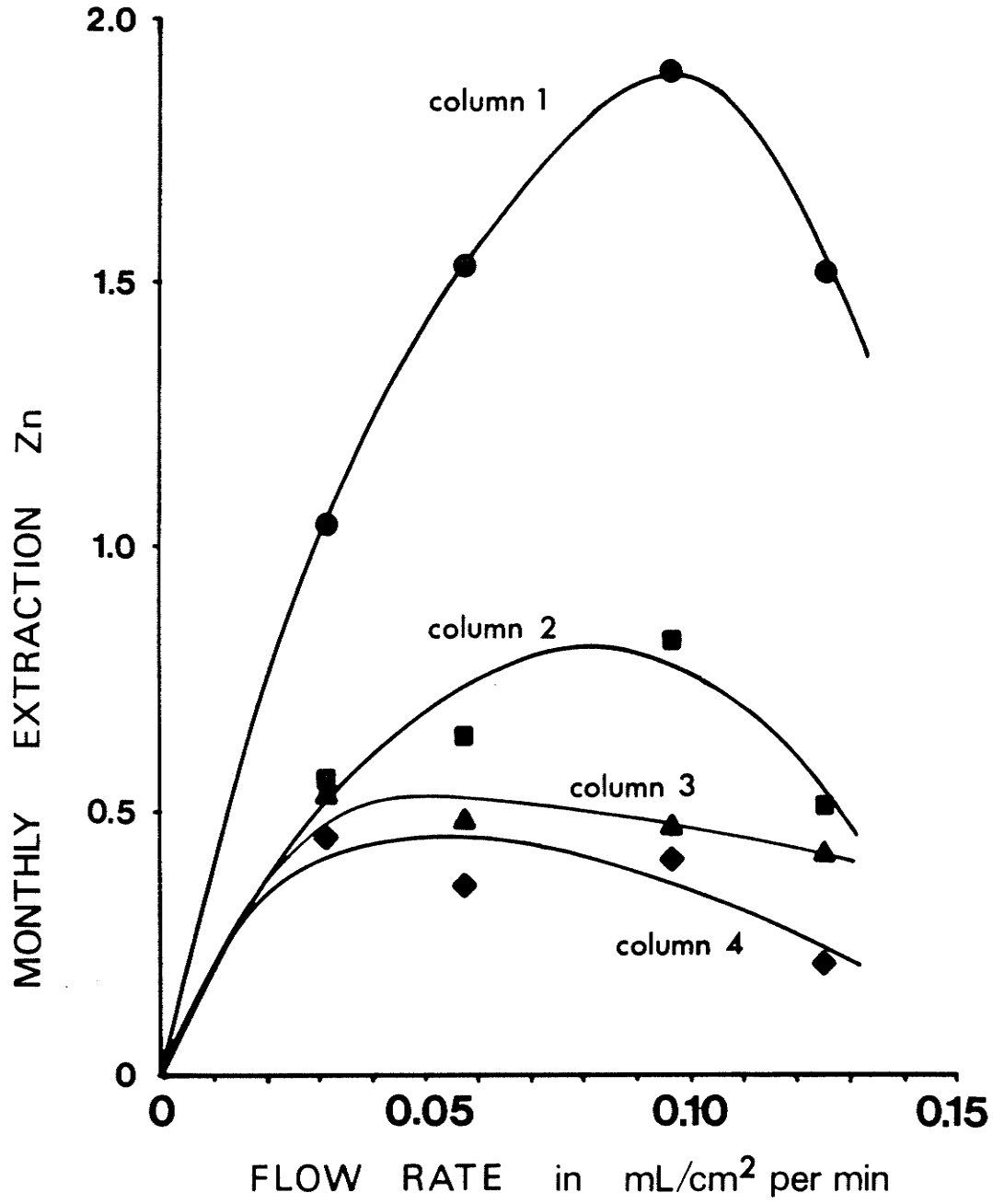
2.0
1.5
1.0
0.5
0
MONTHLY EXTRACTION Zn
column 1
column 2
column 3
column 4
0
0.05
0.10
0.15
FLOW RATE in mL/cm2 per min

At first, the large column was run in a continuous percolation mode, same as the small columns. Upon starting medium percolation, 25 L of liquid were retained in the column bed in addition to the 26 L of water used to wet the sand (see Materials and Methods). It was also found that a further 20 L of medium were circulating inside the column at any one time. With the 50 L of media in the culture carboy, the total volume of liquid in the system during the first two stages of column operation (days 0 - 103) was 121 L (see Table 14). The flow rate used was 4.5 L per hour or 0.032 mL/cm^2 per minute. Initially, the column was inoculated with 4 L each of *T. ferrooxidans* SM-4 and *T. thiooxidans* SM-7 bacterial cultures. However, the effluent pH was quite high at 5.5 so a further 8 L each of SM-4 and SM-7 were added to the system. Even after this second inoculation the pH remained high.

The high effluent pH was probably due to the carbonates present in the ore as $CaCO_3$ and $MgCO_3$. These caused several problems by reacting with H_2SO_4 and precipitating as $CaSO_4$ which plugged up tubing and pumps. The medium had to be cleaned several times by decanting it and filtering out the precipitates (Whatman No. 1 filter paper). Throughout the experiment, the soluble Ca and Mg remained at about 400 to 600 ppm.

Figure 17 shows the time course leaching profile for the large column. During the first phase of the experiment, metal extraction was low and the effluent pH was quite high (Table 15). Samples of effluent tested with a Clark electrode (data not shown) were anaerobic, indicating that oxygen was limiting inside the column. Previous column studies have shown leaching to take place mostly in the uppermost layers of the bed (14). In our case, leaching was probably taking place only at the very

TABLE 14. Volumes in large column

	A Continuous Percolation	B Column Drained	C Pulse Percolation
Total volume inside column (L)	1069	1069	1069
Granite bottom layer and top air space (L)	69	69	69
Volume of ore (L)[1]	600	600	600
Volume of sand (L)[2]	399	399	399
Volume of liquid inside the column (L)[3]	71	51	61
Volume of liquid outside the column (L)	50	70	50
Air space (L)[4]	83	103	93
External oxygen supply (L/30d)[5]	19	32	325

[1]Assuming an average specific gravity of 3 g/cm^3 for the 1.8 tons of 6" - 8" ore used.

[2]Assuming an average specific gravity of 1.63 g/cm^3 for the 650 Kg of sand used, which includes an air space of 154 L (38.7%).

[3]It consists of 26 L for wetting the sand for packing, 25 L retained, and 20 L flowing. For (C) the value is an average value since the liquid is flowing in a 4 hour cycle (2 hours on/2 hours off).

[4]Air space in sand (154 L) minus the liquid volume.

[5]It was calculated assuming the O_2 solubility of 0.258 mM (5.78 mL/L) and 4.5 L/hour liquid percolation in A, the 24 hour drain (20 L liquid space replaced with 20 L air) a week for B, and 9 L air following the liquid every 4 hours in C. The 20% O_2 concentration value in air was used.

TABLE 15. Leaching rates achieved with the large column

	Continuous Percolation	24 hour Drainage	Daily Stoppage	Pulse Percolation	
				Initial	New Medium
g Cu/30d	4.3	7.3	11.9	18.6	47.9
g Zn/30d	50.3	163.4	50.1	83.3	156.4
Cu % extraction/30d	0.011	0.019	0.032	0.049	0.127
Zn % extraction/30d	0.082	0.267	0.082	0.136	0.255
Cu/Zn % ratio	0.13	0.07	0.39	0.36	0.50
Initial pH	5.6	5.5	4.4	3.1	2.6
Final pH	5.5	4.2	3.1	2.6	2.6

Large-scale column leaching experiments were carried out as described in Materials and Methods using HP medium and a mixed culture of SM-4 + SM-7. The metal extraction values were based on the metal content of the ore given in Table 1. The column contained a total of 37.8 Kg Cu and 61.2 Kg Zn. The flow rate used throughout the experiment was 4.5 L/hour or 0.032 mL/cm^2 per minute.

Figure 17. Time course leaching profile of the large column. Experimental procedure was as described in Materials and Methods. Continuous percolation was carried out from days 0 - 87 (Stage 1). Weekly drainage for 24 hours was carried out from days 87 - 103 (Stage 2). Daily stoppage for 2 hours was carried out from days 112 - 131 (Stage 3). Pulse percolation was carried out from days 135 - 194 (Stage 4).

T: inoculation with *T. thiooxidans* SM-7

F: inoculation with *T. ferrooxidans* SM-4

S: spill

D: drainage for 24 hours

C: change in medium (50 L)

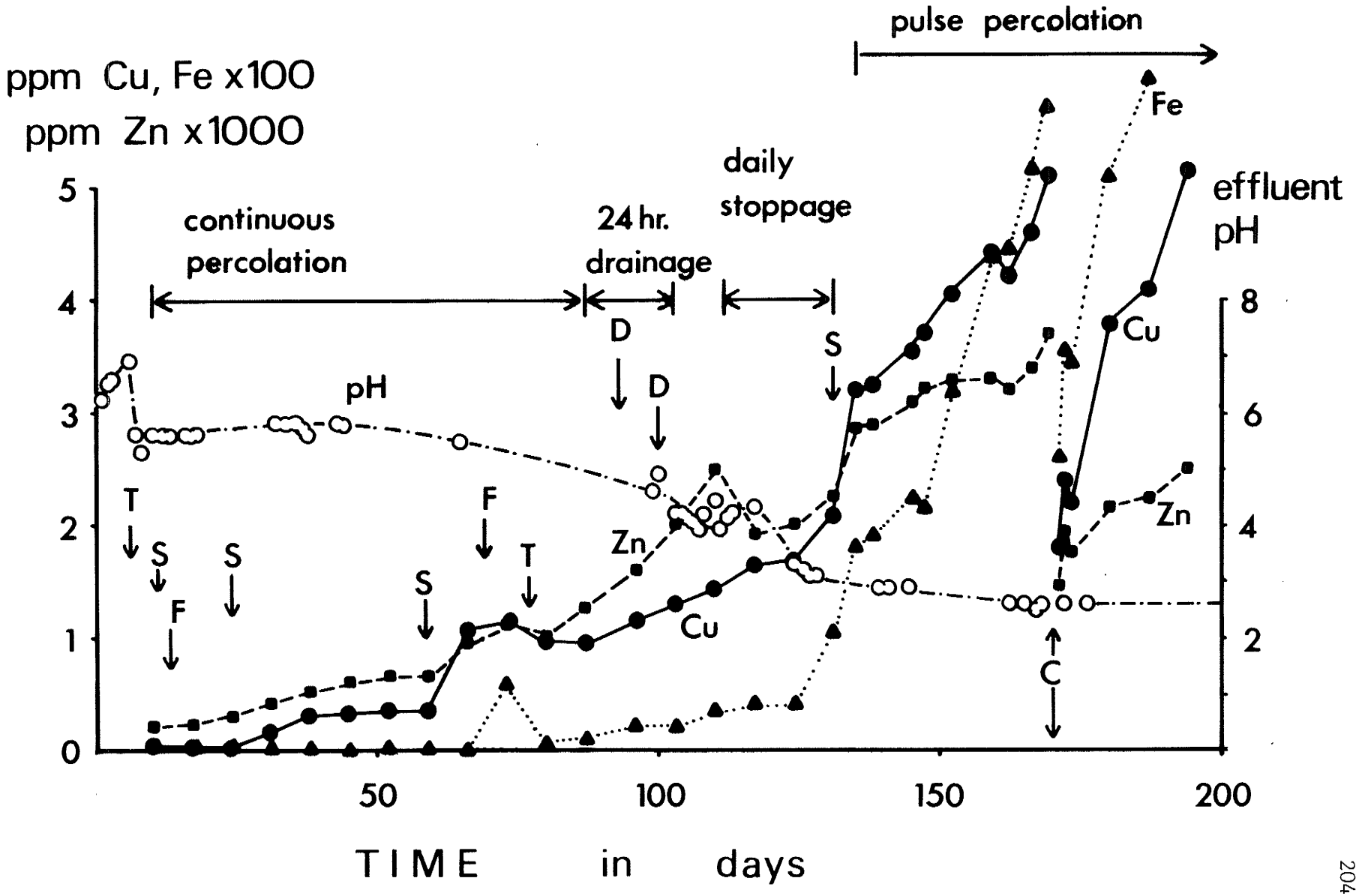
ppm Cu, Fe x100
ppm Zn x1000
pulse percolation
daily
stoppage
continuous
percolation
24 hr.
drainage
effluent
pH
Fe
Cu
Zn
pH
T
S
F
D
C
5
4
3
2
1
0
8
6
4
2
50
100
150
200
TIME in days

top of the column while the rest remained anaerobic and alkaline. Any iron released by leaching was probably precipitating in the column due to the higher pH.

Due to technical difficulties, a number of spills occurred during the course of the experiment, each one followed by a sharp increase in metal extraction. It is possible that bacterial activity was stimulated by air entering the column due to the drainage caused by the spill. An attempt was made to mimic the effects of a spill by draining the column for 24 hours each week for two weeks. This would temporarily increase the air space inside the column bed by 20 L (Table 14). This did improve metal extraction (Fig. 17 and Table 15) but not to the same extent as the spills. A significant lowering of the effluent pH was seen during this stage and (for the first time) iron became prominent in the leaching solution, probably due to less precipitation with the higher acidity.

To try and further improve the aeration problem, the flow of solution was stopped for 2 hours a day, every day (stage 3). The reasoning behind this was that during the interruption of flow, the descending liquid inside the column bed would draw in a volume of air equal to 2 hours x 4.5 L/hour or 9 extra L of air every day. This not only increased Cu extraction but also had a remarkable effect in lowering the effluent pH (Table 15 and Fig. 17). Extraction of Zn was lower than with weekly draining, suggesting that the sudden increase in soluble Zn by weekly draining (Fig. 17) may have been due to a temporary sudden release of labile Zn.

Encouraged by the results obtained from the daily stoppage of the column, we reduced the medium by 10 L to 111 L total liquid volume

(Table 14) and linked the No. 1 pump (culture carboy to column, Fig. 2) to a timer with a four-hour cycle (2 hours on/2 hours off, Mastercraft Multiple Cycle Timer, Canadian Tire Corp., Ltd., Toronto). Thus, the percolation of liquid through the column would be "pulsed"; 9 L of medium would be flowing through the column bed for two hours followed by 9 L of air for two hours. It was hoped that the 9 L pulses of air would provide oxygen to the lower part of the column and help colonization by bacteria. Indeed, the effluent pH decreased even further, indicating increased acid production by bacteria. Up to this point (day 120), sulfuric acid consumption was 2.84 g/Kg ore or 0.71 g/Kg ore per 30 days. With pulse percolation, this figure was in the order of 0.19 g/Kg ore per 30 days.

Metal extraction increased significantly with the improved aeration (17 times the continuous percolation) by 2 hour on/2 hour off cycle (Fig. 17, Table 15). The increase in soluble iron was specially noticeable, probably due to the stabilization of effluent pH. After a month operating the column in the pulse percolation mode (days 135 - 169, Fig. 17), 50 L of the leaching solution were replaced with 50 L of fresh HP medium. This helped to remove a large portion of the soluble carbonate species. After medium replacement, the metal extraction increased yet again (Fig. 17, Table 15).

The estimated total surface area of ore available to the bacteria in the large column is derived in Table 16. In the small column experiments we found the leaching rate to be proportional to the available surface area of ore and inversly proportional to the ore particle size. We can compare the data from the large column to that of the small columns. The average particle diameter for the large column is 17.8 cm, a value

TABLE 16. Dimensional characteristics of ore in the large column

Mass ore used	1800 Kg
Average specific gravity	3 g/cm^3
Average particle diameter	17.8 cm
Estimated particle volume (sphere)	2953 cm^3
Estimated particle surface area (sphere)	995 cm^2
Estimated number of particles	203
Estimated total surface area	202000 cm^2

approximately 10 times that of the ½" - 1" ore from the small column No. 2 in the ore surface area experiments (Table 12). The 10 fold difference in size means that the number of particles per unit volume is 1/1000 and the total surface area per unit volume or unit weight is 1/10 (see Fig. 18). At a flow rate of 0.031 mL/cm^2 per minute, the leaching rates for Cu and Zn with ½" - 1" ore were 0.58 and 0.56 % extraction per 30 days, respectively (Table 13). These values were about 10 times the rates achieved with the large column in the daily stoppage mode (Table 15) with a flow rate of 0.032 mL/cm^2 per minute and only 2 - 4 times those in the pulse percolation mode (0.127 and 0.255 % per 30 days for Cu and Zn, respectively). If we compare the leaching rates from the low grade ore, however, the difference is much greater. Metal extraction rates (%/30d) for SM-4 + SM-7 with HP medium (flow rate = 0.057 mL/cm^2 per minute) on the low grade ore were 4.41 and 9.52 for Cu and Zn, respectively (Table 11). The 40 fold difference (even in comparison to the best leaching rates achieved) with the large column may also be due to the problem of aeration not being completely uniform in the large column.

Figure 18. Surface area ratio of equal weights of spherical particles with different diameters.

$V = \frac{4}{3}\pi r^3$

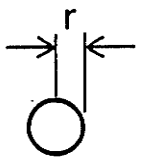

$S = 4\pi r^2$

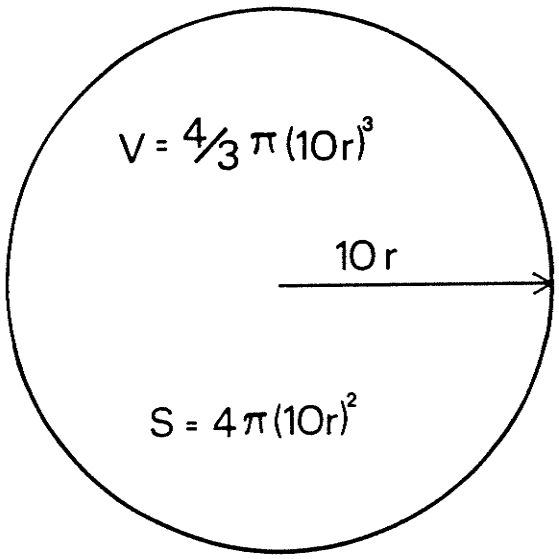

Mass ratio = Volume ratio

$$= \frac{\frac{4}{3}\pi r^3}{\frac{4}{3}\pi(10r)^3} = \frac{1}{1000}$$

Surface area ratio of equal weights:

$$= \frac{1000 \text{ particles}}{1 \text{ particle}} \times \frac{4\pi r^2}{4\pi r^2(10)^2} = \frac{1000}{100} = \frac{10}{1}$$

DISCUSSION

Five strains of *T. ferrooxidans* and two strains of *T. thiooxidans* were isolated from mine water samples and tested for growth on finely ground (-200 mesh) ore in shake-flask leaching experiments. They were shown to be more effective in leaching metals from the ore than the laboratory strains used, probably because of their adaption to, or selection by, their natural habitat in the mine. Both iron-grown *T. ferrooxidans* and sulfur-grown *T. thiooxidans* isolates were capable of leaching Cu and Zn from the ore effectively in shake-cultures, but the leaching efficiency was improved with ore-adapted bacteria. Mixed cultures of *T. ferrooxidans* and *T. thiooxidans* were also effective in leaching but they were not significantly better than the individual organisms. The growth medium had a significant effect in that *T. thiooxidans* seemed to predominate in the low phosphate (LP) medium while *T. ferrooxidans* predominated in the high phosphate (HP) medium. This was probably due to a competition between the two bacterial species.

The shake-flask leaching studies of the finely ground ore by *T. ferrooxidans* and *T. thiooxidans* isolates produced some interesting conclusions with respect to the leaching ability of the two species of bacteria. The Cu/Zn % extraction ratios by *T. ferrooxidans* isolates were always low and in the range of 0.1, while the ratios were higher with *T. thiooxidans* isolates (Tables 3 and 4). Thus, sphalerite (ZnS) was solubilized much faster than chalcopyrite ($CuFeS_2$) by *T. ferrooxidans*. This result agrees with the reported electrode potentials (EP) shown in Table 17 (35). The electrochemical interaction of sulfide minerals favours

TABLE 17. Major minerals present in -200 mesh ore

Mineral	Electrode potential (Volts)*	Percentage content in ore	mol/Kg ore
FeS_2	0.6	51	4.3
$CuFeS_2$	0.4	14	0.76
ZnS	0.23	19	1.9

*Literature values (35) for pH 2.3.

the oxidation of the mineral with the lowest electrode potential and therefore the solubilization of sphalerite is favoured. No doubt, the Fe^{3+} produced by the organism will accelerate the process by maintaining a high redox potential (Eh) in the medium during the experiments.

The increased Cu/Zn % extraction ratios by *T. thiooxidans* is interesting, and may be due to its mode of attack of sulfide minerals, which is fundamentally different from that of *T. ferrooxidans*. *T. thiooxidans* can only oxidize sulfide but not iron and is expected to attack the sulfide portion of minerals without preference for particular metals. Its inability to oxidize ferrous iron to ferric iron should lead to a high Fe^{2+}/Fe^{3+} ratio and therefore a lower Eh. This resulting lower Eh in the medium would be unfavourable for galvanic interactions of sulfide minerals, which was observed in *T. ferrooxidans* leaching. Therefore, a more even and balanced leaching of various metals will be expected with *T. thiooxidans*.

Initial column leaching studies (Tables 7 and 8) demonstrated successful Cu and Zn leaching by *T. ferrooxidans* and a mixed culture of *T. ferrooxidans* and *T. thiooxidans* from crushed ore (-3/4 inch) in columns with ore alone and ore plus smelter slag. The presence of tailings along with the ore inhibited the leaching probably because the raised pH in the column (effluent pH of 5.3) did not allow the growth of the acidophilic bacteria. Bacteria, however, were present in the culture reservoir (as seen by microscopic observation and by measurement of Fe^{2+} and S oxidizing activity in a Gilson Oxygraph, data not shown) although in smaller numbers than in the reservoirs of other columns.

The column leaching studies with ore and sand (Table 9) basically

agreed with the results obtained with the shake-flask experiments in that the leaching by *T. thiooxidans* results in a higher Cu/Zn % extraction ratio than by *T. ferrooxidans*. The difference, however, was smaller than in the shake-flask experiments and the ratio was generally higher in the column leaching (e.g., 0.1 → 0.33 for *T. ferrooxidans*). These results are probably due to the ore size difference in the two studies. The larger particle size (-3/4") in the column studies probably reduced the electrochemical interaction among sulfide minerals which was more pronounced in the shake-flask experiments (-200 mesh) with a more rapid solubilization of sphalerite (ZnS) than chalcopyrite ($CuFeS_2$). The Cu/Zn % extraction ratio was particularly high with the low grade ore where the mineral interaction is expected to be smaller. This was in contrast to a similar column leaching study (51) where the ratios were between 0.06 - 0.16 for a similar particle sized ore as in our experiments.

The column leaching by mixed cultures of *T. ferrooxidans* and *T. thiooxidans* (Tables 10 and 11) was generally faster than the leaching by single strains except the SM-5 + SM-6 column with the low grade ore. The SM-4 + SM-7 column with the low grade ore was exceptionally fast in leaching both Cu and Zn and the acid requirement was also much reduced. Since the ore composition in the mined-out area of the Flin Flon mine is considered to be close to that of the low grade ore used, the SM-4 + SM-7 combination will be the best candidate in any *in situ* leaching experiments.

This study indicates the importance of strain selection in considering a successful bacterial leaching of sulfide ores and the advantage of using mixed cultures of compatible strains of *T. ferrooxidans*

and *T. thiooxidans* to increase the leaching rates of metals by utilizing their respective Fe^{2+} and S oxidizing activities.

In the ore surface area experiments (Table 13), the leaching rates were lower than those in previous experiments (much lower than the rates with the same bacterial cultures, SM-4 + SM-7, on the low grade ore). This was probably due to the ore sample not being as amenable for bacterial action as other samples tested so far. The ore used for the surface area experiments was similar to the high grade ores in terms of higher Cu and Zn contents although it had much lower pyrite and higher pyrrhotite contents (Table 2). The Cu/Zn % extraction ratios were higher, approaching one in many cases.

The leaching rates were linear functions of available surface area of ore (Figure 13). This is consistent with studies using sulfur prills which found bacterial oxidation to be a linear function of surface area per unit weight of sulfur (42). We used the same weights of ore for each experiment so we could compare the ore surface area directly. Leaching activity has been associated with bacteria attached to the sulfide mineral surface (5, 82). In our experiments, bacteria were allowed to grow inside the columns for 2 months before leaching rates were determined. By this time, the ore was probably well colonized and the leaching activity determined likely represents the oxidizing activity of these cells under the conditions used rather than fresh bacterial growth on the ore.

The effect of flow rate on the leaching rates was interesting. Increasing the flow rate will increase the supply of oxygen to the column bed and thus should improve bacterial activity. Indeed, the bacteria's ability to produce sulfuric acid increased with flow rate, as evident

from the decrease in acid consumption (Table 13). The increased oxygen supply must have helped the oxidation of sulfide. At low flow rates, the observed increase in leaching rates with increasing flow rate (Figures 15 and 16) was probably due to the increased oxygen supply. At higher flow rates, however, leaching rates actually decreased , particularly for Zn extraction. We do not know why this inhibition occurs, but it is interesting that the optimal flow rate for Zn extraction increased with increasing surface area of ore. Perhaps the supply of oxygen has to be balanced with the consumption of oxygen for the maximal leaching of metals. Excess oxygen could have deleterious effects on bacteria or physicochemical parameters essential for effective leaching such as pH and Eh of the medium, and the electrolyte concentration (24, 81). Clearly a further detailed study is required.

Because of the mass (volume) to surface area relationship, leaching rate will increase linearly with the inverse of ore particle size as well as with surface area. Although the results in Figures 13 and 14 did not extrapolate to the origin it is possible to make some estimate of the effect on the leaching rates of large ore particles such as those encountered *in situ*. If the lines in Figure 14 are extrapolated to the particle size of 17.8 cm (7"), the monthly extraction rates of 0.24% Cu and 0.28% Zn are obtained. The highest extraction rates actually obtained in the large column leaching experiment (Table 15) were 0.127% Cu and 0.255% Zn, thus 53% and 91% of the values expected. If, on the other hand, rate is assumed to be proportional to the surface area of the ore, then the 7" ore should leach 10 times more slowly than the $\frac{1}{2}$" - 1" ore.

The best leaching rates achieved with the large column were only 2 -

4 times smaller than the leaching rates (column 2 in Table 13) with the ½" - 1" ore fraction in the small column at equivalent flow rates (0.031 - 0.032 mL/cm^2 per minute). They were, however, 40 times smaller than the leaching rates (Table 11) achieved with the low grade ore at twice the flow rate (0.057 mL/cm^2 per minute). Apparently, differences in the ore sample can have a major effect.

In addition to metal extraction, the feasibility of a bacterial leaching process also depends on achieving metal concentrations in the leaching solution that are high enough for efficient processing (34). The volume of leaching solution used in the small column experiments was 500 mL for 2.6 L of ore-sand mixture; the volume of liquid bound in the inter-grain spaces of the sand was considered to be insignificant in comparison to the total volume. In the large column, the volume of bound liquid was considerable (51 L). The total volume of liquid for the large column in the pulse percolation mode was 111 L for 999 L of ore-sand mixture. In terms of ore surface area, these figures translate into 0.39 mL/cm^2 (500 mL/1270 cm^2) and 0.55 mL/cm^2 (111 L/202000 cm^2) for the small and large columns, respectively. Because metal extraction is occurring by way of leaching solution flowing over the surface of the ore particles, the concentration of metals in the solution will be dependent on the volume of leaching solution per unit surface area and the metal concentrations achieved with the large column should be about half those in the small columns. In fact, the values were about 1/5 for Cu and 1/2 for Zn with the ½" - 1" ore at equivalent flow rates. Compared to the low grade ore, these values were even lower.

A number of problems which were almost insignificant with the small

columns became extremely important in the large column. Even though all the ore samples used in these studies contained some carbonates, the sheer amounts of these in the large column caused many problems both with acid consumption and with the formation of gypsum-type precipitates ($CaSO_4$). These precipitates had to be removed by either filtering the solution or replacing it with fresh medium. In the long run, these precipitates should become less of a problem as the medium is continuously replaced from time to time.

The biggest problem with the large column was that of aeration. The small columns had a bed height of only 37 cm while the large column had a bed height of 4 m. This meant that air diffusion was more extensive in the small column supplementing the oxygen supply by percolating liquid. In the large column with continuous percolation probably only the uppermost layer contained oxygen, the rest becoming anaerobic. The aeration problem not only caused low leaching rates, but also high effluent pH due to failure of the bacteria to produce sulfuric acid. In turn, this failure to produce acid caused iron to precipitate inside the column instead of participating in indirect leaching and becoming available for bacterial oxidation in the aerated culture carboy.

By supplying air directly into the column by way of pulse percolation, most of these problems were solved. The leaching rates improved significantly, the effluent pH decreased to within 0.1 units of the pH in the culture carboy, and soluble iron became very prominent. All of this indicated bacterial growth and colonization of the ore. Indeed, the use of pulse percolation should prove to be an effective method for supplying adequate aeration to large ore piles *in situ*.

CONCLUSIONS

This study showed the importance of using indigenous organisms for carrying out successful leaching operations. Indigenous strains of *T. ferrooxidans* appear to have different cell surface properties from the laboratory ATCC strains. These properties manifested themselves in the form of a cell-cell competitive inhibition effect during the oxidation of Fe^{2+}; it may be that these cell surface properties are responsible for the ability of the mine strains to successfully leach the Cu- and Zn-containing sulfide ore samples tested while the ATCC strains could not. *T. ferrooxidans* and *T. thiooxidans* appear to leach sulfide ores by different mechanisms, *T. ferrooxidans* relying on the electrochemical reactions and interactions among sulfide minerals more than *T. thiooxidans* which attacks the sulfide mineral surface directly. However, the kinetics of pyrite oxidation by *T. ferrooxidans* could not be explained solely by soluble Fe^{2+} oxidation and indirect leaching by Fe^{3+}. In mixed cultures, different growth media could influence the predominance of *T. ferrooxidans* over *T. thiooxidans* and vice versa. Thus, it is possible to preferentially leach Cu or Zn by choice of organisms and leaching conditions, as we were able to do. Bacterial leaching activity is a function of available surface area of ore and inversly proportional to ore particle size, as determined by ore particle size experiments. The information from experiments with laboratory-scale columns could be applied to a pilot-scale column leaching experiment with 1.8 tons of ore where leaching was successful. Thus, elementary bacterial leaching studies can be used to predict the feasibility of an *in situ* leaching operation.

REFERENCES

1. Adair, F.W. 1966. Membrane-associated sulfur oxidation by the autotroph *Thiobacillus thiooxidans*. J. Bacteriol. 92: 899-904.

2. Ahonen, L., et al. 1986. The role of pyrrhotite and pyrite in the bacterial leaching of chalcopyrite ores. In Process Metallurgy 4 Fundamental and Applied Biohydrometallurgy. Eds. R.W. Lawrence et al. Elsevier, Amsterdam, pp. 13-22.

3. Andrews, G.F. 1988. The selective absorption of thiobacilli to dislocation sites on pyrite surfaces. Biotechnol. Bioeng. 31: 378-381.

4. Ballentine, R. and D.D. Burford. 1957. Determination of metals (Na, K, Mg, Ca, Mn, Fe, Co, Cu, Zn). In Methods in Enzymology, vol. 3. Eds. S.P. Colowick and N.O. Kaplan. Academic Press, New York, pp. 1002-1034.

5. Bärtels, C.C., et al. 1989. Novel Technique for investigation and quantification of bacterial leaching by *Thiobacillus ferrooxidans*. Biotechnol. Bioeng. 33: 1196-1204.

6. Beck, J.V. 1967. The role of bacteria in copper mining operations. Biotechnol. Bioeng. 9: 487-497.

7. Bennett, J.C. and H. Tributsch. 1978. Bacterial leaching patterns on pyrite crystal surfaces. J. Bacteriol. 134: 310-317.

8. Berry, L.G., et al. 1983. Mineralogy. W.H. Freeman, New York.

9. Berry, V.K. and L.E. Murr. 1978. Direct observation of bacteria and quantitative studies of their catalytic role in the leaching of low-grade, copper bearing waste. In Metallurgical Applications of Bacterial Leaching and Related Microbiological Phenomena. Eds. L.E. Murr et al. Academic Press, New York, pp. 103-136.

10. Blake, R.C. and E.A. Shute. 1987. Respiratory enzymes of *Thiobacillus ferrooxidans* a kinetic study of electron transfer between iron and rusticyanin in sulfate media. J. Biol. Chem. 262: 14983-14989.

11. Booth, I.R. 1985. Regulation of cytoplasmic pH in bacteria. Microbiol. Rev. 49: 359-378.

12. Brierley, C.L. 1982. Microbiological mining. Sci. Am. 247: 42-51.

13. Campbell, M.C., et al. 1985. Biotechnology for the mineral industry. Can. Metall. Q. 24: 115-120.

14. Chaudhury, C.R. and R.Q. Das. 1987. Bacterial leaching-complex sulfides of copper, lead and zinc. Int. J. Mineral Process. 21: 57-64.

15. Cobley, J.G. and J.C. Cox. 1983. Energy conservation in acidophilic bacteria. Microbiol. Rev. 47: 579-595.

16. Cobley, J.G. and B.A. Haddock. 1975. The respiratory chain of *Thiobacillus ferrooxidans*: the reduction of cytochromes by Fe(II) and the preliminary characterization of rusticyanin a novel blue copper protein. FEBS Let. 60: 29-33.

17. Cox, J.C. and D.H. Boxer. 1978. The purification and some properties of rusticyanin, a blue copper protein involved in iron (II) oxidation from *Thiobacillus ferrooxidans*. Biochem. J. 174: 497-502.

18. DiSpirito, A.A. and O.H. Tuovinen. 1982. Uranous ion oxidation and carbon dioxide fixation by *Thiobacillus ferrooxidans*. Arch. Microbiol. 133: 28-32.

19. Ehrlich, H.L. 1981. Geomicrobiology. Marcel Dekker, New York.

20. Ehrlich, H.L. and S.I. Fox. 1967. Environmental effects on bacterial copper extraction from low-grade copper sulfide ores. Biotechnol. Bioeng. 9: 471-485.

21. Espejo, R.T., et al. 1988. Oxidation of ferrous iron and elemental sulfur by *Thiobacillus ferrooxidans*. Appl. Env. Microbiol. 54: 1694-1699.

22. Espejo, R.T. and P. Romero. 1987. Growth of *Thiobacillus ferrooxidans* on elemental sulfur. Appl. Env. Microbiol. 53: 1907-1912.

23. Espejo, R.T. and P. Ruiz. 1987. Growth of free and attached *Thiobacillus ferrooxidans* in ore suspension. Biotechnol. Bioeng. 30: 586-592.

24. Fletcher, M. 1987. How do bacteria attach to solid surfaces? Microbiol. Sci. 4: 133-136.

25. Fukimori, Y., et al. 1988. Fe(II)-oxidizing enzyme from *Thiobacillus ferrooxidans*. FEMS Microbiol. Let. 50: 169-172.

26. Gale, N.L. and J.V. Beck. 1967. Evidence for the calvin cycle and hexose monophosphate pathway in *Thiobacillus ferrooxidans*. J. Bacteriol. 94: 1052-1059.

27. Goulbourne, E.M., et al. 1986. Mechanism of ΔpH maintenance in active and inactive cells of an obligately acidophilic bacterium. J. Bacteriol. 166: 59-65.

28. Harrison, A.P. 1984. The acidophilic thiobacilli and other acidophilic bacteria that share their habitat. Ann. Rev. Microbiol. 38: 265-292.

29. Hooper, A.B. and A.A. DiSpirito. 1985. In bacteria which grow on simple reductants, generation of a proton gradient involves extracytoplasmic oxidation of substrate. Microbiol. Rev. 49: 140-157.

30. Hutchins, S.R., et al. 1986. Microorganisms in reclamation of metals. Ann. Rev. Microbiol. 40: 311-336.

31. Ingledew, J.W. 1986. Ferrous iron oxidation by *Thiobacillus ferrooxidans*. In Biotechnology and Bioengineering Symposium No. 16 Workshop on Biotechnology for the Mining, Metal Refining and Fossil Fuel Processing Industries. Eds. H.L. Ehrlich and D.S. Holmes. John Wiley & Sons, New York, pp. 23-33

32. Ingledew, J.W. 1982. *Thiobacillus ferrooxidans* the bioenergetics of an acidophilic chemolithotroph. Biochim. Biophys. Acta. 683: 89-117.

33. Ingledew, J.W. and A. Houston. 1986. The organization of the respiratory chain of *Thiobacillus ferrooxidans*. Biotechnol. Appl. Biochem. 8: 242-248.

34. Ismay, A., et al. 1986. Engineering prefeasibility for in-place bacterial leaching of copper. In Process Metallurgy 4 Fundamental and Applied Biohydrometallurgy. Eds. R.W. Lawrence et al. Elsevier, Amsterdam, pp. 191-213.

35. Karavaiko, G.I. 1985. In Microbiological Processes for the Leaching of Metals from Ores, State-of-the-art Review. Ed. A.E. Torma. United Nations Environment Program, USSR Commission for UNEP (Center of International Projects, GKNT, Moscow).

36. Karavaiko, G.I., et al. 1984. Distribution and activity of microorganisms in leaching of nonferrous metals at the Nikolaev deposit. Microbiol. 53: 329-335.

37. Keller, L. and L.E. Murr. 1982. Acid-bacterial and ferric sulfate leaching of pyrite single crystals. Biotechnol. Bioeng. 24: 83-96.

38. Kelley, B.C. and O.H. Tuovinen. 1988. Microbiological oxidations of minerals in mine tailings. In Chemistry and Biology of Solid Waste: Dredged Material and Mine Tailings. Eds. W. Salomons and U. Förstner. Springer-Verlag, Berlin, pp. 33-53.

39. Kelly, D.P. and C.A. Jones. 1978. Factors affecting metabolism and ferrous iron oxidation in suspensions and batch cultures of *Thiobacillus ferrooxidans*: relevance to ferric iron leach solution regeneration. In Metallurgical Applications of Bacterial Leaching and Related Microbiological Phenomena. Academic Press, New York, pp. 19-44.

40. Kodama, A., et al. 1970. Studies on the metabolism of a sulfur-oxidizing bacteria. VII.Oxidation of sulfite by a cell-free extract of *Thiobacillus thiooxidans*. Plant Cell. Physiol. 11: 701-711.

41. Kovalenko, T.V., et al. 1982. Effect of Fe(III) ions in the oxidation of ferrous iron by *Thiobacillus ferrooxidans* at various temperatures. Microbiol. 51: 156-160.

42. Laishley, E.J., et al. 1986. Microcrystalline structure and surface area of elemental sulphur as factors influencing its oxidation by *Thiobacillus albertis*. Can. J. Microbiol. 32: 237-242.

43. Lineweaver, H. and D. Burk. 1934. The determination of enzyme dissociation constants. J. Amer. Chem. Soc. 58: 658-666.

44. Lowson, R.T. 1982. Aqueous oxidation of pyrite by molecular oxygen. Chem. Rev. 82: 461-497.

45. Lukow, O.M. 1977. Studies on the sulfur metabolism of *Thiobacillus thiooxidans*. M. Sc. Thesis, The University of Manitoba, Winnipeg, Manitoba.

46. Lundgren, D.G. and M. Silver. 1980. Ore leaching by bacteria. Ann. Rev. Microbiol. 34: 263-283.

47. Lundgren, D.G., et al. 1986. Chemical reactions important in bioleaching and bioaccumulation. In Biotechnology and Bioengineering Symposium No. 16 Workshop on Biotechnology for the Mining, Metal Refining and Fossil Fuel Industries. Eds. H.L. Ehrlich and D.S. Holmes. John Wiley & Sons, New York, pp. 7-22.

48. Mahapatra, S.S.R. and A.K. Mishra. 1984. Inhibition of iron oxidation in *Thiobacillus ferrooxidans* by toxic metals and its alleviation by EDTA. Cur. Microbiol. 11: 1-5.

49. McCready, R.G.L., et al. 1986. Nutrient requirements for the in-place leaching of uranium by *Thiobacillus ferrooxidans*. Hydrometallurgy. 17: 61-71.

50. Mehta, A.P. and L.E. Murr. 1982. Kinetic study of sulfide leaching by galvanic interaction between chalcopyrite, pyrite, and sphalerite in the presence of *Thiobacillus ferrooxidans* (30°C) and a thermophilic microorganism (50°C). Biotechnol. Bioeng. 24: 919-940.

51. Miller, P.C. 1986. Large-scale bacterial leaching of a copper-zinc ore in situ. In Process Metallurgy 4 Fundamental and Applied Biohydrometallurgy. Eds. R.W. Lawrence et al. Elsevier, Amsterdam, pp. 215-239.

52. Morse, J.W., et al. 1987. The chemistry of the hydrogen sulfide and iron sulfide systems in natural waters. Earth Sci. Rev. 24: 1-42.

53. Moses, C.O., et al. 1987. Aqueous pyrite oxidation by dissolved oxygen and ferric iron. Geochim. Cosmochim. Acta. 51: 1561-1571.

54. Oh, J.K. and I. Suzuki. 1980. Respiration in chemoautotrophs oxidizing sulfur compounds. In Diversity of Bacterial Respiratory Systems, vol. 3. Ed. L.J. Knowles. CRC Press Inc. pp. 113-138.

55. Oh, J.K. and I. Suzuki. 1977. Resolution of a membrane-associated thiosulfate-oxidizing complex of *Thiobacillus novellus*. J. Gen. Microbiol. 99: 413-423.

56. Rao, S.R. and J.A. Finch. 1988. Galvanic interaction studies on sulphide minerals. Can. Metall. Q. 27: 253-259.

57. Rodriguez-Leiva, M. and H. Tributsch. 1988. Morphology of bacterial leaching patterns by *Thiobacillus ferrooxidans* on synthetic pyrite. Arch. Microbiol. 149: 401-405.

58. Schaeffer, W.I. and W.W. Umbreit. 1963. Phosphatidylinositol as a wetting agent in sulfur oxidation by *Thiobacillus thiooxidans*. J. Bacteriol. 85: 492-493.

59. Segel, I.H. 1975. System B3. Cooperative (synergistic) pure competitive inhibition by two different nonexclusive inhibitors. In Enzyme Kinetics. I.H. Segel. John Wiley & Sons, New York, pp. 481-488.

60. Silverman, M.P. 1967. Mechanism of bacterial pyrite oxidation. J. Bacteriol. 94: 1046-1051.

61. Southwood, M.J. and A.J. Southwood. 1986. Mineralogical observations on the bacterial leaching of auriferous pyrite: a new mathematical model and implications for the release of gold. In Process Metallurgy 4 Fundamental and Applied Biohydrometallurgy. Eds. R.W. Lawrence et al. Elsevier, Amsterdam, pp. 98-113.

62. Starkey, R.L. 1925. Concerning the physiology of *Thiobacillus thiooxidans*, an autotrophic bacteria oxidizing sulfur under acid conditions. J. Bacteriol. 10: 135-163.

63. Sugio, T., et al. 1988. Existence of a new type of sulfite oxidase which utilizes ferric ions as an electron acceptor in *Thiobacillus ferrooxidans*. Appl. Env. Microbiol. 54: 153-157.

64. Sugio, T., et al. 1988. Synthesis of an iron-oxidizing system during growth of *Thiobacillus ferrooxidans* on sulfur-basal salts medium. Appl. Env. Microbiol. 54: 150-152.

65. Sugio, T., et al. 1987. Purification and some properties of sulfur: ferric iron oxidoreductase from *Thiobacillus ferrooxidans*. J. Bacteriol. 169: 4916-4922.

66. Sugio, T., et al. 1985. Role of a ferric ion-reducing system in sulfur oxidation of *Thiobacillus ferrooxidans*. Appl. Env. Microbiol. 49: 1401-1406.

67. Sugio, T., et al. 1981. The purification and some properties of a factor having a stimulating effect on iron-oxidizing activity of *Thiobacillus ferrooxidans*. Agric. Biol. Chem. 45: 405-412.

68. Suzuki, I. 1974. Mechanisms of inorganic oxidation and energy coupling. Ann. Rev. Microbiol. 28: 85-101.

69. Suzuki, I. 1965. Oxidation of elemental sulfur by an enzyme system of *Thiobacillus thiooxidans*. Biochim. Biophys. Acta. 104: 359-371.

70. Suzuki, I. and M. Silver. 1966. The initial product and properties of the sulfur-oxidizing enzyme of thiobacilli. Biochim. Biophys. Acta. 122: 22-33.

71. Suzuki, I., et al. 1988. Determination of activity parameters in *Thiobacillus ferrooxidans* strains as criteria for mineral leaching effiency. I. Growth characteristics and effect of metals on growth and on sulfur or ferrous iron oxidation. In Biominet Proceedings SP87-10. Ed. R.G.L. McCready. CANMET, Ottawa, pp. 179-209.

72. Takakuwa, S., et al. 1979. Some properties of cell-sulfur adhesion in *Thiobacillus thiooxidans*. J. Gen. Appl. Microbiol. 25: 21-29.

73. Torma, A.E. 1977. The role of *Thiobacillus ferrooxidans* in hydrometallurgical processes. In Advances in Biochemical Engineering, vol. 6. Eds. T.K. Ghose et al. Springer-Verlag, New York, pp. 1-37.

74. Torma, A.E. 1971. Microbiological oxidation of synthetic cobalt, nickel and zinc sulfides by *Thiobacillus ferrooxidans*. Rev. Can. Biol. 30: 209-216.

75. Toro, L., et al. 1986. Ions and precipitates in the biooxidation of ferrous sulphate solution by *Thiobacillus ferrooxidans*. In Process Metallurgy 4 Fundamental and Applied Biohydrometallurgy. Eds. R.W. Lawrence et al. Elsevier, Amsterdam, pp. 476-478.

76. Tributsch, H. and J.C. Bennett. 1981. Semiconductor-electrochemical aspects of bacterial leaching. I. Oxidation of metal sulphides with large energy gaps. J. Chem. Tech. Biotechnol. 31: 565-577.

77. Tributsch, H. and J.C. Bennett. 1981. Semiconductor-electrochemical aspects of bacterial leaching. Part 2. Survey of rate-controlling sulphide properties. J. Chem. Tech. Biotechnol. 31: 627-635.

78. Tuovinen, O.H., et al. 1971. Tolerance of *Thiobacillus ferrooxidans* to some metals. A. van Leeuwenhoek. 37: 489-496.

79. Umbreit, W.W., et al. 1949. Manometric techniques and tissue metabolism, 2nd ed. Burgess Publishig Co., Minneapolis.

80. Wakao, N., et al. 1984. Bacterial pyrite oxidation III. Adsorption of *Thiobacillus ferrooxidans* cells on solid surfaces and its effect on iron release from pyrite. J. Gen. Appl. Microbiol. 30: 63-77.

81. Wardell, J.M., et al. 1983. Microbes and surfaces. In Microbes in their Natural Environments-34th Symposium of the Society for General Microbiology. Eds. J.H. Slater et al. Cambridge University Press, England, pp. 351-378.

82. Yeh, T.Y., et al. 1987. Use of epifluorescence microscopy for characterizing the activity of *Thiobacillus ferrooxidans* on iron pyrite. Biotechnol. Bioeng. 30: 138-146.